Regioselective [^{18}F]fluoropropionylation of Peptides and Proteins in Aqueous Solution

WESTER H.J., GUHLKE S., STÖCKLIN G.
Institut für Nuklearchemie, Forschungszentrum Jülich, 52425 Jülich, Germany

In order to label peptides and proteins with fluorine-18 ($T_{1/2}$=110 min), we have investigated the applicability of our previously developed ^{18}F-fluoropropionylation method [1] in aqueous solutions. For ^{18}F - labeling of biomolecules containing multiple nucleophilic groups, regioselective acylation exploiting the different pK_a values seems to be of great interest. The selectivity is of crucial importance when a nucleophilic group in the pharmacophoric moiety should not be attacked by the labeling agent [2,3].

Initial studies were performed using phenylalanyl glycine (phe-gly), tyrosyl lysine (tyr-lys) and valyl lysine (val-lys) as model systems. Starting with the 2-bromopropionyl-(9-anthryl)methylester precursor, the acylating species 2-[^{18}F]fluoropropionyl-para-nitrophenylester (2-[^{18}F]PNPE) was synthesised as described previously [1]. In the general labeling procedure, 10µl of 2-[^{18}F]PNPE in DMF was reacted with 5µmol of the peptides or protein in 100-200 µl buffer-solution for 15 min at 22°C. To prevent the competing hydrolysis of the 2-[^{18}F]PNPE, pH control is of major importance. It was found, that ^{18}F-fluoropropionylation of phe-gly only occured with low RCY (about 30% at pH 7.4 using amine concentrations of about 150 µmol/ml) (Tab.1). In addition, peptides with side chain amino groups, as represented by val-lys and tyr-lys, could not be labeled regioselectively at the N_α-position by pH-control only.

To overcome these problems, different aminolysis catalysts were tested. Comparison of the catalytic effects of 1-hydoxybenzotrizole (HOBt), 1-hydroxy-2-pyridone, 2-hydroxypyridine and imidazole, HOBt seems to be the catalyst of choice (Fig.1). Under conditions described in Fig.1, the RCY of the ^{18}F-fluoroacylation of phe-gly increased from 15% to 70% using HOBt. In addition, regioselective ^{18}F-fluoroacylation of N_α- or N_ε- amino groups was possible (Table 1). So, the N_α/N_ε - product ratio of the ^{18}F-fluoroacylation of val-lys was changed to the reciprocal value with addition of the catalyst, leading to 69% N_α-[^{18}F]fluoroacylated product.

Similar results were obtained with proteins. While the reaction of avidine with 2-[^{18}F]PNPE without HOBt only leads 10±2% RCY (1mg avidine, pH 8.4, 10 min), the presence of HOBt gives rise to product yields of 61±6%, again demonstrating the impressive efficiency of the catalyst. Furthermore, the biologic activity of the ^{18}F-fluoroacylated avidine remained unchanged, as was determined by affinity-chromatography with immobilized biotin.

In conclusion 2[^{18}F]PNPE in combination with HOBt as catalyst exhibits two principal advantages for the labeling of bioactive peptides and proteins:

- *pH controlled regioselective fluoroacylation avoids attack of nucleophilic pharmacophoric moieties without educt protection*
- *considerable reduction of educt concentration facilitates product separation*

Table 1: RCY and product ratios of the [^{18}F]-fluoropropionylation of model peptides in catalysed and non-catalysed reactions (15 min, 22°C).

model-peptide	$c_{peptide}$ [mmol/ml]	pH	RCY (%)	catalyst (HOBt)	N_α/N_ε-ratio
phe-gly	0.04	7.5	15	no	/
	0.04	7.5	70	0.05 mol/l	/
tyr-lys	0.05	6.7	N_ε= 12; N_α=51	0.1 mol/l	4.25
	0.05	10	N_ε= 59; N_α=5	0.1 mol/l	0.08
val-lys	0.05	7.2	N_ε= 61; N_α=19	no	0.31
	0.05	7	N_ε= 18; N_α=69	0.1 mol/l	3.83

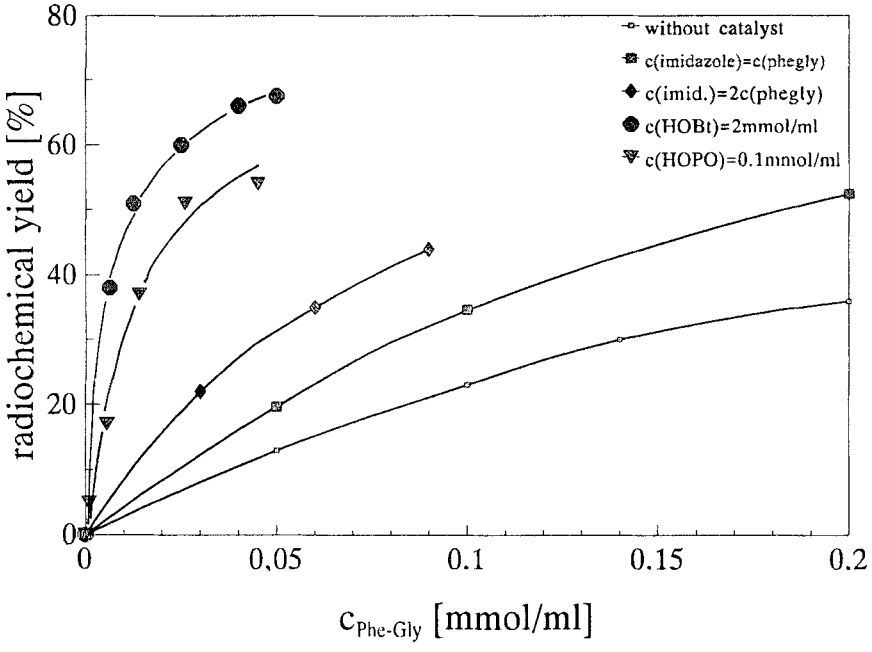

Figure 1: RCY (based on 2-[^{18}F]PNPE) of ^{18}F-fluoropropionylation of phe-gly as a function of educt concentration for different catalysts.

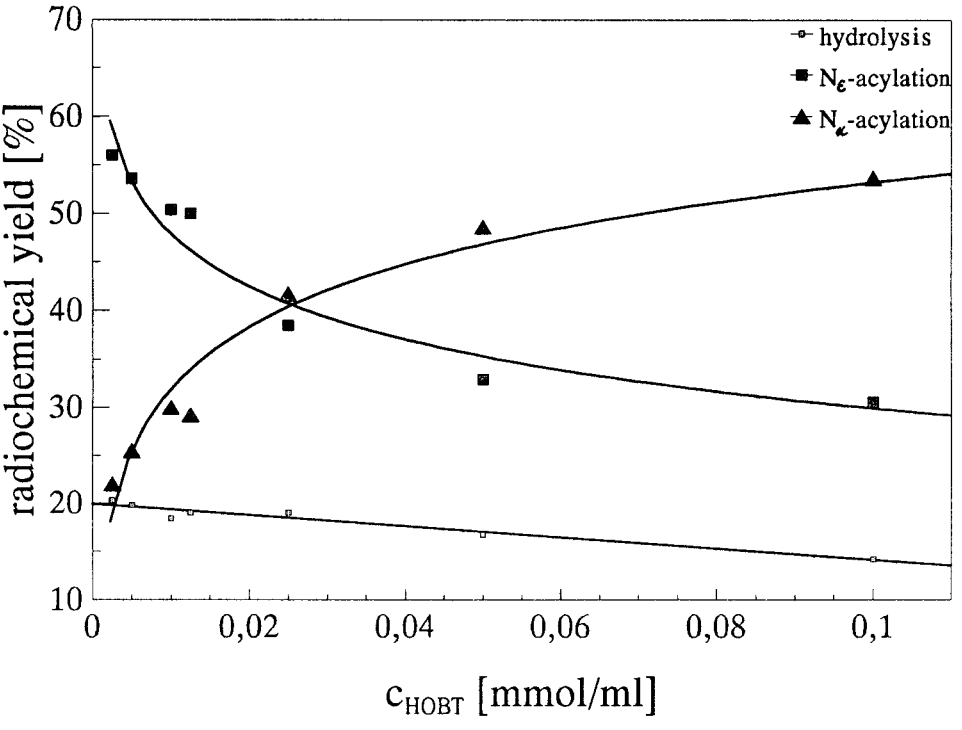

Figure 2: RCY of N_α-and N_ε-2-[^{18}F]fluoropropionylation of val-lys as a function of HOBt concentration ($c_{val\text{-}lys}$=0.05 mmol/ml, 22°C, 15 min, pH 7.3)

[1] Guhlke.S., Coenen H.H., Stöcklin G., J. Label. Compd. Radiopharm. **32**: 108-110, 1993 (abstr.)
[2] Garg S., Garg P.K., Zalutzky M.R., J. Label. Compd. Radiopharm. **32**: 212-213, 1993 (abstr.)
[3] Guhlke S., Wester H.J., Bruns C., Stöcklin G., J.Nucl.Med. **34**(5): 80, 1993 (abstr.)

^{11}C-Labelling of macromolecules using [^{11}C]cyanogen bromide

WESTERBERG, G., and LÅNGSTRÖM, B. Uppsala University PET Centre, UAS S-751 85, Uppsala, Sweden.

The biological activity exhibited by many macromolecules make them interesting as tracers for the study of a range of physiological processes such as blood flow, metabolism, tissue perfusion and receptor binding. PET also presents a possibility for the assessment of macromolecular biodistribution kinetics. In this study [1], a general method for the labelling of polypeptides and polysaccharides using [^{11}C]cyanogen bromide is presented. Human serum albumin (HSA) and human iron-free transferrin (Tf) were treated with [^{11}C]cyanogen bromide of high specific radioactivity under physiological conditions to give high yields of labelled protein in short synthesis times.

Protein labelling - Cyanogen bromide has for long been used in protein chemistry as a sequencing agent for the selective cleavage of peptide chains on the carboxyl side of methionine residues [2]. Incubating proteins at physiological pH with tracer amounts of cyanogen bromide however, does not seem to cause any cleavage of the peptide chain. Thus, in a typical experiment starting with 8.5 GBq [^{11}C]cyanogen bromide, 2.0 GBq of ^{11}C-albumin was obtained in >98% radiochemical purity in 17 - 19 minutes synthesis time counted from [^{11}C]cyanogen bromide corresponding to a decay-corrected radiochemical yield of 76 %. The labelled proteins were characterized using both high performance liquid chromatography and high performance capillary electrophoresis [3]. No fragmentation of the proteins resulting from the treatment with [^{11}C]cyanogen bromide was observed.

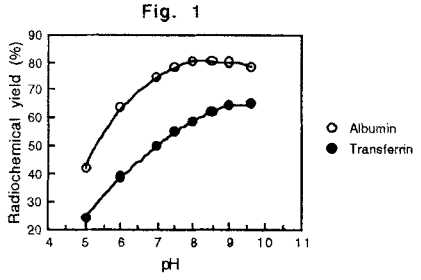

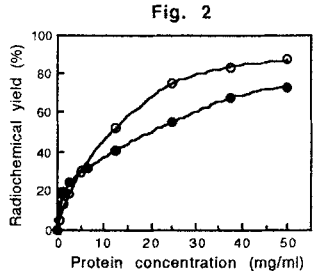

The yield of labelled protein as a function of pH was investigated in the pH-range 5 - 9.5, as illustrated in Fig. 1. After incubation for 5 min, a sample was withdrawn and analyzed by anion-exchange chromatography. The yield of labelled product was obtained from the radiochromatograms after decay-correction. In order to verify the yields obtained by chromatography, an aliquot of the reaction mixture was withdrawn and the proteins precipitated using TCA. In all cases, the yields obtained by these two methods corresponded within ± 2 %.

The variation in yield of labelled protein with the protein concentration was determined at pH 8.0 analogously to the pH-dependence experiments, Fig. 2. The concentration of protein was varied over the range 0.25 - 50 mg ml^{-1}. The specific activity of the labelled proteins varied with the amount of protein used between 10.7 - 141 GBq μmol^{-1} (0.289 - 3.8 Ci μmol^{-1}) as indicated in Fig. 3.

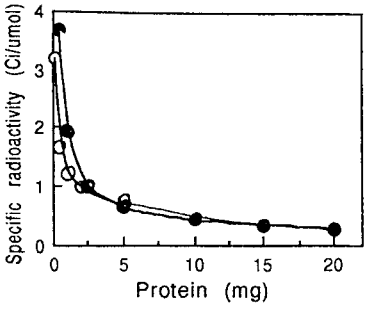

Fig. 3

The [^{11}C]cyanogen bromide was trapped at room temperature in 300 µl 50 mM potassium phosphate buffer (pH-range 5 - 7.5) or 50 mM borate buffer (pH-range 7.5 - 9.5) in a 0.9 ml mini-vial equipped with a septum. When the radioactivity had reached a maximum, the solution was transferred to a conical 3 ml septum-equipped reaction vessel containing the protein in the phosphate or borate buffer above (100 µl) to give a total volume of 400 µl. The reaction mixture was then incubated at 40 °C. After incubation , the reaction mixture was either injected onto a gel-permeation HPLC column (Zorbax GF-250 10µm, 250 x 10 mm ID), or eluted on a single-use Sephadex® G25 cartridge, using normal saline or 50 mM sodium bicarbonate as the eluent. The high molecular weight fraction was passed through a sterile filter (Dynagard ME, 0.22 µm) into a sterile ampoule to provide a solution ready for i.v. injection.

Polysaccharide labelling - Hyaluronic acid (1-[β-4-D-glucoronic acid (1-β-3) *N*-acetyl-D-glucosamine-1-]$_n$-β-4) is a glucosaminoglycan which has attracted considerable interest in recent years, particularly for its role in rheumatoid arthritis and in hepatic diseases. The widespread use of cyanogen bromide for the activation of polysaccharide gels for affinity chromatography [4] suggested that [^{11}C]cyanogen bromide might be a useful reagent for the labelling of these compounds. Using a procedure similar to the protein experiments, ^{11}C-hyaluronic acid (HA) and various molecular weight fractions of dextrane were prepared to illustrate the potential usefulness of [^{11}C]cyanogen bromide for polysaccharide labelling.

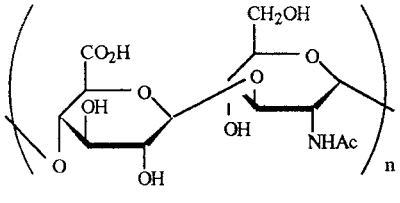

hyaluronic acid

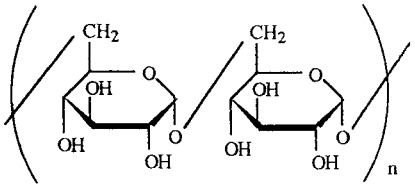

dextrane

In the labelling of polysaccharides, the [^{11}C]cyanogen bromide was trapped at room temperature in 300 µl of water. A solution of the polysaccharide (0.5 - 1.0 ml, 0.1 - 5 mg ml^{-1}) was added and the reaction mixture heated at 40 - 80 °C. The reaction mixture was then either eluted on a single-use Sephadex® G25 cartridge using normal saline as the eluent, or passed through an ultrafilter (Millipore UFP1 THK24). The residue was resuspended in saline and sterile filtered.

The labelled proteins may become interesting as tracers for pulmonary flow investigations using PET. Further applications of labelled HSA include measurement of regional haematocrit and myocadial perfusion. Labelled transferrin may become interesting as a tracer for the assesment of pulmonary permeability and for studies of the transferrin receptor [5]. The ^{11}C-hyaluronic acid is of interest for the study of hyaluronic acid bioavailability and extent of extrahepatic elimination in liver diseases. The experimental labelling procedure is general, and might also be of interest for ^{14}C-labelling of proteins for *in vitro* use.

References

1. Westerberg, G., and Långström, B. (1993) *J. Biol. Chem., Submitted.*
2. Gross, E., and Witkop, B. (1962) *J. Biol. Chem. 237, 1856 - 1860.*
3. Westerberg, G., Kilár, F., Lundqvist, H., and Långström, B. (1993) *J. Chromatogr., In press.*
4. Kohn, J., Wilchek, M. (1984) *Appl. Biochem. Biotech. 9, 285.*
5. Mintun, M. A., Dennis, D.R., Welch, M.J., Mathias, C.J., and Schuster, D.P. (1987) *J. Nucl. Med. 28, 1704 - 1716;* Brudin, L.H., Valind, S.O., Rhodes, C.G., Turton, D.R., and Hughes, J.M. (1986) *J. Appl. Physiol. 60, 1155 - 1163*

Reduction in Non-specific Uptake of Indium-111 from Using Semi-rigid Cyclohexyl EDTA Immunoconjugates

SRIVASTAVA, S.C.; MEASE, R.C.; MEINKEN, G.E.; GESTIN[1], J.F.; JOSHI, V.; PYATT, B.; MAUSNER, L.F.; and CHATAL[1], J.F. Medical Department, Brookhaven National Laboratory, Upton, NY 11973, USA, and [1]INSERM, Unit 211, University of Nantes, Nantes, France.

Monoclonal antibodies (MAb) labeled with In-111 continue to find widespread use for imaging tumors and other in-vivo pathology. The most commonly used bifunctional chelating agent (BCA) is DTPA-dianhydride (DTPA-DA) but its use results in high non-specific retention of In-111 in liver and other tissues. However, a number of modified DTPA analogs have shown some improvement (1,2). This study was done to further improve In-111-MAb distribution by using semi-rigid cyclohexyl EDTA analogs as BCA (3). Two BCA, 4-isothiocyanato-trans-1,2-diaminocyclohexane-N,N,N',N'-tetraacetic acid (4-ICE) and N-[methyl(2-isothiocyanato ethyl) carbamide]-trans-1,2-diaminocyclohexane N,N',N'-triacetic acid (CDTA-EN-SCN), synthesized as previously reported (3,4), were used to prepare In-111-anti-CEA $F(ab')_2$ conjugates. Typical labeling conditions were as follows: To ~400 μg of the immunoconjugate (1.5 - 3.0 BCA/MAb) in 30μl 0.1M $NaHCO_3$ were added a 0.2M acetate buffer, pH 5.0, 0.1M citrate buffer pH 5.0, and 10μl of In-111 Cl_3 in 0.05M HCl. Final concentrations were acetate 0.2M, citrate 0.02M, and the pH was 5.0. The mixture was incubated for 2h at 25°C and then purified using Centricon C-30 membrane filters (pretreated with HSA). The labeling yields were 90-95% with DTPA-DA (control) and 4-ICE, and in the range of 35-75% for CDTA-EN-SCN. Aggregate formation (size exclusion HPLC) was less than 2% except for DTPA-DA where it was ~15%. Following incubation of all purified preparations with mouse serum at 37°C for 4 days, >95% In-111 remained bound to the antibody fragment. Immunoreactivity retention as determined from solid-phase antigen binding assays was 80 ± 5% for all labeled conjugates. Biodistribution studies were carried out in human tumor-xenografted nude mice (LS-174T cells). The results are shown in Table 1. Tumor (T) to blood (B), liver (L), and kidney (K) ratios, at 24 and 96h, respectively, were: DTPA-DA, T/B 6.7 and 54, T/L 2.2 and 1.8, T/K 1.0 and 0.8; CDTA-EN-SCN, T/B 6.1 and 124, T/L 3.3 and 3.7, T/K 1.1 and 1.0; 4-ICE, T/B 6.3 and 133, T/L 3.9 and 3.8, T/K 1.4 and 2.4. These results demonstrate that our semi-rigid bifunctional chelating agents CDTA-EN-SCN and 4-ICE produce considerably improved tumor to normal organ uptake ratios of the In-111 labeled anti-CEA $F(ab')_2$ antibody. Use of 4-ICE gave the best overall distribution. Whereas the tumor uptake using 4-ICE is comparable with that using DTPA-DA, non-specific organ uptake is substantially reduced, especially in liver, kidneys, and bone (Table 2). This 6-coordinate ligand, functionalized at the 4-carbon of the cyclohexyl moiety for conjugation to antibodies, is worthy of further investigations for labeling MAbs with In-111. Imaging studies in patients are currently in progress.

1. Brechbiel, M.W.; Gansow, O.A.; Atcher, R.W.; et al., Inorg. Chem. 25:2772 (1986).
2. Sumerdon, G.A.; Rogers, P.E.; Lombardo, C.M.; et al., Nucl. Med. Biol. 17:247 (1990).
3. Mease, R.C.; Gestin, J.F.; Meinken, G.E.; Srivastava, S.C. J. Label. Compd. Radiopharm. 30:196 (1991).
4. Mease, R.C.; Meinken, G.E.; Srivastava, S.C. J. Label. Compd. Radiopharm. 32:410 (1993).
5. Srivastava, S.C.; and Mease, R.C. Nucl. Med. Biol. 18:589 (1991).

This work was supported by the U.S. Department of Energy under contract No. DE-AC02-76CH00016. Thanks are due to J. C. Saccavini, Compagnie ORIS Industrie, Gif Sur Yvette, France for providing the antibody used in these studies.

Table 1. Tissue Distribution (% dose/g) of ^{111}In-Labeled Anti-CEA F(ab')$_2$* in Nude Tumor Mice

Tissue/ Organ	DTPA-DA		CDTA-EN-SCN		4-SCN-CDTA (4-ICE)	
	24h	96h	24h	96h	24h	96h
Tumor	30.17 ± 6.99	13.34 ± 1.69	25.41 ± 5.38	10.81 ± 0.06	28.27 ± 5.94	11.61 ± 3.96
Blood	4.53 ± 0.46	0.25 ± 0.03	4.14 ± 0.39	0.09 ± 0.03	4.50 ± 0.54	0.09 ± 0.03
Liver	13.87 ± 0.80	7.35 ± 1.2	7.59 ± 0.72	2.88 ± 0.35	7.20 ± 0.50	3.09 ± 0.30
Muscle	0.85 ± 0.11	0.40 ± 0.09	0.68 ± 0.09	0.16 ± 0.03	0.82 ± 0.07	0.10 ± 0.02
Kidney	31.62 ± 2.04	17.25 ± 1.11	24.15 ± 3.28	11.20 ± 1.55	20.5 ± 2.1	4.78 ± 0.67
Spleen	5.53 ± 0.60	4.11 ± 0.65	3.81 ± 0.35	1.60 ± 0.44	4.30 ± 0.29	1.46 ± 0.11
Bone	2.22 ± 0.23	1.59 ± 0.11	1.78 ± 0.25	0.63 ± 0.06	2.00 ± 0.09	0.77 ± 0.04
Whole Body (% Dose remaining)	95.1 ± 2.3	59.6 ± 4.0	80.0 ± 6.2	27.1 ± 2.4	81.7 ± 1.9	27.5 ± 8.1

Table 2. Improvement in Tumor/Organ Ratios of ^{111}In anti-CEA F(ab')$_2$ Immunoconjugates*

Ratio, Tumor To:	DTPA-DA		4-ICE		Improvement Factor 4-ICE/DTPA-DA	
	24 h	96 h	24 h	96 h	24 h	96 h
Blood	6.7	54	6.3	133	0.9	2.5
Liver	2.2	1.8	3.9	3.8	1.8	2.1
Kidney	1.0	0.8	1.4	2.4	1.4	3.0
% dose per g in tumor	30.2	13.3	28.3	11.6	0.9	0.9

In-111-Anti-CEA F(ab')2 Tumor to Organ Ratios at 24 h

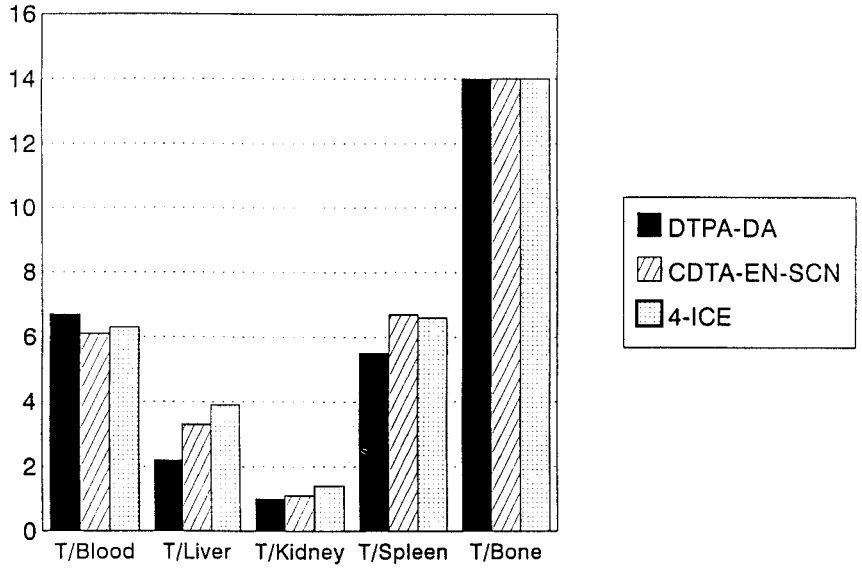

In-111-Anti-CEA F(ab')2 Tumor to Organ Ratios at 96 h

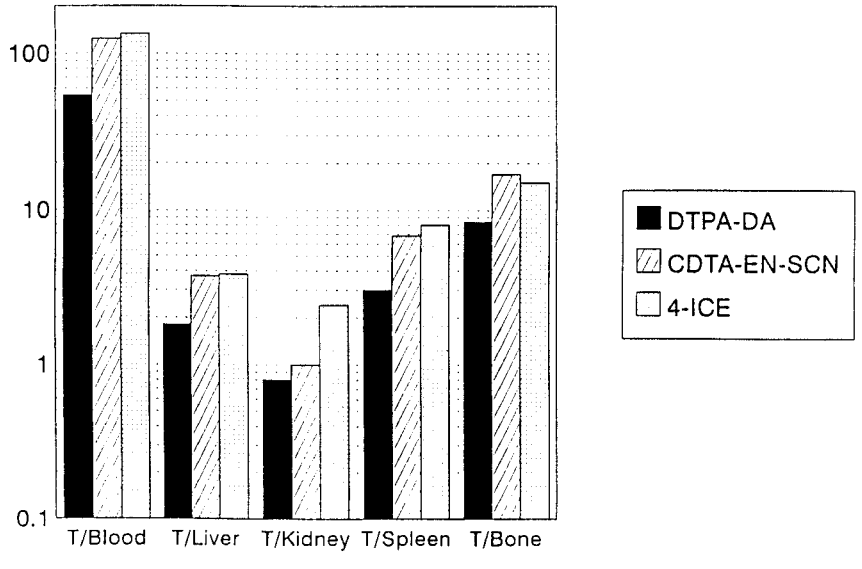

IN VITRO EVALUATION AND TISSUE DISTRIBUTION OF Tc-99m MONOCLONAL ANTIBODIES PREPARED BY DIRECT AND PREFORMED CHELATE METHODS.

JOHN E., WILDER S., ESHIMA D*., THAKUR M.L.
Dept. of Nuclear Medicine, Thomas Jefferson University, Philadelphia, PA - 19107 and * Dept. of Nuclear Medicine, Emory University School of Medicine, Atlanta, GA - 30322.

The use of Tc-99m labeled monoclonal antibodies (MAbs) has continued to grow rapidly. Although direct labeling techniques are simple and permit kit formulations for instant preparations (1,2), Tc-99m bound to MAbs by direct methods is generally considered to be unstable. Also, nonspecific binding (approx. 20%) of Tc-99m to ε amino groups of lysine tends to increase liver uptake and reduce its concentration in tumors (3). Contrary to this, preformed chelate techniques are thought to be highly stable and to prevent nonspecific binding.

The purpose of this investigation was to prepare a specific, nonspecific, and control Tc-99m labeled MAbs using an ascorbic acid direct labeling method, and to compare the stabilities, structural perturbations, if any, and tissue distribution in tumor bearing mice, with a preformed chelate technique.

Specific preparations (scheme I) were made in which aliphatic ε-amino groups of lysines were blocked with fluorescein isothiocyanate (FITC) prior to labeling with Tc-99m. In nonspecific preparations all sulfhydryl groups were blocked with sodium iodoacetate following AA reduction and prior to labeling with Tc-99m. Unblocked, AA reduced MAbs labeled with Tc-99m served as the control preparation.

For the preformed chelate , a tetrafluoro-activated ester of a triamide thiolate ligand (N_3S) synthesized in Dr. Eshima's laboratory was used. Tc-99m chelation with the ester was facilitated (scheme II) by exchange with Tc-99m gluconate at 75°C for 30 minutes. Unbound Tc-99m was eliminated using a C-18 Sep Pak cartridge. The chelate was then conjugated to MAbs by incubation in Na_2CO_3 buffer, pH 10, for 30 min. at 22°C. Unbound chelate was eliminated by molecular filtration and labeled MAbs were analyzed by ITLC and HPLC.

Human immunoglobulin (HIgG) labeled by AA (control) and preformed chelate (N_3S) techniques were challenged with 100 and 250 molar excess of cysteine, DTPA, and HSA at 37°C for up to four hours; radioactivity associated with the protein was determined and is shown in Table I.

Antihistone antibody TNT-1 obtained from Dr. Epstein's laboratory at USC was labeled with Tc-99m using the AA (three preparations) and N_3S techniques. Four hour tissue distribution studies were performed in mice bearing experimental embryonal carcinomas. Results are given in Table II.

Structural perturbations of MAbs following radiolabeling were examined under identical nonreduced and DTT reduced PAGE analyses (4). Gels were stained, cut and counted for distribution of activity. Results are shown in Table III.

Table I indicates that Tc-99m labeled by both AA and N_3S methods were stable with HSA, but upon incubation with even 100 molar excess of cysteine, approximately 35% of the radioactivity was associated with protein. Surprisingly, Tc-99m labeled by the N_3S method was slightly less stable to DTPA challenge (4 hr, 85% vs 94%) than that labeled by the AA technique.

With N_3S preparation, the tumor uptake was as high as the AA specific preparation (2±0.2% vs 2±0.4%). The liver uptake with N_3S preparation, however, was as high as the regular AA preparation (25.7±2.5% vs 23.1±5.0%) and much higher (25.7±2.5% vs 15.1±2.2%) than the AA specific preparation. The reasons for the higher liver uptake with the preformed chelate are not well understood at this time. As given in Table III, SDS-PAGE analyses of N_3S preparations show that 72% of the Tc-99m is

bound to the apparent M.W. 150 KD, compared to that of only 46.4% with the AA method. This is favorable over the AA preparation.

In summary, our preliminary comparitive results indicate that MAbs labeled by the preformed chelation technique may have limited advantage over the AA technique. However these may be outweighed by the lengthy and inconvenient preparations required by the preformed chelate technique in clinical pharmacy settings. Further work with other DADT agents continues in our laboratory. (Supported by NIH grant CA-R0151960)

References

1. M.L. Thakur, J. DeFulvio. J. Immunol. Methods 1991;237:217-224.
2. E. John, M.L. Thkaur et al. J. Nucl. Med. 1993:34;260-267.
3. E. John, S. Wilder, M.L. Thakur et al. J. Nucl. Med. 1993:34;246P.
4. E. John, S. Wilder, M.L. Thakur. submitted to Nucl. Med. Comm.

TABLE I

Stability Studies
(% Tc-99m associated with proteins at 37°C)

	^{99m}Tc-HIgG(AA method)				^{99m}Tc-HIgG-N_3S			
	0.5 hr	2 hr	3 hr	4 hr	0.5 hr	2 hr	3 hr	4hr
1:100 Cys	70	48	43	38	68	42	36	35
1:250 Cys	65	41	40	34	54	36	30	32
1:100DTPA	97	96	95	95	96	91	89	88
1:250DTPA	97	96	96	94	89	87	86	85
1:100HSA	98	94	91	88	98	98	98	98
1:250HSA	88	78	76	74	98	93	87	87

TABLE II

4 hr Biodistribution of ^{99m}Tc- labeled MAb in mice (% ID/organ, N = 5)

	^{99m}Tc-TNT-1-FITC (specific)	^{99m}Tc-TNT-1-1A (nonspecific)	^{99m}Tc-TNT-1AA (control)	^{99m}Tc-TNT-1N_3S (preformed chelate)
Muscle	0.36 ± 0.03	0.27 ± 0.08	0.33 ± 0.07	0.33 ± 0.05
Intestine	1.56 ± 0.42	0.84 ± 0.25	1.44 ± 0.44	1.20 ± 0.4
Heart	1.49 ± 0.38	0.49 ± 0.08	2.07 ± 1.4	1.20 ± 0.06
Lungs	2.37 ± 0.41	0.59 ± 0.19	2.92 ± 0.71	7.80 ± 3.2
Blood	6.50 ± 0.86	1.66 ± 0.59	4.89 ± 1.5	5.20 ± 0.60
Spleen	13.9 ± 3.5	15.7 ± 1.6	32.8 ± 3.7	14.2 ± 3.5
Kidney	13.9 ± 2.9	8.27 ± 1.0	14.2 ± 1.3	13.8 ± 2.2
Liver	15.1 ± 2.2	26.7 ± 4.0	23.1 ± 5.0	25.7 ± 2.5
Tumor	2.05 ± 0.41	0.89 ± 0.16	1.72 ± 0.77	2.02 ± 0.23

TABLE III

SDS-PAGE RESULTS

% Radioactivity associated with radiolabeled MAbs with and without DTT digestion

	w/o DTT		with DTT	
M.W. (kD)	AA	N_3S	AA	N_3S
150	46.4	72.0	----	7.2
100	10.8	11.0	9.3	10.2
50	14.1	5.3	28.4	51.0
25	28.5	11.7	62.3	31.0

DIRECT METHOD - SCHEME I

1) Specific Preparation

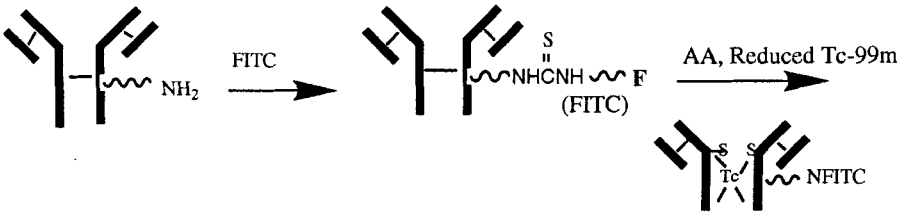

2) Nonspecific Preparation

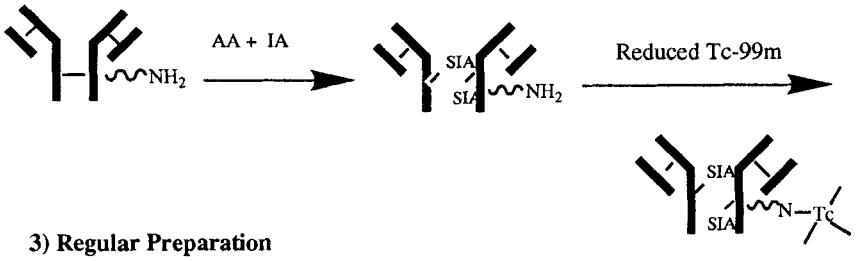

3) Regular Preparation

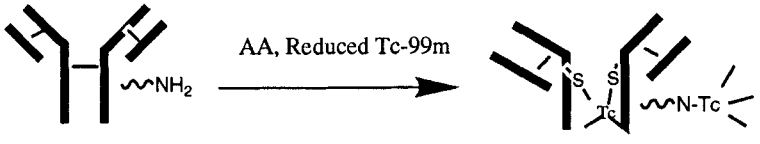

PREFORMED CHELATE - SCHEME II

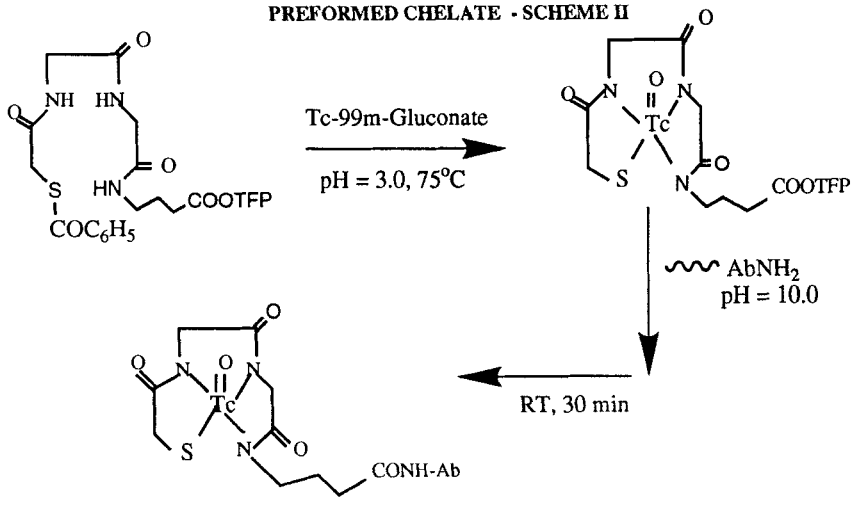

CATABOLISM OF LABEL FROM MEL-14 F(ab')$_2$ FRAGMENT RADIOHALOGENATED USING *N*-SUCCINIMIDYL 3-HALOBENZOATES.

GARG, P.K., GARG, S., ZHAO, X.G., WELSH, P.C., and ZALUTSKY, M.R.
Department of Radiology, Duke University Medical Center, Durham, NC 27710, USA.

An understanding of the nature of the labeled species created by the catabolism of labeled monoclonal antibodies (MAbs) should facilitate the development of better methods for labeling these molecules for *in vivo* use. Studies were performed to investigate various catabolites present in normal tissues following injection of anti-proteoglycan chondroitin MAb Mel-14 F(ab')$_2$ labeled using *N*-succinimidyl 3-[^{125}I]iodobenzoate (SIB) and *N*-succinimidyl 3-[^{211}At] astatobenzoate (SAB). Labeling of Mel-14 F(ab')$_2$ was accomplished using previously described procedures (1,2) that are summarized in Figure 1. Protein associated activity was greater than 99% for both labeled Mel-14 F(ab')$_2$ preparations.

Three hours after injection of radiolabeled MAb fragment, BALB/c mice were euthanized and blood, urine, spleen, kidney, lungs, and liver (^{125}I only) were obtained. Tissues were homogenized, centrifuged and the supernatants were separated. Aliquots of serum, urine and organ supernatants were analyzed by a) size-exclusion HPLC using a Bio-Sil SEC-250 column; b) tandem 10% SDS-PAGE gel under non-reducing conditions; and c) after precipitation of proteins from the supernatants, by HPLC using a reverse-phase C-18 column.

With both ^{125}I and ^{211}At, >98% of activity in serum eluted as unmodified F(ab')$_2$ on size-exclusion HPLC. An SDS-PAGE gel was run to quantitate the size distribution of radiolabeled macromolecules in tissues. The autoradiograph from the ^{125}I study is shown in Figure 2. A duplicate gel was cut up and counted to calculate the distribution ratio between F(ab')$_2$:Fab:heavy & light chain bands from each tissue. A ratio of 1:0.5:1.5 for spleen, 1:0.06:0.05 for lungs, 1:10:20 for kidneys and 1:1:1 for liver was observed. Similar trends were seen with ^{211}At-labeled F(ab')$_2$.

With ^{125}I-labeled F(ab')$_2$, low molecular weight compounds (<10 kD) accounted for between 1-5% of the activity from liver, lungs and spleen compared to 40% for kidneys; for ^{211}At, a larger fraction of radioactivity was present as low molecular weight species in spleen (40%) and lungs (15%) and the kidneys. Using reverse-phase HPLC, more than 90% of the ^{125}I activity from urine was eluted with a retention time corresponding to an iodobenzoic acid (IBA)-lysine conjugate standard; of the remainder, 1% eluted as iodide and 2% as IBA. The more extensive dehalogenation of the ^{211}At-labeled F(ab')$_2$ was reflected by the fact that 37% of the activity in the urine was present as astatide. Also, in kidneys, lungs, and spleen astatide accounted for 6, 9, and 16% of total tissue activities, respectively, compared to only about 1% for iodide in these tissues. In addition to iodide, low levels of IBA, IBA-lysine, and IBA-glycine were also detected. In kidneys, IBA was the primary low molecular weight component with varying amounts of IBA-glycine and IBA-lysine. Iodide levels in kidney were <0.5%. Reverse-phase HPLC of kidneys showed approximately equal levels of astatide and ABA, no evidence of glycine or lysine conjugate formation, and the presence of multiple unknown peaks accounting for about half of the low molecular weight activity. These results suggest different distributions of labeled catabolites from F(ab')$_2$ labeled using SIB and SAB and explain the higher retention of ^{211}At compared to^{131}I activity in normal tissues observed in previous studies (3). In conclusion, we believe that analyses of this type may provide valuable input for the design of improved methods for labeling MAbs and their F(ab')$_2$ fragments.

References:

1. Garg, P.K., Archer Jr., G.E., Bigner, D.D., and Zalutsky, M.R., Appl. Radiat. Isot. **40**, 485-490 (1989).

2. Zalutsky, M.R., Garg, P.K., Friedman, H.S., and Bigner, D.D., Proc. Natl. Acad. Sci., USA. **86**, 7149-7153 (1989).

3. Garg, P.K., Harrison, C.L., and Zalutsky, M.R., Cancer Res. **50**, 3514-3520 (1990).

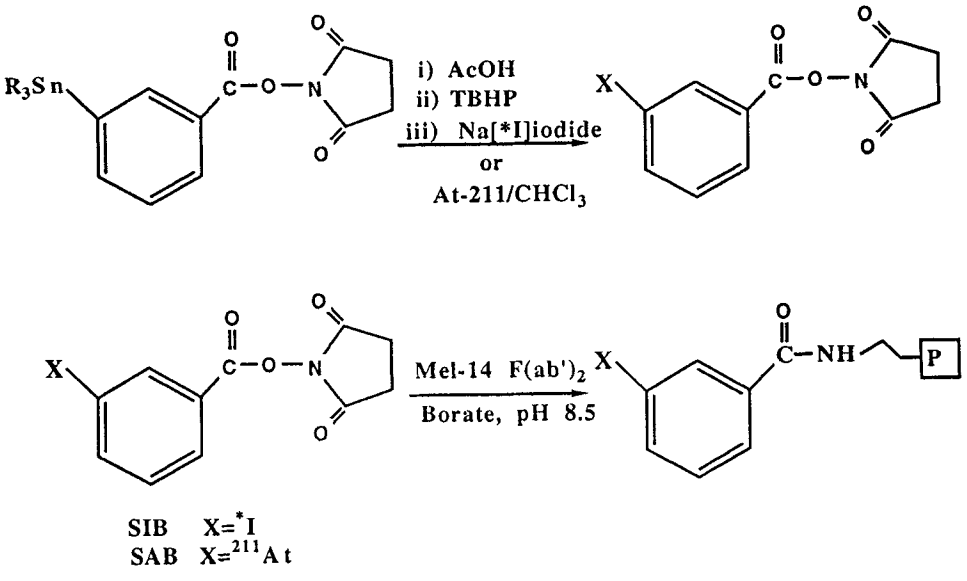

Figure 1. Radiohalogenation of Mel-14 F(ab')$_2$ using SIB or SAB

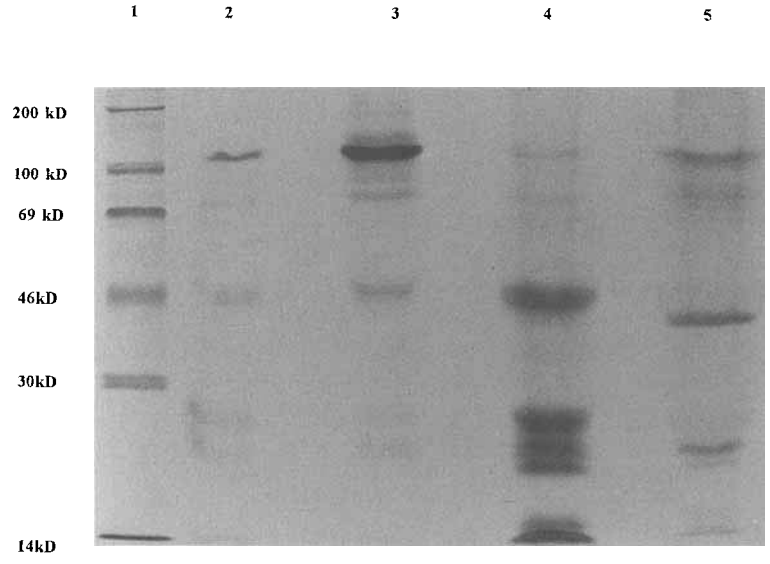

Figure 2. Autoradiograph of SDS-PAGE of ^{125}I-labeled Me1-14 F(ab')$_2$ in tissue extracts; molecular weight standards (lane 1); spleen (lane 2); lung (lane 3); kidney (lane 4); and liver (lane 5).

Comparison of Two Bifunctional Chelates for Labeling ^{64}Cu to Mab 1A3 and 1A3-F(ab')$_2$: Chemistry and Animal Biodistribution

C.J. Anderson[1], B.E. Rogers[1], J.M. Connett[2], L.W. Guo[2], S.W. Schwarz[1], K.R. Zinn[3] and M.J. Welch[1]. [1]Mallinckrodt Institute of Radiology and [2]Department of Surgery, Washington University Medical School, St. Louis, MO and [3]University of Missouri Research Reactor, Columbia, MO.

Copper-64 (β^+, $T_{½}$ = 12.8 h) has shown potential as a radionuclide for PET radiopharmaceuticals.(1) In the labeling of monoclonal antibodies (Mab) and proteins it has been demonstrated that ^{64}Cu must be complexed by a macrocyclic bifunctional chelate conjugated to the Mab or protein for stable binding.(2) The anti-colorectal monoclonal antibody (Mab) 1A3(3) and the 1A3-F(ab')$_2$ fragments have been labeled with ^{64}Cu using the bifunctional chelate 6-bromoacetamidobenzyl-1,4,8,11-tetraazacyclotetradecane-N,N',N'',N'''-tetraacetic acid (Br-benzyl-TETA or BAT) and evaluated by animal biodistribution.(4) Tumor uptake in a hamster model for both ^{64}Cu-labeled intact 1A3 and 1A3-F(ab')$_2$ was superior to both ^{111}In- and ^{125}I-labeled antibodies; however, the kidney uptake of ^{64}Cu-TETA-1A3-F(ab')$_2$ was high. Another macrocyclic bifunctional chelate, 4-[(1,4,8,11-tetraazacyclotetradec-1-yl)-methyl]benzoic acid (CPTA) has been conjugated to an intact Mab and labeled with ^{67}Cu, and has demonstrated stable binding *in vivo*.(5) In the present study ^{64}Cu has been labeled to intact Mab 1A3 and 1A3-F(ab')$_2$ using either BAT or CPTA as the bifunctional chelate (figure 1). The two bifunctional chelates are compared with respect to their conjugation to Mab 1A3 and 1A3-F(ab')$_2$ and labeling with ^{64}Cu. The biodistribution of all ^{64}Cu-labeled conjugates are compared in two animal models.

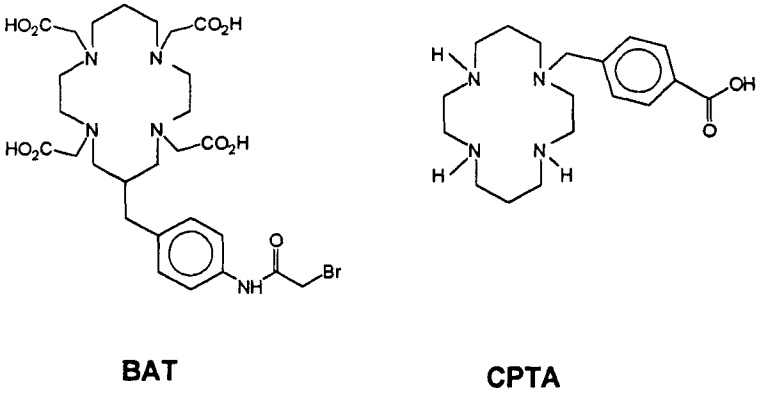

BAT **CPTA**

FIGURE 1

The bifunctional chelate BAT was synthesized as previously described[6,7] and conjugated to Mab 1A3 and 1A3-F(ab')$_2$ using the linker 2-iminothiolane.[4] The benzyl-TETA-1A3-F(ab')$_2$ fragments were purified by FPLC to remove a 40,000 Da impurity present after conjugation prior to labeling with ^{64}Cu.[8] The bifunctional chelate CPTA was synthesized by the one-step procedure of Studer and Kaden.[9] The conjugation of CPTA to Mab 1A3 or 1A3-F(ab')$_2$ was carried out in a method similar to that described by Smith-Jones and co-workers[5] using the coupling agents N-Hydroxysulfosuccinimide (sulfo-NHS) and 1-Ethyl-3-(3-Dimethylaminopropyl)carbodiimide Hydrochloride (EDC). FPLC purification of the CPTA-1A3-F(ab')$_2$ conjugate was not necessary, and the labeling with ^{64}Cu was accomplished in ammonium acetate buffer, pH 5.5. The immunoreactivities (IR) of both ^{64}Cu-labeled intact 1A3 conjugates were > 90%, whereas the IRs of both ^{64}Cu-labeled 1A3-F(ab')$_2$ conjugates were 80-82%.

Biodistribution studies on ^{64}Cu-labeled intact Mab 1A3 and 1A3-F(ab')$_2$ conjugated to either CPTA and BAT were performed in Golden Syrian hamsters bearing GW39 human colon cancer tumors and Sprague-Dawley rats. The biodistribution data of ^{64}Cu-CPTA-1A3 and ^{64}Cu-benzyl-TETA-1A3 in both the hamster and rat animal models were comparable (data not shown). The biodistribution data of the ^{64}Cu-labeled fragments with both conjugates at 24 hours post-injection are presented in Tables 1 and 2. In the hamster model, the tumor uptake is similar for both ^{64}Cu-labeled conjugates. In both the hamster and rat animal models the kidney uptake of ^{64}Cu-CPTA-1A3-F(ab')$_2$ is approximately 2.5 times greater than that of ^{64}Cu-benzyl-TETA-1A3-F(ab')$_2$. Other notable differences in the biodistribution include a more rapid blood clearance and higher liver uptake for ^{64}Cu-CPTA-1A3-F(ab')$_2$.

Table 1

Biodistribution in Golden Syrian Hamsters
24 hours post-injection

%ID/g

Organ	^{64}Cu-CPTA-1A3-F(ab')$_2$	^{64}Cu-TETA-1A3-F(ab')$_2$
Blood	0.92 ± 0.20	1.60 ± 0.26
Liver	2.71 ± 0.47	2.10 ± 0.56
Tumor	9.0 ± 1.14	10.1 ± 3.46
Kidney	23.6 ± 2.41	7.62 ± 2.03
Muscle	0.27 ± 0.04	0.22 ± 0.05

Table 2

Biodistribution in Sprague-Dawley Rats
24 hours post-injection

%ID/g

Organ	^{64}Cu-CPTA-1A3-F(ab')$_2$	^{64}Cu-TETA-1A3-F(ab')$_2$
Blood	0.21 ± 0.01	0.49 ± 0.21
Liver	2.30 ± 0.40	1.05 ± 0.40
Kidney	27.6 ± 2.25	11.6 ± 4.4
Muscle	0.11± 0.04	0.14 ± 0.06

In summary, ^{64}Cu has been labeled to Mab 1A3 and 1A3-F(ab')$_2$ using the macrocyclic bifunctional chelates BAT and CPTA. There was no significant difference in the animal biodistribution of the ^{64}Cu-labeled intact Mab; however, the accumulation of ^{64}Cu-CPTA-1A3-F(ab')$_2$ in the kidneys was 2.5 times greater than that of ^{64}Cu-TETA-1A3-F(ab')$_2$. Although the conjugation of CPTA to 1A3-F(ab')$_2$ is preferable to that of BAT to 1A3-F(ab')$_2$, the high kidney uptake precludes the application of ^{64}Cu-CPTA-1A3-F(ab')$_2$ for human use.

Acknowledgements: This work was supported by NIH grant 2 RO1 CA44728 and DOE grant DE-FG02-84ER60218.

REFERENCES

1. Philpott G.W., Schwarz S.W., Anderson C.J., et al. - J. Nucl. Med. 34:81P (1993) (abstract).
2. Cole W.C., DeNardo S.J., Meares C.F., et al. - Nucl. Med. Biol. 13:363 (1986).
3. Connett J.M., Fenwick J.J., Timmcke A.E. and Philpott G.W. - Proc. Am. Assoc. Cancer Res. 28:352 (1987) (abstract).
4. Anderson C.J., Connett J.M., Schwarz S.W., et al. - J. Nucl. Med. 33:1685 (1992).
5. Smith-Jones P.M., Fridrich R., Kaden T.A. et al. - Bioconj. Chem. 2:415 (1991).
6. Moi M.K., Meares C.F., McCall M.J., Cole W.C. and DeNardo S.J. - Anal. Biochem. 148:249 (1985).
7. McCall M.J., Diril H. and Meares C.F. - Bioconj. Chem. 1:222 (1990).
8. Anderson C.J., Schwarz S.W., Connett J.M. et al. - J. Nucl. Med. 34:28P (1993) (abstract).
9. Studer M. and Kaden T.A. - Helv. Chim. Acta 69:2081 (1986).

Optimization of the $^{64/67}$Cu labelling of Cyclam Derivatives and the In Vivo Evaluation of both ^{67}Cu and ^{125}I Labelled B12 Anti MCA Monoclonal Antibody. P.M.SMITH-JONES*, H.AKOPRIOVOVA, T.KADEN£ and H.MÄCKE. Institute of Nuclear Medicine, Kantonsspital Basel, Basel, Switzerland. £:Institut für Anorganische Chemie der Universität Basel, Basel, Switzerland. *:Present address Sandoz Pharma, PKF, 4002 Basel, Switzerland.

The high kinetic stability of the Cu^{2+} complex formed with the chelator 4-[(1,4,8,11-tetraazacyclotetradec-1-yl)methyl]benzoic acid (CPTA) has been demonstrated in vitro and in vivo conjugated to the AB35 MoAb (1,2). In this study we have examined the kinetics of formation of various cyclam derivatives (cf figure 1). The labelling procedure of CPTA/Mab conjugates has been optimized and a further in vivo comparison between ^{67}Cu and ^{125}I labelled Mab is presented with the B12 anti MCA Mab.

For the unconjugated ligands all the N alkylated ligands (CPTA, Cyc1 and Cyc2) demonstrated a faster overall Cu^{2+} complexing rate, in a non complexing buffer system (pH 3-6), than both cyclam and the C alkylated derivative Cyc3. This faster incorporation of Cu^{2+} into the macrocyclic ligand was found to be due to the differences in the protonation constants, which in turn produced more of the reactive LH species in the pH range studied.

A succinate buffering system (3) was confirmed to further enhanced the complexation rate with Cu^{2+}, for both the unconjugated ligands and the CPTA/B12 conjugate, rather than the more conventional acetate. The effect of elevated Zn^{2+} levels (^{67}Cu is normally produced from a Zn target) was also examined and a 50 fold excess of Zn^{2+} was found only to have a slightly detrimental effect.

Both the pre and post labelling approaches were applied with ^{67}Cu but the prelabelling approach was abandoned because of inconsistent results. The final labelling method used a 1:1 reaction ratio of Cu^{2+} to available CPTA sites (1.8 µM, CPTA/B12) in 0.1 M sodium succinate (pH 6.0) produced over 80 % incorporation within 20 minutes. A similar procedure using a three fold excess of Cu^{2+} saturated all available CPTA binding sites within 5 minutes. Animal studies compared the biodistribution of ^{67}Cu and ^{125}I labelled B12 in ZR75 tumour bearing nude mice following the coinjection of 10µg ^{125}I/B12 and 10 µg ^{67}Cu/CPTA/B12 in the tail vein. The respective immunoreactivities of the two radiolabelled antibodies were 70 % and 60 %. The animal studies showed a similar biodistribution of ^{67}Cu and ^{125}I one day p.i., but all later time points (up to six days) showed an increasing ^{67}Cu/^{125}I ratio at the tumour. The maximum tumour uptake was demonstrated on the fourth day p.i. where a tumour accumulation of 27.5 ± 3.4 %ID/g for ^{67}Cu and 4.8 ± 0.4 %ID/g for ^{125}I was achieved.

This study was supported by the Swiss national Science foundation (Grant No 31-32586.91).

References

1) Smith-Jones P., Fridrich R., Kaden T., Novak-Hofer I., Siebold K., Tschudin D. and Mäcke H.. Bioconjugate Chem., **2**, 415-421 (1991)

2) Studer M., Kaden T.. and Mäcke H.. Helv.Chim.Acta., **73**, 149-153 (1990)

3) Wu Y. and Kaden T.. Helv.Chim.Acta.,**68** , 1611-1616 (1985).

Figure 1 Cyclam derivatives

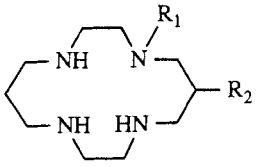

Cyclam	R_1= H	R_2= H
CPTA	R_1= $CH_2(C_6H_4)COOH$	R_2= H
Cyc1	R_1= $CH_2(C_6H_4)CONHCH_2(CH_3)_2$	R_2= H
Cyc2	R_1= $CH_2(C_6H_4)NO_2$	R_2= H
Cyc3	R_1= H	R_2= $CH_2(C_6H_4)NO_2$

^{90}Y-Labeled 17-1A Monoclonal Antibody Prepared Using The New Bifunctional Chelating Agent DOTA-NHS

ZHOU, Y.G.; KHAZAELI, M.B.; and BUCHSBAUM, D.J.
Departments of Radiation Oncology and Medicine, The University of Alabama at Birmingham, Birmingham, AL 35233

Radiolabeled monoclonal antibodies have shown great potential in diagnostic imaging and radioimmunotherapy of cancer. Antibodies labeled with ^{131}I have been used widely for these purposes. However, ^{131}I is not an ideal radionuclide for most imaging or therapeutic applications because of its dehalogenation *in vivo* following catabolism resulting in uptake of free radioiodine into stomach and thyroid, unfavorable gamma emissions, an 8-day physical half-life and marrow toxicity.

^{90}Y is one of the optimal radionuclides for use in radioimmunotherapy. Its 64.2 h half-life is long enough for tumor localization. It is a pure beta emitter with a shorter path length than gamma emitters, decreasing toxicity to other organs. It has an intermediate energy (2.27 MeV maximum energy) with a range of 1 to 1,000 cell diameters. It has a stable daughter product and good chelation properties.

The chelating agents cyclic DTPA anhydride and 1-(p-aminobenzyl)DTPA have been used for the preparation of ^{90}Y-labeled MoAbs (1,2). But, the ^{90}Y has been lost *in vivo* from those complexes since they are unstable under physiologic conditions, and significant amounts of ^{90}Y were incorporated into bone.

DOTA(1,4,7,10- tetrazacylodocane-N,N',N'',N'''- tetraacetic acid) and its analogue p-nitrobenzyl-DOTA hold ^{90}Y stably under physiological conditions in human serum. Radiopharmaceuticals prepared using this DOTA analogue have received growing attention. But, the p-nitrobenzyl-DOTA synthesis is a long procedure. The overall yield of the 9-step synthesis sequence starting from nitrophenylalanine is 5.6% (3).

As an alternative to the DOTA analogue, we have now synthesized a N-hydroxysuccinimide ester of DOTA (DOTA-NHS). The DOTA-NHS ester was conjugated to monoclonal antibody 17-1A which has specificity for colorectal and pancreatic carcinomas, and the conjugate was then labeled with ^{90}Y.

DOTA was prepared by condensation of the cyclen in water with bromoacetic acid (4) which had previously been neutralized with NaOH. The mixture was heated, and the temperature was kept to 70-

75^{0}C and 6 N NaOH solution was added dropwise. The pH was monitored continuously. For most of the reaction time, the pH was maintained between 9 and 10. After 5 h reaction, the mixture was cooled and was acidified to pH 2.5, then purified by ion-exchange chromatography(AG 50W-x 8 hydrogen form and AG 1-x 8 formate form).

DOTA was reacted with N-hydroxysuccinimide and N, N'-dicyclohexylcarbodiimide in DMSO solvent and the reaction mixture was stirred at room temperature for 24 h, then filtered. The filtrate containing the activated ester DOTA-NHS/DMSO was stored at 4^{0}C in a moisture-free environment.

For 17-1A MoAb conjugation, an aliquot of the desired volume of DOTA-NHS/DMSO and 17-1A MoAb were added in 0.1 M $NaHCO_3$, pH 8.1. The 17-1A MoAb concentration was 10 mg/ml. A volume 0.05 ml containing 0.5 mg antibody was used. The 17-1A-DOTA conjugate was purified from free DOTA by passage through a column of Sephadex G-50 fine.

For labeling, 0.1 mCi of $^{90}YCl_3$ in 0.1 M ammonium acetate buffer (pH 5.5) was added to 17-1A-DOTA-NHS (pH 6.0) at room temperature. for 6 h. Identification and separation of labeled antibody was done by HPLC. The labeling efficiency depended on the DOTA-NHS/17-1A molar ratio. The labeling efficiency was 15%, 25% and 40% when the DOTA-NHS/17-1A molar ratio was 20/1, 60/1, and 100/1, respectively.

In summary, ^{90}Y-labeled 17-1A monoclonal antibody has been prepared using the new bifunctional chelating agent DOTA-NHS. In the future, we will study the immunoreactivity of such radioimmunoconjugates and their biodistribution and therapeutic effects in animal tumor xenograft systems.

References:

1. Hnatowich, D.J.; Vrizi, F. and Doherty, P.W. J. Nucl. Med. 26, 503-509 (1985)
2. Srivastava, S.C. and Mease, R.C. Nucl. Med. Biol. 18, 589-603 (1991)
3. Renn, O. and Meares, C.F. Bioconjugate Chem. 3, 563-569 (1992)
4. Gansow, O.A. and Kumar, K. U.S. Patent No. 4, 923, 985 (1990)

The biokinetics of ^{169}Yb- and ^{153}Sm-labelled somatostatin analogues in comparison with ^{111}In-octreotide - Preliminary results

SCHOMÄCKER, K.; SCHEIDHAUER, K.; SCHARL*, A.; SCHICHA, H.; HAUSCH, A.; SCHULZ, M.; SCHULTE, S.; SHUKLA**, S.K. Clinic of Nuclear Medicine and *Clinic of Obstetrics and Gynaecology, Cologne Medical School, **Nuclear Research Council of Italy, Hospital St. Eugenio (Department of Nuclear Medicine)

The somatostatin analogue pentatreotide which attaches ^{111}In between four carboxyl groups of a DTPA-moiety has been used for a receptor mapping and demonstration of different tumours. The aim of this study is to use the pentatreotide as vehicle for the in vivo transportation of the lanthanides ^{153}Sm and ^{169}Yb.

For the labelling of pentatreotide we used the radionuclides in chloride form. We carried out two quality control methods both HPLC (Equipment:Knauer - Dual Gradient System, Column: WATERS-Bondapak, C-18, 125 Å, 10 mm, Flux:1ml/min, Eluent 1: Methanol, Eluent 2: 0,005 M Acetate-buffer, pH: 5, Gradient: within 20 min from 60 % Methanol to 40 % Methanol) and the "cartridge method" which is recommended by the producer for the quality control of ^{111}In-pentatreotide. The results of the quality control (Table 1) showed that it was difficult to label the commercially available somatostatin kit (Octreoscan) with ^{169}Yb or ^{153}Sm. We attribute this matter to the metal concentration which is adjusted due to the limited specific activity of the metal chlorides which were used for labelling. Only after the increasing of the concentration of citrate ions in the labelling medium a reasonable radiochemical purity became possible, but if the citrate concentration became too high the radiochemical purity decreased again. As a consequence of these experiments the chemical compositions of the final solutions were as shown in Table 2. 100 µl of these solutions were injected via the tail vein into tumour bearing mice with a tumour transplanted in the hind limb. The animals were killed 24 h p.i. and the biodistributions after the application of the three different labelled pentatreotides were compared.

Some of the results are shown in Figure 1-4. The results can be summarized as follows:

We found clear differences between the biodistribution of the ^{111}In-pentatreotide and the lanthanide- (^{153}Sm, ^{169}Yb) pentatreotide in tumour bearing mice. The lanthanide-pentatreotides showed higher tumour uptake, stronger bone accumulation, slower blood clearance and elimination via kidneys and higher uptake in liver and spleen than the ^{111}In-pentatreotide. This biological behaviour is caused both by a lower stability of the lanthanide-pentatreotide-complex and a lower specific radioactivity connected with a higher probability of intravasal colloid formation in comparison with the indium compound.

For using somatostatin as carrier for therapeutically relevant radionuclides (^{153}Sm, ^{90}Y) the binding between the radioactive metal and the somatostatin dervative must be stabilized by replacing the commonly used DTPA by other "bridge molecules".

Table 1. Results of quality control

Radioactive Products	Radiochemical purity, measured by	
	HPLC	Cartridge
^{111}In-Pentatreotide	98,5 % (N=20)	96,9 % (N=20)
^{153}Sm-Pentatreotide		
Na_3Cit/H_3Cit: 4,91/0,37 mg	21,3 % (N=20)	24,3 % (N=20)
Na_3Cit/H_3Cit: 50/4 mg	96,5 % (N=20)	98,6 % (N=20)
Na_3Cit/H_3Cit: 150/12 mg	78,6 % (N=20)	75,4 % (N=20)
^{169}Yb-Pentatreotide:		
Na_3Cit/H_3Cit: 4,91/0,37 mg	1,4 % (N=20)	1,0 % N=20)
Na_3Cit/H_3Cit: 50/4 mg	95,9 % (N=20)	97,1 % (N=20)
Na_3Cit/H_3Cit: 150/12 mg	33,8 % (N=20)	35,9 % (N=20)

Table 2. Composition of 1 ml final solution

	^{111}In-Pentatreotide	^{153}Sm-Pentatreotide	^{169}Yb-Pentatreotide
Pentatreotide:	10,00 µg		
Trisodium citrate:	4,91 mg	50,00 mg	50,00 mg
Citric acid	0,37 mg	4,00 mg	4,00 mg
Inositol:	10,00 mg		
Gentisic acid:	2,00 mg		
HCl, 0.02 M	q. s. ad 1,00 ml		

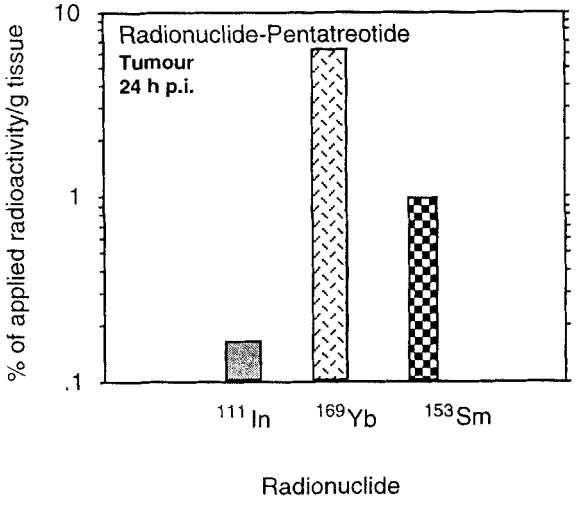

Fig. 1. Radioactivity-concentration in tumour 24 h after application of different labelled pentatreotides

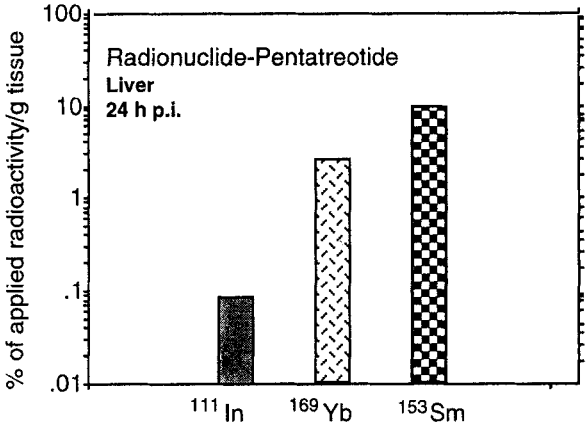

Fig. 2. Radioactivity-concentration in the liver 24 h after application of different labelled pentatreotides

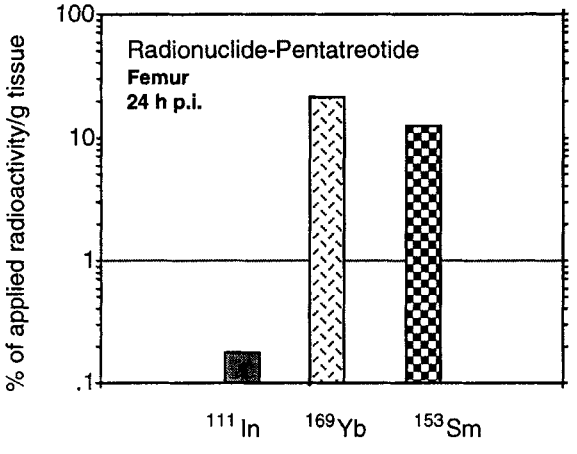

Fig. 3. Radioactivity-concentration in the liver 24 h after application of different labelled pentatreotides

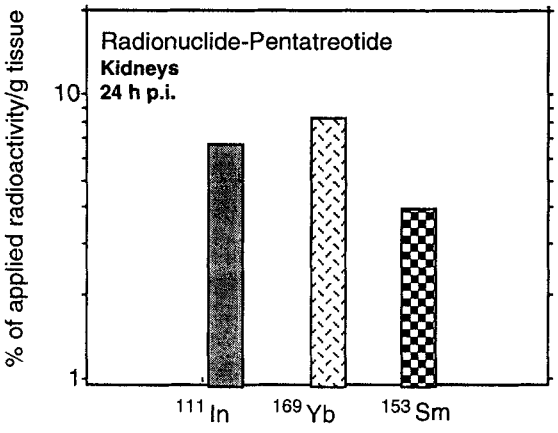

Fig. 4. Radioactivity-concentration in the lkidneys 24 h after application of different labelled pentatreotides

An Automated Synthesis of 2-[^{11}C]Thymidine Utilising [^{11}C]Phosgene.

STEEL, C.J.; LUTHRA, S.K.; BROWN, G.D.; SERGIS, A.N.; TOCHON-DANGUY[1], H.; TILSLEY, D.W.O.; OSMAN, S.; WATERS, S.L.; JONES, T.; PRICE, P.; LABAR[2], D. and BRADY*, F. MRC Cyclotron Unit*, Hammersmith Hospital, Ducane Road, London W12 OHS, U.K., [1]Centre for Positron Tomography, Austin Hospital, Heildelberg Victoria 3084, Australia, [2]Faculte de Medecine, Universite Catholique de Louvain, Louvain-La-Neuve, Belgium.

2-[^{11}C]Thymidine has been proposed as an agent for measuring tumour proliferation rate *in vivo* by PET[1,2]. 2-[^{11}C]Thymidine can be synthesised from 2-[^{11}C]thymine by adding the deoxyribose moiety enzymatically using thymidine phosphorylase.

We have previously described the synthesis of the intermediate [^{11}C]thymine from anhydrous [^{11}C]urea[3]. The latter was prepared from the reaction of [^{11}C]phosgene with liquid ammonia. We have now extended this work to the synthesis of 2-[^{11}C]thymidine and have developed a microprocessor controlled automated synthesis system suitable for routine production of 2-[^{11}C]thymidine (Figure 1).

[^{11}C]Methane is converted to [^{11}C]phosgene[4,5]. [^{11}C]Phosgene is then reacted with liquid ammonia to give [^{11}C]urea[3]. A mixture of diethyl-β-methylmalate (DEMM) (10 μL) and ethanol (10 μL) were then transferred from a teflon loop into vessel 1 containing anhydrous [^{11}C]urea (Figure 1). Fuming sulphuric acid (100 μL) was then added to the reaction mixture in vessel 1 from a second teflon loop. The mixture is heated at 130 ^{0}C for 5 min. After cooling, water (0.5 mL) was added to the mixture and the solution neutralised on a resin column (AG 11 A8). 2-[^{11}C]Thymine is typically produced in 70% radiochemical yield in 15 mins from [^{11}C]urea. The neutral solution of 2-[^{11}C]thymine is then transferred into vessel 2 containing thymidine phosphorylase and 2'-deoxyribose phosphate (3 mg) in water (100 μL). After mixing for 3 min at room temperature, the reaction mixture (2 mL) is then injected onto the HPLC column ("μ"Bondapak C_{18}, 10 x 250 mm i.d.). The column is eluted with a mixture of ethanol and water [6:94] at a flowrate of 3.0 mL min^{-1}. 2-[^{11}C]Thymidine elutes at 10 min and 2-[^{11}C]thymine at 7 min. The radiochemical yield of 2-[^{11}C]thymidine is typically 55% from [^{11}C]urea in 20 min. Specific activity is 29.6 - 51.8 GBq μmol^{-1} (0.8 - 1.4 Ci μmol^{-1}) at EOS.

The complete synthesis is carried out using in a fully automated microprocessor controlled system (Figure 1). The automated system produces up to 2.4 GBq (65 mCi) 2-[^{11}C]thymidine suitable for human injection in 45 mins from EOB. The decay corrected radiochemical yield of 2-[^{11}C]thymidine is 13-14% from [^{11}C]methane.

Work is in progress to further simplify and improve the conversion of 2-[^{11}C]thymine to 2-[^{11}C]thymidine. To achieve this we have immobilised the enzyme thymidine phosphorylase on a triazine activated agarose. Triazine Activated Agarose 4XL gel was washed with sodium acetate (50 mM, pH 5.0). The gel was mixed with a solution of thymidine phosphorylase in sodium acetate (50 mM) for 2 h at 4 ^{0}C. After washing in water, remaining active sites on the gel were blocked by reaction with 2-ethanolamine.

Solutions of 2-[^{11}C]thymine or thymine containing 2'-deoxyribose phosphate were passed through a column of the immobilised enzyme. Conversion of thymine to thymidine is essentially quantitative. The conversion of 2-[^{11}C]thymine to 2-[^{11}C]thymidine has also been achieved using this approach and the conditions are being optimised .

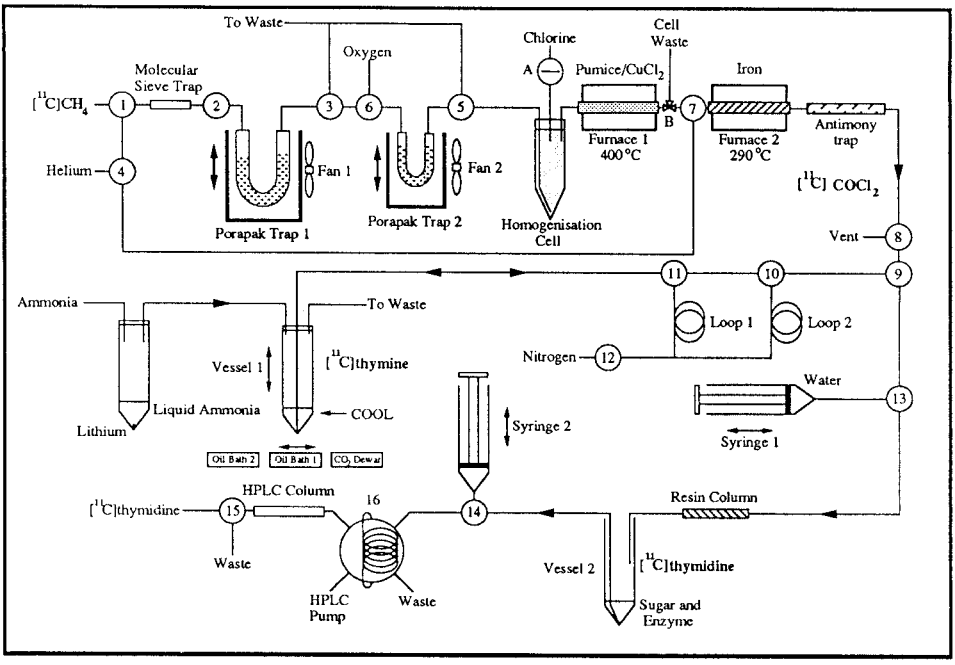

Figure 1. Schematic diagram of the automated synthesis of 2-[^{11}C]thymidine. The shielded synthesis system is operated using an external Toshiba EX-40+ programmable logic controller (PLC). In a typical procedure, [^{11}C]methane from the cyclotron is condensed in Porapak trap 1 over 3 mins. The volume is then reduced by transferring [^{11}C]methane in a flow of helium through valves 4, 1, 2, 3 and 6 into Porapak trap 2 over 2.5 mins. Porapak trap 2 is then taken up to room temperature (1.5 mins). [^{11}C]Methane is then carried from Porapak 2 in a flow of oxygen through valve 5 into the homogenisation vessel which has been pre-filled with chlorine. The reactants are then passed through furnace 1 containing a mixture of pumice and copper chloride at 400 ^{0}C producing [^{11}C]carbon tetrachloride. The latter is then oxidised to [^{11}C]phosgene by passing it in a stream of oxygen through furnace 2 containing iron filings at 290 ^{0}C. [^{11}C]Phosgene is passed through valves 8, 9, 10 and 11 into anhydrous liquid ammonia, distilled from lithium, to form [^{11}C]urea (5 mins). Excess liquid ammonia is removed by gently warming the vial in oil bath 1 at 85 ^{0}C for 5 mins. The precursor DEMM and ethanol in loop 1 are then transferred using a stream of nitrogen via valves 11 and 12 into vessel 1 containing [^{11}C]urea. Fuming sulphuric acid in loop 2 is added in a stream of nitrogen to vessel 1 via valves 10 and 12. [^{11}C]Thymine is formed by heating this mixture in oil bath 2 at 130 ^{0}C for 5 mins. Reaction vessel 1 is then cooled and water is added via valves 13, 9, 10 and 11. The reaction mixture is the withdrawn into syringe 1 and passed through valve 13 onto the neutralisation resin over 4 mins. From the neutralisation column it is passed into vessel 2 containing thymidine phosphorylase and 2'-deoxyribose phosphate. The reaction mixture containing 2-[^{11}C]thymidine is taken up through valve 14 into syringe 2 and then injected onto the HPLC column via valve 16. Valve 15 is used to collect the fraction containing 2-[^{11}C]thymidine.

The Porapak traps are raised and lowered pneumatically. Valves 1-15 are of the following type; 1-4, 6 and 12 (stainless steel, solenoid, Skinner), 5, 7, 14 and 15 (PTFE, solenoid, ASCO), 8-13 (pneumatic, Rheodyne) and 16 (6 port stainless rotary, pneumatic, Rheodyne). Valves A and B are 3 port polycarbonate valves (Vygon).

References
1. Vander Borght T., Labar D., Pauwels S., Lambotte L. - Appl. Radiat. Isotopes. 42: 103(1991).
2. Vander Borght T., Pauwels S., Lambotte L., De Saeger C., Bekers C. - J. Label. Comp. Radiopharm. 28: 819(1990).
3. Steel C.J., Brown G.D., Dowsett K., Turton D.R., Luthra S.K., Tochon-Danguy H., Waters S.L., Price P. and Brady F. - J. Label. Comp. Radiophar. 32: 178(1993).
4. Landais P., and Crouzel C. - Appl. Radiat. Isot. - 38: 297(1987).
5. Brady F., Luthra S.K., Tochon-Danguy H., Steel C. J. - Appl. Radiat Isot. 42: 621(1991).

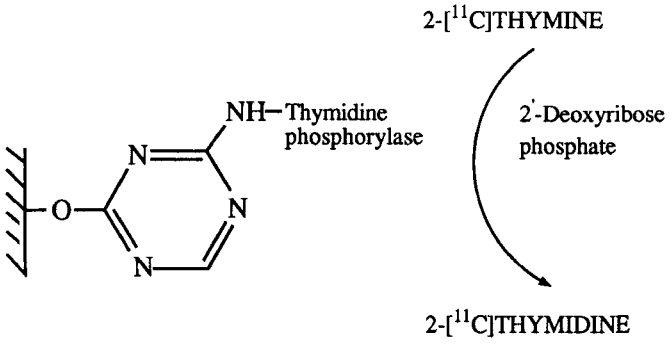

Figure 2. Conversion of 2-[^{11}C]thymine to 2-[^{11}C]thymidine by immobilised thymidine phosphorylase.

Rapid One-Pot Method for Synthesizing Substituted [^{11}C]Amides.

ROGERS, G.A.; STONE-ELANDER, S.; and INGVAR, M. Neuroscience Research Institute, University of California, Santa Barbara, CA 93106 and Departments of Pharmacy and Clinical Neurophysiology, Karolinska Hospital, Stockholm.

For PET screening of the biodistribution of a series of compounds, we found it useful to develop a general, rapid method for radiolabeling substituted benzamides. The reaction of [^{11}C]CO_2 with Grignard reagents formed from bromobenzenes allowed the desired flexibility in the aromatic structure and the potential to couple the suitably-activated [^{11}C]benzoates to a variety of amines. As previously observed in radiotracer synthesis, high incorporations of [^{11}C]CO_2 were obtained using aromatic Grignard reagent in THF. Because of time constraints, it was desirable to quench excess Grignard reagent and activate the trace amount of labelled benzoate without isolation or purification. Benzoates can be activated most conveniently with carbonyl diimidazole (CDI), as CO_2 and imidazole (Im) are the only biproducts. Coupling of the resulting benzoyl imidazolide with an amine can be carried out in the same reaction vessel with yields typically >95%.

In initial attempts to couple the [^{11}C]benzoate with piperidine, the excess Grignard reagent was quenched with ImHCl in DMF, which led to the reduced aromatic ring (i.e. with net ArBr to ArH). Subsequent activation with CDI and coupling with piperidine proceeded in 97% overall conversion (based on the [^{11}C]acid; by radioanalytical HPLC) with a synthesis time of 22 min from E.O.B. However, UV analysis of the chemical components in the reaction mixture revealed that the byproduct from the Grignard reagent eluted immediately prior to the amide from a reversed-phase C18 column. As a result, the product amide was severely contaminated. The observation that the bromaromatic starting material for the Grignard reagent eluted significantly later than the corresponding product amide provided the solution to the separation problem above. It was successfully regenerated by quenching the Grignard reagent with a freshly prepared solution of Br_2/THF immediately prior to addition of ImHCl. This procedure provided the desired [^{11}C]amide in high radiochemical conversions (>90% based on [^{11}C]CO_2) in reaction times as short as 22 min from E.O.B.

Purification was rapidly performed by diluting the reaction mixture with water and eluting the solution through a C-18 SepPak to remove hydrophilic components of the reaction mixture. The product [^{11}C]amide could be eluted free from the bromoaromatic byproduct by acetonitile/water. Alternatively, isolation could be easily performed using reversed-phase HPLC.

In summary, a rapid procedure for synthesizing substituted benzamides labeled with ^{11}C in the amide group has been demonstrated. This four-step, one-pot method has been used to synthesize the first of a series of new compounds for PET with a total synthesis time on the order of 20-25 min and high isolated yields (>80% based on [^{11}C]CO_2).

REACTION SCHEME [1]

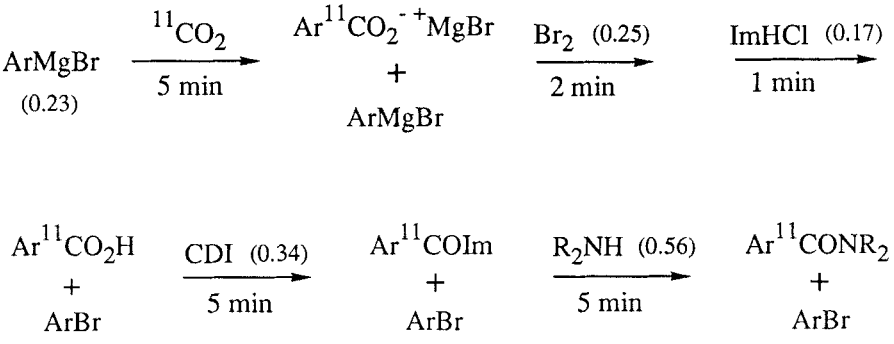

[1] Numbers in parentheses refer to quantities of reagents in mmol

Preparation of [*N-methyl*-^{11}C]Propionyl-L-carnitine for Human Biodistribution Studies

RAYMOND J. DAVENPORT[1], VICTOR W. PIKE[1], DAVID R. TURTON[1] and SANDRA MUCK[2]
[1]MRC Cyclotron Unit, Hammersmith Hospital, Ducane Road, London W12 0HS, U.K.
[2]Sigma Tau, Industrie Farmaceutiche Riunite S.p.A., Via Pontina km 30,400 - 00040 Pomezia, Rome, Italy.

L-Carnitine (I) is essential for fatty acid metabolism, the main source of energy for the heart, and acts as a carrier for the transport of free fatty acids into mitochondria, preceding their metabolism through β-oxidation and Krebs cycle. Normally, L-carnitine is produced in the liver and kidney and distributed via the plasma to tissues. L-Carnitine may enter cells to form acyl carnitines which reversibly cross cell membranes. Hence, plasma contains significant endogenous levels of many acyl carnitines. Propionyl-L-carnitine (PLC) (II) is under investigation as a therapeutic for peripheral artery disease, coronary artery disease and chronic heart failure.[1] The beneficial affects of PLC in these conditions are assumed to result from the delivery of essential L-carnitine to tissues and of propionate to mitochondria, the latter producing an anaplerotic (energy-producing) effect.

Despite the extensive literature on carnitine and acyl carnitines there are no studies addressing the absolute quantitation of uptake by myocardial and skeletal muscle in man as a function of plasma concentration. In addition since acyl carnitine retention in tissue is a function of both its tissue uptake and release, only tracer studies employing radiolabelled acyl carnitine can provide accurate information on turnover in man. L-Carnitine has previously been labelled with carbon-11 ($t_{1/2}$ = 20.4 min; β^+ = 99.8 %),[2] but we are unaware of any biological studies with this tracer. We set out to label PLC isotopically with carbon-11, initially in the *N*-methyl position, for studies of the distribution, retention and turnover of this potential therapeutic in man using positron emission tomography (PET).

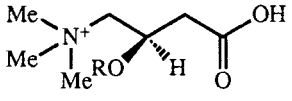

I, R = H
II, R = EtCO

We considered that [*N-methyl*-^{11}C]PLC could be prepared by direct methylation of *nor*PLC with [^{11}C]iodomethane, produced conventionally from cyclotron-produced [^{11}C]carbon dioxide (Figure 1).[3,4] Various conditions were examined for this reaction, based on the use of ethanol as solvent and the generation of *nor*PLC free base from the hydrochloride *in situ* by the action of an excess of a hindered base, such as 2,6-di-*t*-butyl-pyridine or 1,2,2,6,6-pentamethyl piperidine. Conditions for product analysis were found on TLC (silica-C18: EtOH-Et_2O-H_2O-HCl; 50:40:10:0.01 by vol.) with detection by ninhydrin and autoradiography, and on HPLC using a silica-NH_2 column (30 x 4.6 mm; Phenomenex Ltd) eluted at 1 mL/min with acetonitrile-THF-*aq*. KH_2PO_4 (0.05M)/1-butanesulphonic acid (0.015M) (70:5:25 by vol.), with detectors for absorbance at 205 nm and radioactivity. Analysis revealed selective ^{11}C-methylation at the nitrogen of *nor*PLC under a variety of reaction conditions. Optimal labelling (*ca* 50% radiochemical yield) was achieved by heating a solution of no-carrier-added [^{11}C]iodomethane, *nor*PLC (10 mg) and 1,2,2,6,6-pentamethyl piperidine (10 mg) in ethanol (200 μL) in a sealed vial at 120 °C (bath temperature) for 10 min.

The development of a satisfactory preparative separation of [*N-methyl*-^{11}C]PLC from *nor*PLC and byproducts presented some difficulty. HPLC on "semi-preparative" silica gel, reverse phase silica C-18 and silica-NH_2 columns, gave poor separations or were inconvenient with respect to eluent, time of elution or volume of elution. Excellent separations were found on strong cation exchange columns (*e.g.* Partisil™ 10 SCX; 250 x 4.6, 7 or 9 mm) eluted with ammonium phosphate solutions

($NH_4H_2PO_4$; 0.05–0.2M). Separation on the 7 mm diameter column delivered pure [*N-methyl*-^{11}C]PLC in a volume conveniently small (*ca* 10 mL) for intravenous injection (Figure 2). The radiosynthesis may be performed in remotely controlled apparatus within 40 min from the end of radionuclide production.

This tracer will enable the fate of the L-carnitine moiety in PLC to be followed kinetically in man, assuming that demethylation *in vivo* is not greatly significant over the time course of the proposed PET studies. It is also considered that labelling in the propionate group of PLC by the reaction of [1-^{11}C]propionyl chloride[5] on L-carnitine has potential for investigating the fate of the propionate group and hence the anaplerotic effect, especially in myocardium.

Acknowledgement. The authors are grateful to Dr Antonio Longo (Sigma Tau S.p.A.) and Professor Paulo Camici for their support and encouragement.

References

1. See *Cardiovascular Drugs and Therapy*, 1991, Vol. 5, Supplement 1.
2. M. Holschbach, W. Hamkens, W. Roden and L.E. Feinendegen, *J. Label. Compd. Radiopharm.*, 1990, 29, 599.
3. D.R. Turton, F. Brady, V.W. Pike, A.P. Selwyn, M.J.Shea, R.A. Wilson and C.M. DeLandsheere, *Appl. Radiat. Isot.*, 1984, 35, 337.
4. C. Crouzel, B. Långström, V.W. Pike and H.H. Coenen, *Appl. Radiat. Isot.*, 1987, 38, 601.
5. S.K. Luthra, V.W. Pike and F. Brady, *Appl. Radiat. Isot.*, 1990, 41, 471.

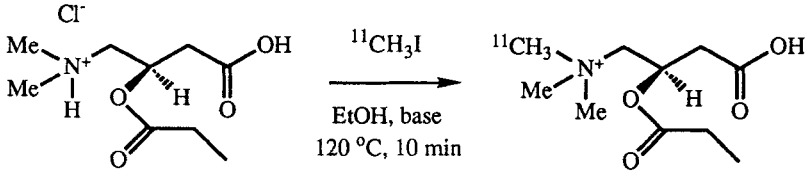

Figure 1. The preparation of [*N-methyl*-^{11}C]propionyl-L-carnitine

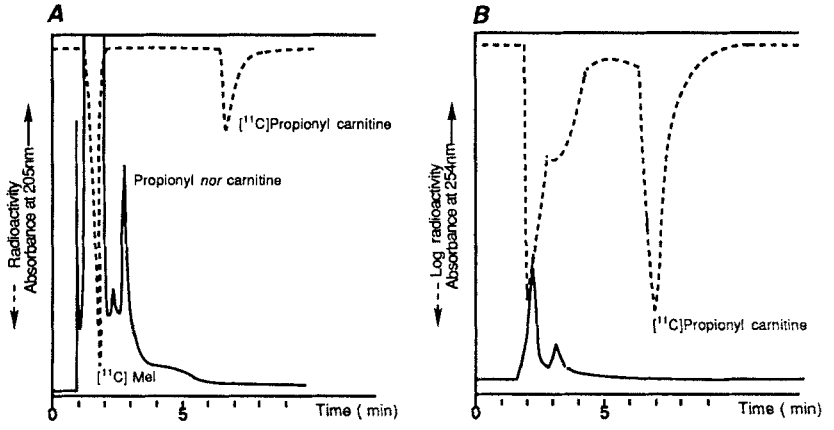

Figure 2. Analysis of crude product from the ^{11}C-methylation of *nor*PLC-HCl on Partisil™ 10 SCX (250 x 4.6 mm i.d.) eluted with 0.05M-$NH_4H_2PO_4$ at 3 mL/min (Panel A). Preparative separation [^{11}C]PLC on a 7 mm diameter column, eluted with 0.1M-$NH_4H_2PO_4$ solution at 4 mL/min (Panel B).

Microprocessor-Controlled Open Vessel System for the Production of No-Carrier-Added 1-[^{11}C]-1-Aminocyclobutane-1-Carboxylic Acid

GOODMAN, M.M.; DEVINNEY, J.L.; KABALKA, G.W.; LADETSKY, M.; HUBNER, K.F.; MEYER, M.A.; and LAMBERT, S.J. Biomedical Imaging Center, University of Tennessee at Knoxville, Knoxville, TN 37920 USA

1-[^{11}C]-1-Aminocyclobutane-1-carboxylic acid (1-[^{11}C]ACBC) is an alicyclic amino acid analog that has a high affinity to a variety of tumors (1). Unlike the carbon-11 labeled naturally occurring amino acid L-[methyl-^{11}C]methionine, 1-[^{11}C]ACBC is selectively taken up by intracranial tumors but not by normal brain tissue. Therefore, 1-[^{11}C]ACBC has the advantage of a much higher tumor-to-normal brain tissue concentration when compared to L-[methyl-^{11}C]methionine (2).

1-Aminocyclobutane-1-carboxylic acid (ACBC) is also a selective ligand and antagonist for the excitatory amino acid receptor subtype N-methyl-D-aspartic acid (NMDA), specifically the strychnine-insensitive [^{3}H]glycine recognition site (3). The NMDA receptor has been implicated in CNS disorders such as epilepsy, stroke, Huntington's disease, Alzheimer's disease and schizophrenia (4). Thus, 1-[^{11}C]ACBC may also be an important research probe and potential imaging agent for measuring the density of binding sites and characterization of the binding site of the NMDA receptor.

Recently we reported the development of an automated high pressure stainless steel amino acid synthesis unit for the production of carrier-added 1-C-11 amino acids employing the Bucherer-Strecker synthesis (5). Because high specific activity radiotracers are required for receptor studies we now report the development of a new microprocessor-controlled, glass open vessel system for the routine, reliable, clinical production of no-carrier-added 1-[^{11}C]ACBC.

The automated synthesis unit is shown in Figure 1. The unit is comprised of 5 major subunits:

1. A 10mL crimp top reaction vial (180mm X 25mm) and block heater
2. One 6-position and one two position, three-way air actuated teflon rotary Rheodyne valves interfaced to a 8085 microprocessor control unit which directs the passage of solutions to and from the reaction vessel
3. Six reagent vials and reservoirs
4. A strong and weak cation exchange column purification and filter sterilization unit
5. Six two-way and one three-way Angar electric actuated pinch valves interfaced to the 8085 microprocessor control unit to regulate the application of the reaction mixture onto, and flow of the column eluents through, the purification and filter sterilization unit.

No-carrier-added 1-[^{11}C]ACBC was synthesized in 25 min with a radiochemical yield of 40% EOB utilizing the set of subprograms shown in Table 1. The carbon-11 hydrogen cyanide was collected in the unit in a 1.5 mL aqueous solution of $(NH_4)_2CO_3$ and cyclobutanone. The reaction mixture was heated at 104° C in the block heater and reflux maintained in the vessel by the circulation of cold air through a copper coil fitted at the top of the vessel. The reaction mixture was cooled prior to neutralization by passage through small bore teflon

tubing immersed in an ice bath. Reagent addition, solution transfers, and column elution was achieved by the application of gas pressure. The radiochemical purity exceeded 98% and was determined via HPLC equipped with a radioactivity detector and via TLC with a Bioscan 200 Scanner. The HPLC stationary phase was a Whatman analytical Patrisil SAX 4.6 X 250 mm column with a mobile phase of 50 mm $KHPO_4$ at a flow rate of 1.0 mL/min, rt=4.5 min. The TLC stationary phase was a reversed phase silica gel chiral plate with a mobile phase of CH_3CN:H_2O:CH_3OH 20:5:5, rf=0.40.

References

1. Wise R.J., Thomas D.G., Lammertsma A.A., and Rhodes C.G. - Prog.Exp.Tumor Res. 27: 154-169(1984)
2. Hubner K.F., King P., Gibbs W.D., Partain C.L., Washburn L.C., Hayes R.L., Holloway E. - Medical Radionuclide Imaging 1980; Vienna, Austria, International Atomic Energy Agency, 1981, Vol II, pp. 515-529
3. Hood W.F., Sun E.T., Compton R.P., and Monahan J.B. - Eur.J.Pharmacol. 161: 281-282(1989)
4. Ortwine D.F., Malome T.C., Bigge C.F., Drummond J.T., Humblet C., Johnson G., and Pinter G.W. - J.Med.Chem. 35: 1345-1370(1992)
5. Goodman M.M., DeVinney J.L., Longford C.P.D., Ladetsky M., Kabalka G.W., Larsen J., Hubner K.F. and Buonocore E. - J.Lab.Cmpds.Radiopharm. 30: 184-186(1991)

Figure 1. 1-[^{11}C-ACBC Automated Synthesis Unit

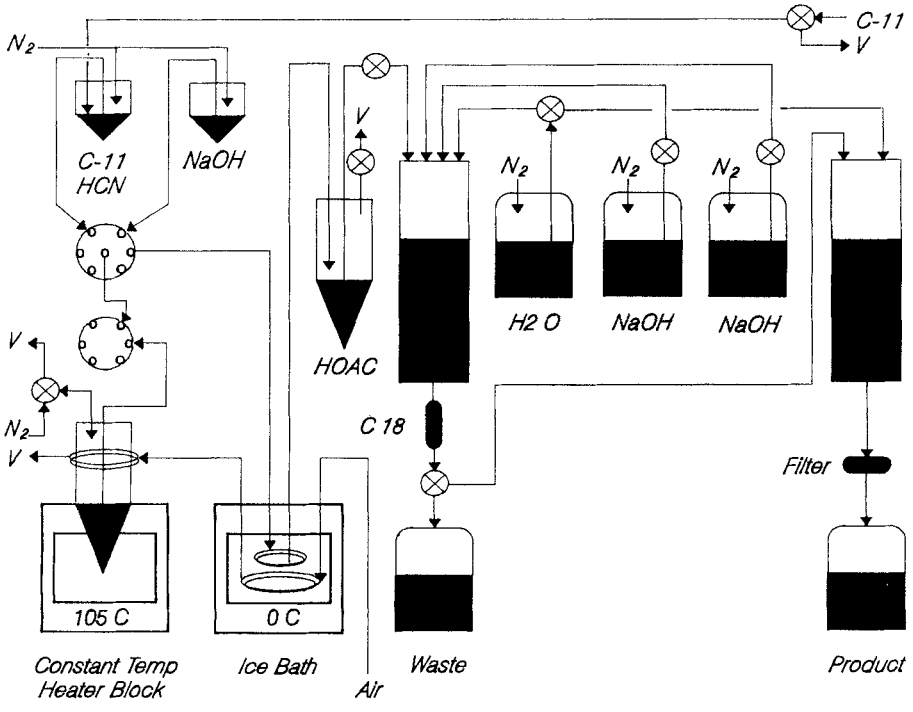

TABLE 1. 1-C-11 ACBC Synthesis Program

COMMAND FILE/DESCRIPTION	TASK DESCRIPTION/TIME REQUIRED
COLLECTION POSITION: A path in the valves is opened for introduction of C-11 HCN into vial A.	Valves are positioned. 10 min.
A TO VESSEL: C-11 CN is transferred to glass reaction vessel (GRV)	Vial containing C-11 CN/$(NH_4)_2CO_3$, NH_4Cl, and cyclobutanone is pressurized to add C-11 CN to GRV. 0.25 min.
HEAT POSITION: GRV valves to reagent vials are closed.	Valves in GRV are closed. Vent valve open. 0 min.
HEAT VESSEL 1: GRV is heated to form hydantoin.	GRV solution is heated at 104° C. 4 min.
TRANSFER POSITION: B TO VESSEL: 6.25 N NaOH is transferred to GRV.	Vial containing 1 mL 6.25 N NaOH is pressurized to add to GRV. 0.25 min.
HEAT POSITION: HEAT VESSEL 2: GRV is heated to form amino acid.	GRV solution is heated at 104° C. 10 min.
TRANSFER TO COLUMN: TRANSFER POSITION: Reaction mixture is transferred to HOAc vial.	GRV solution is cooled, added to 4.25 mL 25% HOAc and HOAc mixed. 1.25 min.
TRANSFER POSITION: HOAc mixture is transferred to strong cation column.	Mixture is transferred onto strong cation resin. 1.0 min.
WATER 1: Water transferred through cation column.	Water reservoir vial is pressurized to elute 30 mL of H_2O through strong cation column and C-18 Seppak to waste. 2 min.
BASE 1: 0.4 NaOH is transferred through cation column	NaOH reservoir vial 1 is pressurized to elute 30 mL of 0.4 M NaOH through strong cation column to waste. 2 min.
BASE 2: 0.4N NaOH is transferred through cation columns to elute amino acid	NaOH reservoir vial 2 is pressurized to elute 40 mL of 0.4 M NaOH through strong and weak cation columns to elute and filter amino acid into sterile product vial. 3.25 min.
WATER 2: Amino acid is transferred to product vial.	Water vial is pressurized to elute 10 mL of H_2O through weak cation column to elute and filter amino acid into sterile product vial. 0.5 min.

The Quality of [^{13}N] Ammonia Produced by Using Ethanol as a Scavenger.
CHANNING M.A., DUNN B.B., KIESEWETTER D.O., PLASCJAK P. AND ECKELMAN W.C. PET Department, National Institutes of Health (NIH), Bethesda MD 20892.

Production of [^{13}N] ammonia has been of importance in cardiac imaging. Production of [^{13}N] via $^{16}O(p,\alpha)^{13}N$ on pure water produces [^{13}N] nitrate as the major species. Early efforts to produce ammonia in the target produced a decreasing yield of ammonia with increasing μAh. Welch and Straatman in 1973 reported 7% ammonia at <1eV/molecule and 0.3% ammonia at > 1 eV [1]. Parks and Krohn used a recirculating target system to produce ^{13}N from the 18 MeV proton beam. Any combination of current intensity and time that resulted in 18 mCi produced 96-99% nitrate[2]. Tilbury and Dahl in 1979[3] used a closed system to produce ^{13}N. Maximal ammonia(40%) was produced at 0.01 μAh falling to a plateau of 5% at 1 μAh. The addition of small amounts of organic and inorganic modifiers resulted in improved yields of [^{13}N]-ammonia. They added either ethanol or formic acid and found increased [^{13}N]-ammonia yields with a drop off at 6-7 μAh. They obtained high yields at $\leq$ 1 μAh whether helium or nitrogen was used as the purge gas, but less than 10% when oxygen was used. At the Princeton meeting, Patt et al.[4] showed dose effects up to 80 μAh. Yields of nitrate were reduced by the free radical scavenger "$K_2[Fe(CN)_6]$". Wieland et al[5] produced high yields of ammonia using 5 mM ethanol in a pressurized target . At the Paris meeting, Ferrieri et al.[6] reported on the fate of ethanol after 2 minute irradiations. Using radioactive ethanol as a tracer, they found 97% of the added ethanol as carbon dioxide and only a small amount of formaldehyde.

The 9.5 mL water target in use at NIH for [^{13}N]-ammonia production (Japan Steel Works) is constructed of titanium with transfer lines of stainless steel and teflon. The yield at NIH using either He or oxygen purged solutions is 100 mCi at 20 μA x 5 min. This irradiation time (1.7 μAh) is approximately that found by Tilbury and Dahl to produce high ammonia yields. We have repeated their experiments using water containing 5 mM ethanol with and without various purges. The control experiments without 5 mM ethanol showed a low yield of ammonia regardless of the purge. The presence of 5 mM ethanol produced high yields of ammonia also independent of the

purge. Oxygen was deleterious to the yield of ammonia to a small but not significant extent even when 5 mM EtOH was present. The major impurity in these samples was [^{13}N]-nitrate **(Table 1)**.

Table 1. YIELD OF AMMONIA UNDER VARIOUS CONDITIONS USING WATER WITH AND WITHOUT 5 mM ETHANOL (ETOH).*

SOLUTION	% [^{13}N] AMMONIA
5 mM ETOH	97 ± 3 (n=12)
5 mM ETOH (< 1.4 ppm OXYGEN)	94 ± 4 (n= 4)
5 mM ETOH, OXYGEN SAT. (> 14 ppm)	91 ± 0.6 (n=3)
WATER (< 1.4 ppm OXYGEN)	10 ± 10 (n=5)
WATER, OXYGEN SAT (>14 ppm)	1.6 ±0.2 (n=3)

---

*For 0.83 μA-h, the average ^{13}N yield was 60 to 70 mCi.

Control samples of ethanol, acetaldehyde, and formaldehyde were submitted to an outside testing laboratory (Leberco Testing, Inc.) to verify their ability to analyze low level samples and to validate the accuracy of a qualitative formaldehyde test reagent "Fast Formalert" from Organon Teknika. All values were in good agreement. Subsequent production runs were submitted and found to have less than 2 ppm formaldehyde. These values agreed with the fast formalert test.

For production, [^{13}N]-ammonia is produced by irradiating 5 mM ethanol in water for 5 minutes at 10 uA in a sealed target. The solution is passed through a Bio-REX AG^{tm} 1-X8 anion exchange membrane in series with a Millipore Vented Millex-GS 0.22 μm filter unit. About 35 mCi is collected. The routine quality control for [^{13}N]-ammonia includes the colormetric test for formaldehyde and cation exchange chromatography for the presence of the rapidly eluting oxides of nitrogen. The absence of nitrites and nitrates has been confirmed by anion chromatography. The HPLC chromatography

uses a Westcan silica base cation column (50 x 4.6 mm, 3 μm) for separation and quantification of the ammonia. The eluent is 3 mM nitric acid. Radiochemical purity is determined using a NaI detector and specific activity can be obtained by using a Model 213A Westcan conductivity detector.

A specific activity of ≥ 800 Ci/mmol is achieved. The limit of detection for the latter is 3 ng. The radionuclidic purity is >99%. When the [^{13}N] ammonia is transferred from the target through a strong anion exchange resin membrane (25 mm, AG1-X8), all anionic impurities are removed. The final radiochemical and radionuclidic purity is ≥ 99% which meets the criteria set by the USP.[7]

The effect of ethanol must be to produce an overall reducing media. Oxygen can be deleterious because it reacts with the hydrated electron to produce the oxidizing agent, hydroxy radical. These hydroxy radicals and those produced directly react with ethanol (primarily the alpha hydrogen) to produce the weakly reducing ethanol radical. The solution is therefore reducing, but the exact mechanism of ammonia formation is still in question.

---

[1]Welch M.J. and Straatman M.-- Radiochim. Acta 20:124 (1973.
[2]Parks N.J.and Krohn K.A. --Int. J. Appl. Radiat. Isot. 29: 754 (1978)
[3]Tilbury R.S. and Dahl J.R. -- Radiat. Res. 79:22 (1979).
[4]Patt J.T., Nebeling B., Stocklin G. -- J. Label. Compd. Radiopharm. 30: 122 (1991).
[5]Wieland B. et al.-- Appl. Radiat. Isot. 42: 1095 (1991)
[6]Ferrieri R.A. et al. -- J. Label. Compd. Radiopharm. 32: 461 (1993).
[7]United States Pharmacopeia-NF XXII. Ammonia N13 for Injection., United States Pharmacopeia Convention, Inc. Rockville MD, 1990, p. 2367.

^{18}F-Labeled Analogs of Arachidonic acid ; Synthesis and Preliminary In Vivo Distribution in Rats of Methyl ω-[^{18}F] Fluoroarachidonate.

NAGATSUGI, F.; HOKAZONO, J.; SASAKI, S.; MAEDA, M. Faculty of Pharmaceutical Sciences, Kyushu University, 3-1-1 Maidashi, Higashi-ku, Fukuoka 812 Japan

Arachidonic acid has important roles in the physiology and pathology of the central nervous system. The metabolic turnover of membrane phospholipids has been shown to be closely related to the regulation of functions that are linked to neuronal transmission (1,2) and arachidonic acid is one of the most common fatty acid found in the brain phospholipid. Intravenously injected 1-[^{14}C]arachidonic acid has been shown to be incorporated selectively into brain phosphatidyl inositol (3). Therefore, the development of arachidonic acid analogs labeled with positron emitting nuclides would be of very interest as possible radiopharmaceuticals for studying brain phospholipid turnover. Arachidonic acid labeled with ^{11}C at the carboxylic carbon has recently been prepared and its uptake in animal brains studied (4). Since labeling with the longer lived nuclide fluorine-18 permit longer PET imaging intervals than the 20 min half-life carbon-11, fluorine-18 labeled arachidoic acid analogs are expected to be more useful as phospholipid metabolic tracers for the brain by PET. We report here the first synthesis of [^{18}F]-fluoroarachidonic acid through [^{18}F]fluoride ion displacement and the preliminary biodistribution in rats.

Our synthetic route to fluoroarachidonic acid, involving the introduction of a fluorine atom through nucloeophilic substitution using fluoride ion, is depicted in Scheme 1. The tosylate precursor was prepared from arachidonic acid according to a modified literature procedure (5). The C_{20}-carbon skeleton was constructed by coupling of the aldehyde with the Wittig reagent. This synthetic approach also seems suitable for the preparation of ω-^{18}F-labeled eicosapentaenoic acid as well as other functionalized arachidonic acid analogs.

Scheme 1

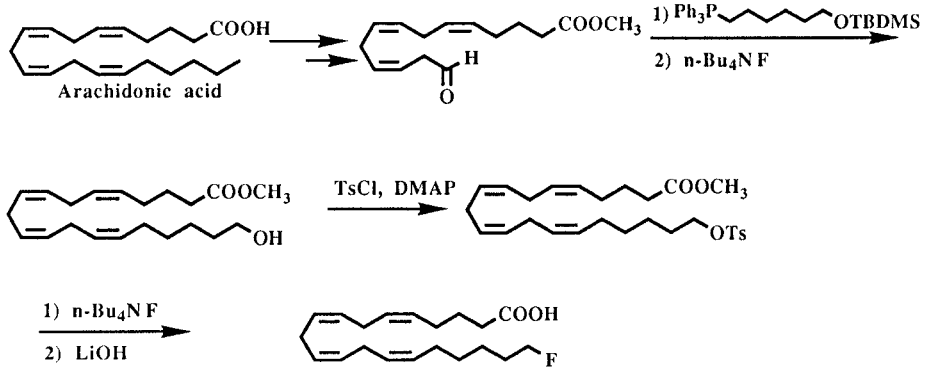

The radiosynthesis was achieved by [^{18}F]fluoride (n-Bu$_4$N^{18}F) ion displacement on the tosylate precursor (Scheme 2). Various conditions were explored for this exchange reaction. Optimal reaction conditions were found to be a 20 min reaction time at 90°C in acetonitrile, using the tosylate and n-Bu$_4$N^{18}F. Methyl ω-[^{18}F]-fluoroarachidonate was purified by HPLC with a reverse phase column using CH_3CN-H_2O (7:3). The HPLC purification provided a product with high radiochemical (>98 %) and chemical purity. Total synthetic time including HPLC purification was 100 min. Isolated radiochemical yields (not corrected decay) at the end of synthesis (EOS) was 37%. The conversion to the labeled free acid was accomplished by the hydrolysis with 1N KOH.

Scheme 2

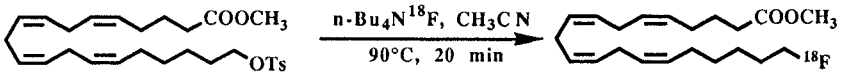

Preliminary biodistribution in Wistar male rats under fasting condition at various time after intravenous injection of methyl ω–[^{18}F]fluoroarachidonate is shown in Table 1. The ^{18}F concentration in the heart was initially high but the radioactivity then declined rapidly. The initial uptake of ^{18}F activity in the brain was low, but the radioactivity then increased slowly and at 60 min the brain level was seen to approach that of the blood. The bone radioactivity increased with time, but the level was not so high, indicating *in vivo* defluorination may not occur remarkably. Further *in vivo* characterization of this agent are in progress, and biodistribution of ω–[^{18}F]fluoroarachidonic acid will be also presented.

Table 1. Tissue distribution in rats following *i.v.* administration of methyl [^{18}F]fluoroarachidonate

	Uptake (%dose/g) [a)]			
	1 min.	5 min.	30 min.	60 min.
blood	0.62±0.16	0.35±0.07	0.36±0.05	0.27±0.03
lung	1.70±0.03	1.83±0.15	1.65±0.44	1.06±0.04
liver	1.95±0.81	3.29±0.37	3.15±0.97	2.57±0.98
kidney	1.15±0.44	1.54±0.17	1.62±0.09	1.36±0.23
small intestine	0.58±0.01	0.86±0.09	0.88±0.05	0.68±0.13
heart	3.06±0.38	1.96±0.60	0.96±0.07	0.68±0.09
bone	0.12±0.04	0.29±0.18	0.66±0.09	0.78±0.14
brain	0.17±0.01	0.19±0.02	0.26±0.02	0.26±0.04

a) Mean±SD of three or two rats

1) Bazan N.G., *Biochim. Biophys. Acta.*, **218**: 1 (1970).
2) Abdel-Latif A.A., *Pharmacol. Rev.*, **38**, 227: (1986).
3) DeGeorge J.J. et al., *J. Neurosci. Res.*, **24**: 413 (1989).
4) Channing M.A. et al.,*J. Label. Compd. Radiopharm.*,**XXXII**: 539 (1993).
5) Manna S., et al., *Tetrahedron Lett.*, **24**: 33 (1983).

Synthesis and Biodistribution of F-18 Labeled Analog of D-Fructose: 1-Deoxy-1-[^{18}F]fluoro-D-fructose.

HARADAHIRA, T.[1]; TANAKA, A.[2]; MAEDA, M.[2]; ICHIYA, Y[3].; and MASUDA, K.[3] [1]Research Development Corporation of Japan, Tokyo, 100 Japan; [2]Faculty of Pharmaceutical Sciences and [3]Faculty of Medicine, Kyushu University, Fukuoka, 812 Japan.

Recently a great variety of metabolic tracers have been developed for the measurements of regional biochemical functions by positron emission tomography (PET).[1] Some of them were elegantly designed to be metabolically trapped in a particular metabolic process. 2-Deoxy-2-[^{18}F]fluoro-D-glucose ([^{18}F]FDG), a representative metabolic trapping tracer, undergoes trapping in tissues after the formation of [^{18}F]FDG-6-phosphate by hexokinase in the glycolytic pathway. D-Fructose, a physiological ketohexose, can behave as a substrate similarly to D-glucose for energy production in humans.[2] We are interested in developing F-18 labeled D-fructose analogs which undergo metabolic trapping in the processes of D-fructose metabolism and evaluating their potentials as PET tracers for the measurement of human energy metabolism.

D-Fructose is primarily converted to D-fructose-1-phosphate by fructokinase in human tissues such as the liver, gut and kidneys, after which the phosphate is cleaved by aldolaseB to glyceraldehyde and dihydroxyacetone phosphate. These trioses are subsequently utilized in the glycolytic-gluconeogenic pathway. D-Fructose is also known to be phosphorylated to fructose-6-phosphate by hexokinase, although the affinity of this enzyme for D-fructose is considerably lower than for D-glucose[3]. The metabolism of D-fructose by fructokinase could be blocked by introducing a fluorine atom, in the place of hydroxyl group, at C-1 of D-fructose. It was therefore expected that F-18 labeled analog of D-fructose, 1-deoxy-1-[^{18}F]fluoro-D-fructose (1-[^{18}F]FDFrc), might be subjected to metabolism primarily by hexokinase and the resulting 1-[^{18}F]FDFrc-6-phosphate remains unchanged in the tissues because of the presence of fluorine atom at C-1. Our *in vitro* metabolic study of nonradioactive 1-FDFrc using F-19 NMR spectroscopy has shown that 1-FDFrc is phosphorylated by yeast hexokinase. Thus, our initial attention to the developments of F-18 labeled fructoses was given to the synthesis of 1-[^{18}F]FDFrc and its *in vivo* behavior in animals. This paper describes new syntheses of both 1-FDFrc and 1-[^{18}F]FDFrc as well as the preliminary result of biodistribution of 1-[^{18}F]FDFrc in rats.

Nonradioactive 1-FDFrc has previously been prepared via nucleophilic fluorination of 2,3; 4,5-di-O-isopropylidene-1-O-(trifluoromethanesulfonyl)-D-fructopyranose (**1**) with tris(dimethylamino) sulfonium difluorotrimethylsilicate.[4] We have modified this synthetic procedure for the preparation of 1-[^{18}F]FDFrc using [^{18}F]fluoride ion. Nucleophilic fluorination of **1** with tetrabutylammonium fluoride in THF at 70°c for 90 min gave 1-deoxy-1-fluoro-2,3;4,5-di-O-isopropylidene-D-fructopyranose (**2**) in 88% yield after purification by silica gel column chromatography. Excellent conversion of **2** into 1-FDFrc was accomplished by the acid hydrolysis with 90% (v/v) CF_3COOH at room temperature for 15 min. The overall yield of 1-FDFrc from **1** was 83% after chromatographic purifications. Aminopolyether supported potassium [^{18}F]fluoride ($K^{18}F$/Kry222) was used as a [^{18}F]fluorinating agent in the radiosynthesis of 1-[^{18}F]FDFrc. Reaction of **1** with $K^{18}F$/Kry222 in CH_3CN at 90°C for 30 min gave ^{18}F-intermediate (**3**), which was separated from unreacted [^{18}F]fluoride and aminoplyether through Silica Sep-Pak filtration using $CHCl_3$ as a eluent. The deprotection of **3** into 1-[^{18}F]FDFrc was achieved by the treatment with 90% (v/v) CF_3COOH at room temperature for 20 min. After neutralization of the acidic solution of 1-[^{18}F]FDFrc with AG11X8 resin column and subsequent purification with both C18 and Alumina Sep-Pak columns, an aqueous solution of 1-[^{18}F]FDFrc was obtained in 20% radiochemical yield (decay uncorrected) based on the initial activity of $K^{18}F$/Kry222, with a total synthesis time of 100 min from start of the radiofluorination. The radiochemical purity of 1-[^{18}F]FDFrc was greater than 99% by radio-TLC analysis.

Biodistribution study of 1-[^{18}F]FDFrc in rats (Fig. 1) showed initial high uptake and subsequent rapid washout of the radioactivity in the principal tissues (kidney , liver , small intestine) for D-fructose metabolism, indicating no metabolic trapping of this tracer by the enzymes such as fructokinase in these organs. The uptake of 1-[^{18}F]FDFrc in the brain having the high level of hexokinase activity was the lowest among the organs examined, which may arise from the low BBB permeability of this tracer similarly to D-fructose. The radioactivity in the brain, however, tended to increase with time, suggesting that the expected metabolic trapping of 1-[^{18}F]FDFrc by hexokinase was occurring.

This work was supported by a Grant-in-Aid for Cancer Research from the Ministry of Education, Science and Culture, Japan.

1. Stöklin G. - Eur. J. Nucl. Med., 19, 527 (1992)
2. Chen M. and Whistler R. L. - Adv. Carbohydr. Chem. Biochem., 34, 286 (1977)
3. Gumaa K. A. and McLean P. - FEBS Lett., 27, 293 (1972)
4. Card P. J. and Hitz W. D. - J. Am. Chem. Soc., 106, 5348 (1984)

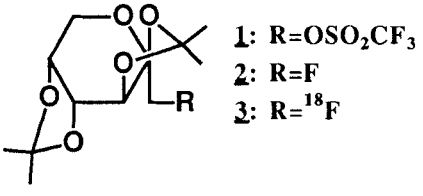

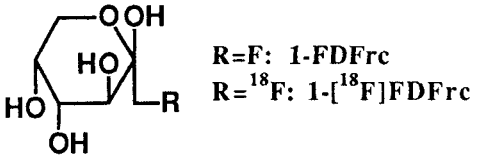

Fig. 1 Tissue Distribution of Radioactivity in Rats Following Intravenous Injection of 1-[^{18}F]FDFrc

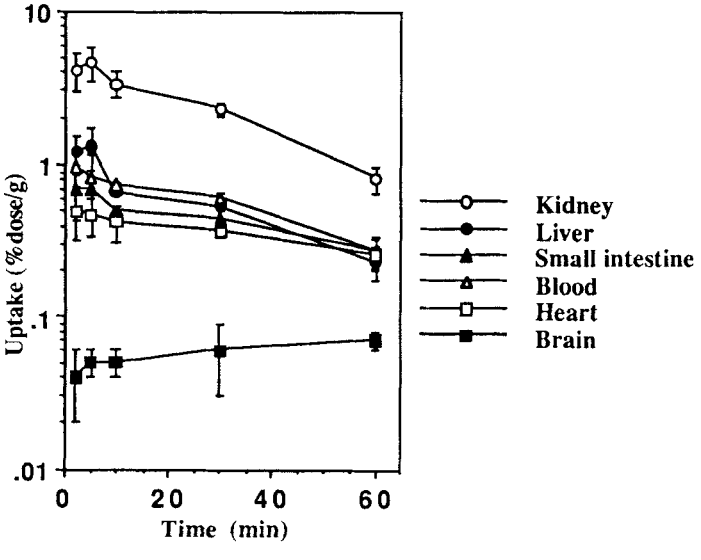

Protein Incorporation of L-[*methyl*-^{3}H]Methionine, L-[*1*-^{14}C]Leucine and L-[2-^{18}F]Fluorotyrosine in the Brain and Tumor Tissues

ISHIWATA, K.; KUBOTA*, K.; MURAKAMI**, M.; KUBOTA*, R.; SASAKI, T.; ISHII, S.; and SENDA M. (Positron Medical Center, Tokyo Metropolitan Institute of Gerontology, Tokyo, *The Research Institute for Tuberculosis and Cancer, Tohoku University, Sendai, **Research Institute for Brain and Blood Vessel-Akita, Akita, Japan, Japan)

In order to compare potential of L-[*methyl*-^{11}C]methionine (^{11}C-Met), L-[*1*-^{11}C]leucine (^{11}C-Leu) and L-2-[^{18}F]fluorotyrosine (^{18}F-Tyr) as tracers for measuring protein synthesis rate by PET, incorporation of three tracers into the acid-precipitable fraction (APF) of mouse brain and tumor tissues was studied. Labeled proteins in the APF was further separated from lipids and nucleic acids.

L-[*methyl*-^{3}H]methionine (^{3}H-Met), L-[*1*-^{14}C]leucine (^{14}C-Leu) and ^{18}F-Tyr were injected i.v. simultaneously into two groups of mice bearing FM3A mammary carcinomas: control and cycloheximide-treated group (100 mg/kg, i.p.) to inhibit the protein synthesis *in vivo*. Distribution was measured as % injected dose per g tissue. Brain and tumor tissues were homogenized in $HClO_4$, and divided to the acid-soluble fraction and APF by centrifugation. From the APF, lipid fraction was extracted with $CHCl_3/CH_3OH$. The residual precipitate was incubated in 0.3 M KOH solution at 37 °C for 60 min. The solution was acidified with $HClO_4$ at 0 °C and centrifuged. The supernatant (alkaline-labile fraction) was separated from precipitate. Finally, the precipitate was heated in 0.5 M $HClO_4$ solution at 95 °C for 15 min, and the solution was divided to the acid-labile fraction and the precipitated proteins by centrifugation at 0 °C.

In the control mice, the uptake and their incorporation into APF of all three amino acids in the brain and FM3A increased with time. The cycloheximide-treatment significantly reduced the incorporation into the APFs of all three tracers to 6-31% and 3-11% of the control in the brain and tumors, respectively. The total uptake of ^{14}C-Leu by the brain and tumors decreased rapidly, while the uptake of both ^{3}H-Met and ^{18}F-Tyr still increased with at most 28% reduction.

In the APFs of brain and FM3A, the protein fraction was a major component in the control (^{14}C-Leu > ^{18}F-Tyr > ^{3}H-Met) as shown in Table 1. The amounts of the ^{14}C in the lipids and alkaline-labile fraction were negligible both in brain and tumors; however, certain amounts of the ^{3}H were detected in these two fractions and the ^{18}F was detected in the lipid fraction. Proportions of these fractions were significantly increased in the cycloheximide-treated mice. Presence of the alkaline-labile fraction means the ^{3}H-Met was incorporated into RNA. Similar percentages were found in the acid-labile fractions of all three amino acids, suggesting that this fraction probably represents the labeled basic proteins such as chromosomal histones.

These results demonstrate that all three amino acids are incorporated into proteins as a main metabolic pathway, however, ^{3}H-Met and ^{18}F-Tyr are also used in other pathways, especially under suppressed proteins synthesis. Therefore, among the positron emitting analogs of three amino acids investigated, ^{11}C-Leu is the best choice for assessing the protein synthesis rate *in vivo* by PET.

Table 1. The effects of cycloheximide on incorporation of radioactivity into high-molecular weight materials in mice bearing FM3A tumors 60 min after i.v. injection of ^{3}H-Met, ^{14}C-Leu and ^{18}F-Tyr.

			% of acid-precipitable fraction			
			Lipid Fr.	Alkaline-labile Fr.	Acid-labile Fr.	Protein Fr.
Brain	Control	^{3}H-Met	7.1 ± 1.8***	4.5 ± 0.7***	5.3 ± 1.1	82.9 ± 1.6***
		^{14}C-Leu	1.2 ± 0.3	0.7 ± 0.3	3.9 ± 0.8	94.3 ± 1.2
		^{18}F-Tyr	5.4 ± 2.1**	0.8 ± 0.4	3.0 ± 0.7	90.8 ± 2.3*
	Cycloheximide	^{3}H-Met	14.7 ± 2.2***	13.8 ± 4.0***	4.6 ± 2.3	67.1 ± 4.9***
		^{14}C-Leu	5.3 ± 2.2	bg	4.4 ± 3.0	90.4 ± 3.0
		^{18}F-Tyr	21.3 ± 2.8***	3.9 ± 0.7***	9.4 ± 2.0*	65.4 ± 1.9***
FM3A	Control	^{3}H-Met	2.4 ± 0.2***	5.6 ± 0.4***	7.2 ± 1.6	84.6 ± 1.8***
		^{14}C-Leu	0.9 ± 0.3	1.2 ± 0.1	5.0 ± 1.3	93.1 ± 1.2
		^{18}F-Tyr	5.1 ± 1.5***	3.0 ± 1.7	4.9 ± 1.2	87.0 ± 3.3**
	Cycloheximide	^{3}H-Met	12.2 ± 0.5***	22.8 ± 1.3***	12.3 ± 2.2***	52.7 ± 1.7***
		^{14}C-Leu	6.7 ± 0.6	5.4 ± 0.4	3.1 ± 2.0	84.8 ± 2.1
		^{18}F-Tyr	38.7 ± 3.5***	7.8 ± 0.9**	9.1 ± 1.9**	44.4 ± 2.3***

Mean ± sd (n = 4). bg: background radioactivity level.

*p<0.05, **p<0.01, ***p<0.001 (Student's t-tests between ^{14}C-Leu and the other amino acids).

COMPARISON OF BIODISTRIBUTION IN 2-METHYL-FATTY ACIDS LABELED AT DIFFERENT POSITIONS

OGAWA, K.; NOZAKI, T.; SASAKI, T.*; ISHIWATA, K.*; SENDA, M.*
School of Hygienic Sciences, Kitasato University, Sagamihara, Kanagawa, 228 Japan; * PET Center, Tokyo Metropolitan Institute of Gerontology, Sakae-cho, Itabashi-ku, Tokyo, 137 Japan

We reported previously on the malonic ester synthesis of 2-methyl[$^{11}CH_3$]-fatty acids using $^{11}CH_3I$ and their behavior in mouse (1). In order to study in detail the difference in the organ distribution of radioactivity due to the labeling position in 2-methyl-fatty acids, we synthesized the following compounds and measured the time course of their DAR in mouse organs: 3-^{14}C-propanoic acid [1], 1-^{14}C-propanoic acid [2], 2-methyl[$^{14}CH_3$]-butanoic acid [3], 1-^{14}C-2-methyl-butanoic acid [4], 2-methyl[$^{14}CH_3$]-hexanoic acid [5], 1-^{14}C-2-methyl-hexanoic acid [6], 3-^{14}C-butanoic acid [7], 1-^{14}C butanoic acid [8], and 3-^{14}C-2-methyl-butanoic acid [9]. Some of them are labeled also with ^{11}C.

Compounds 1, 3 and 5 were prepared by the malonic ester synthesis from the diethyl malonate or corresponding diethyl alkylmalonates with $^{14}CH_3I$ in good yields (> 60 %). By the use of $CH_3{}^{14}CH_2I$, Compounds 7 and 9 were similarly obtained in 68 % and 78 % yields, respectively (2). Compounds 4 and 6 were prepared by the Grignard reaction of $^{14}CO_2$ with sec-butyl magnesium chloride and 2-methyl-pentyl magnesium bromide, respectively, both in 45 % yield. Compounds 1 and 8 were purchased from NEN. Their saline solutions were injected intravenously into mice. After preset times, the mice were sacrificed and the radioactivity in their organs was measured by liquid scintillation method.

Figure 1 shows the relationship between the chain length and the DAR in mouse brain at 20 min after the injection for 2-methyl[$^{14}CH_3$]-fatty acids. The DAR became maximum around this time for any chain length. Figure 2 shows the time couse of DAR in mouse brain for some fatty acids labeled at different positions. Markedly lower brain uptake was observed for all the carboxyl-labeled compounds, Compounds 2, 4, 6, and 8, than the methyl-labeled compounds, Compounds 1, 3 and 5. The same was true for the upkake by most other organs. Further resemlances in the biodistribution were observed, in general, among the methyl-labeled compounds as well as among the carboxyl-labeled compounds. This is probably due to the β-oxydation of 2-methyl-fatty acids to give Compound 2 and Compound 1 from the other carboxyl-labeled fatty acids and 2-methyl-labeled acids, respectively. Compound 7 was quite similar with Compound 8 and also with 1-^{14}C-acetic acid in the biodistribution. This implies rapid β-oxidation of 7 and 8. Compound 9 showed slower respiratory excretion and blood clearance than Compound 7. This suggests that the β-oxydation is slower for 2-methyl-fatty acids to give propanoic and than for straight-chain fatty acids to give acetic acid.

Since 2-methyl[$^{11}CH_3$]-fatty acids are much different from the same compounds labeled at the carboxyl carbon, the 2-methyl compounds obtained by the malonic ester synthesis can be expected to offer valuable information in biochemistry as well as useful tracers in nuclear medicine.

(1) K. Ogawa, K. Niisawa, M. Sasaki and T. Nozaki, J. Labeled. Compd. Radiopharm., XXX, 417(1991).
(2) A. Gee, Acta Universitatis Upsaliensis(Fac. Sci.), No. 299, 1991,Upsala.

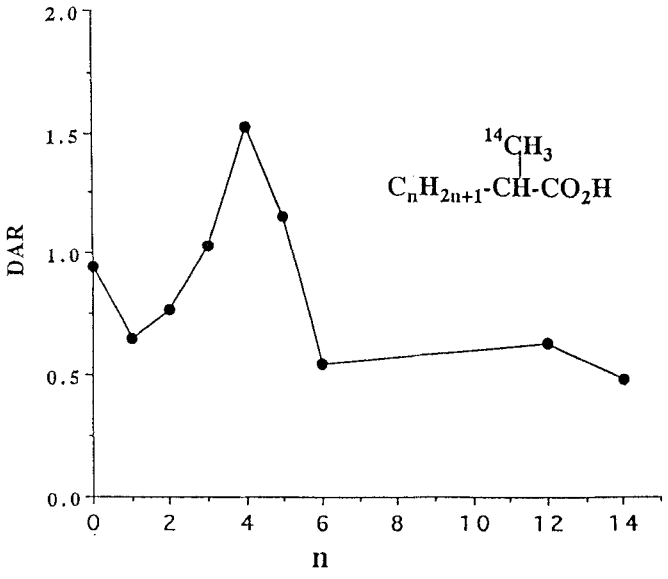

Fig. 1 DAR in Mouse Brain vs Chain Length of 2-Methyl-Fatty Acid
20 min. after i. v. injection

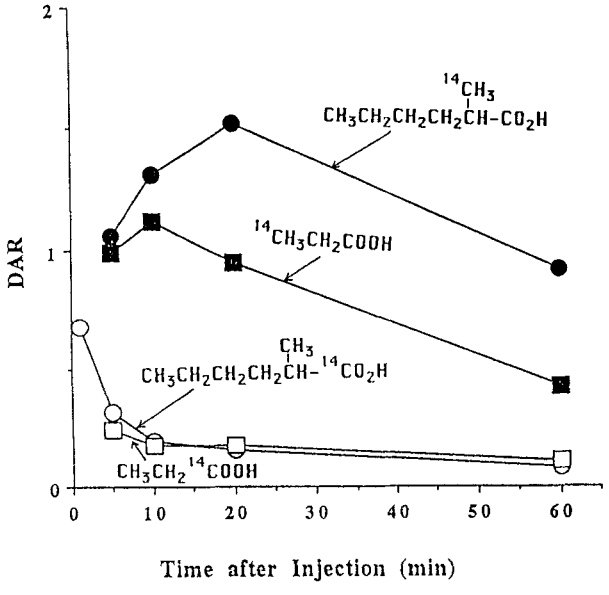

Fig. 2 Carbon-14 Concentration in Mouse Brain

Species-Dependent Binding of Copper(II) Bis(thiosemicarbazone) Complexes to Serum Albumin. MATHIAS, C.J.; Bergmann, S.R.*; and GREEN, M.A. *Cardiovascular Division, Washington University School of Medicine, St. Louis, MO 63110 and Department of Medicinal Chemistry, Purdue University, West Lafayette, IN 47907-1333.

Copper-62 labeled pyruvaldehyde *bis*(N^4-methylthiosemicarbazonato)copper(II), Cu-PTSM, has shown promise as a generator-based PET radiopharmaceutical for evaluation of regional tissue perfusion (1-4). In the process of development and validation of a solvent-extraction technique for determination of [^{62}Cu]Cu-PTSM in blood, we observed significant inter-species variations in the binding of Cu-PTSM to serum albumin (5). For example, when the partitioning of [^{67}Cu]Cu-PTSM between the plasma and red blood cell (RBC) fractions of whole blood was examined, ~35% of tracer was found to be associated with the plasma phase in dog blood, while in human blood at the same hematocrit ~75% of the radiotracer was associated with the plasma phase (5). The plasma phase of these blood samples was clearly identified as the source of this inter-species variation through "cross-over" experiments; human RBC suspended in dog plasma exhibit tracer partitioning identical to whole dog blood, while dog RBC suspended in human plasma exhibit [^{67}Cu]Cu-PTSM partitioning identical to whole human blood (5). When tracer partitioning was examined with RBC suspended in either dog or human albumin solutions (35 mg/mL saline), the observed [^{67}Cu]Cu-PTSM partitioning was virtually identical to that observed with plasma. Thus, there appears to be significant inter-species variability in the albumin binding of Cu-PTSM (*i.e.* $K_{human\ albumin} > K_{dog\ albumin}$; equation 1). We report here the use of ultrafiltration to further investigate the albumin binding of [^{67}Cu]Cu-PTSM and related [^{67}Cu]copper(II) *bis*(thiosemicarbazone) complexes.

$$\text{Cu-PTSM} + \text{Albumin} \underset{k_2}{\overset{k_1}{\rightleftharpoons}} (\text{Cu-PTSM})\cdots\text{Albumin} \qquad (1)$$

$$K = \frac{[(\text{Cu-PTSM})\cdots\text{Albumin}]}{[\text{Cu-PTSM}][\text{Albumin}]}$$

Protein binding of [^{67}Cu]Cu-PTSM was measured in human plasma, dog plasma, human serum albumin (HSA), and dog serum albumin solutions using Amicon Centrifree™ 30,000 Dalton NMWL ultrafiltration devices. Approximately 1 μCi [^{67}Cu]Cu-PTSM (estimated specific activity >2 x 10^6 mCi/mole) in 1-2 μL 50% ethanol was added to 1 mL of each protein solution, mixed, transferred to the ultrafiltration device, and centrifuged at 1000 x *g* for 20 minutes at room temperature using a 45° fixed-angle rotor. The fraction of "free" (unbound) [^{67}Cu]Cu-PTSM in the solution was calculated as:

$$\left[\frac{\text{Cu - PTSM Concentration in Ultrafiltrate}}{\text{Cu - PTSM Concentration in Unfiltered Protein Solution}}\right]$$

As a control, ultrafiltration studies were concurrently carried out following addition of [^{67}Cu]Cu-PTSM to normal saline alone, providing a measure of the extent of [^{67}Cu]Cu-PTSM binding to the ultrafiltration membrane. Significant binding of [^{67}Cu]Cu-PTSM to the ultrafiltration membrane was consistently observed (*i.e.* the percentage of unbound or "free" [^{67}Cu]Cu-PTSM in saline appears to be <100%, despite the absence of protein for binding; Table 1). Nevertheless, it is clear

Table 1. Evaluation of [^{67}Cu]Cu-PTSM Binding to Proteins by Ultrafiltration.

Solvent	"Free" [^{67}Cu]Cu-PTSM in Solution (%)*	*n*
Normal Saline (Control)	60.6 ± 5.6	22
Human Serum Albumin†	3.1 ± 0.8	12
Dog Serum Albumin††	23.0 ± 4.5	12
Human Plasma	1.6 ± 0.6	9
Dog Plasma	22 ± 1	2

*Values shown represent the mean ± standard deviation of *n* measurements.

†Human serum albumin, essentially fatty acid and globulin free (Sigma Chemical Co., St. Louis, MO); 35 mg/mL saline.

††Dog serum albumin, essentially fatty acid free (Sigma Chemical Co., St. Louis, MO); 35 mg/mL saline.

that the [^{67}Cu]Cu-PTSM tracer is bound more strongly by human albumin than dog albumin (Table 1). As in the previously reported studies of [^{67}Cu]Cu-PTSM partitioning in blood, the extent of protein binding in plasma is similar to that observed with saline solutions of serum albumin from that same species (Table 1). Similar ultrafiltration studies with related [^{67}Cu]copper(II) *bis*(thiosemicarbazone) complexes (6) suggest that the inter-species variability in albumin binding is highly compound specific. While a number of copper(II) bis(thiosemicarbazone) complexes can be identified that, like Cu-PTSM, exhibit significantly stronger binding to HSA than to dog serum albumin, other compounds in this series are found to exhibit no preferential association with HSA.

Further studies will be required to fully assess the significance of the inter-species variability in Cu-PTSM binding to serum albumin; however, the reported attenuation of [^{62}Cu]Cu-PTSM myocardial uptake in humans at high rates of myocardial blood flow (4 and S.R. Bergmann, unpublished results) could indicate that, contrary to expectations from PET studies in the dog model (3), k_2 (equation 1) can become the rate-limiting step for myocardial extraction of tracer.

This work was supported by a grant from the National Cancer Institute (RO1-CA-46909).

1. Green, M.A., Mathias, C.J., Welch, M.J., *et al.* - J. Nucl. Med. 31:1989 (1990).
2. Van der Wall, E.E., Sochor, H., Righetti, A., and Neimeyer, M.G., eds. - What's New in Cardiac Imaging? Kluwer, Dordrecht, pp165-177, (1992).
3. Herrero, P., Markham, J., Weinheimer, C.J., *et al.* - Circulation 87:173 (1993).
4. Beanlands, R., Muzik, O., Mintun, M., *et al.* - J. Nuclear Med. 33:684 (1992).
5. Mathias, C.J., Bergmann, S.R., and Green, M.A. - Nucl. Med. Biol. 20:343 (1993).
6. John, E.K.; and Green, M.A. - J. Med. Chem. 33:1764 (1990).

Cu-62-PTSM AND MITOCHONDRIAL ELECTRON TRANSPORT SYSTEM

TANIUCHI, H.; FUJIBAYASHI, Y.; WADA, K.; KONISHI*, J.; and YOKOYAMA, A. Faculty of Pharmaceutical Sciences and School of Medicine*, Kyoto University, Sakyo-ku, Kyoto, 606, JAPAN

In vivo behavior of copper, which is essential metal considerably related with *in vivo* oxidation-reduction, is very attractive to us. Previously a new $^{62}Zn/^{62}Cu$ generator system, feasible for clinical purpose, has been developed in our laboratory (1). Using this system, we have been evaluating various ^{62}Cu-labeled complexes concerning their tissue-selectivity, *in vivo* oxidation-reduction and so on. In these experiments it has been shown that Cu-bisthiosemicabazone complexes (Cu-DTS) reveals excellent uptake and retention to the brain and the heart (2, 3). Based on these results, Green and his co-workers have reported that Cu-pyruvaldhyde-bis(N^4-methylthiosemi-carbazone) (Cu-PTSM) (Fig. 1) is a most potential tracer for the evaluation of cerebral and myocardial blood flow with PET (4, 5). With regard to the retention mechanism of Cu-DTS complexes, Petering et al. have indicated that in Ehrlich ascites tumor cells, Cu(II)-DTS was reduced in the cytosol to Cu(I) by non-speific reduction system (6, 7). However, the retention mechanism of Cu-PTSM in the brain is still unclear. Thus, we have studied the retention mechanism of Cu-PTSM with electron spin resonance (ESR). Among the subcellular components, Cu(II)-PTSM was reduced by the enzymatic system and reaction site was located only in the mitochondrial fraction (8). This was completely different from any of the previously proposed contrivances (6, 7, 9). In this study, we attempted to analyze in relation with the reduction of Cu-PTSM in detail. With regard to study of the reaction site in the brain mitochondria, we focused on the electron-transport chain, which is well-known as an electron-rich system of mitochondria. Then we examined the effect of inhibitors of the electron-transport chain had effects on the reduction of Cu(II)-PTSM to Cu(I), using antimycin A, malonate and retenone. Next, for confirming the specificity for the reduction on the brain mitochondria, we analyzed the intracellular reaction site of the liver and Ehrlich ascites cell, compared with the brain.

The electron-transport chain accepts the electron flow from two substrates, NADH and succinate. When the electron-transport chain was inhibited by antimycin A, which inhibits the point after meeting each electron flow, the reduction of Cu-PTSM was activated compared with non-treated mitochondria. Rotenone, which inhibits the electron-transport from NADH, activated the reduction as well as antimycin A. On the other hand, malonate inhibiting the electron flow from succinate didn't have effect on the reduction at all (Fig. 2). From these results it is suggested that the reduction site of Cu-PTSM was located on the upper stream of the inhibition site by rotenone. The Cu-PTSM was not reduced by

NADH, one of the electron-transport chain substrates and potent reductant. Thus, only complex I including NADH dehydrogenase was satisfied with the present requirements for the candidate of the reduction site. Moreover this suggestion was supported by the similarity of the reduction potential of Cu-PTSM (- 208 mV) (6) and that of the reaction in the complex I. From these results, this enzyme system might relate with the reduction of Cu-PTSM. Interestingly, this phenomenon was observed only in the brain. When studied in the liver, the reduction ability was observed in the mitochondria fraction as well as in the cytosol fraction. In the Ehrlich ascites cell, that was found only in the cytosol fraction (Fig. 3), a similar finding as Petering, et al (7). These results suggested that the reduction of Cu-PTSM observed in the brain was a unique reaction only in the brain but not general in all tissues.

With regard with intracellular fate of Cu-PTSM, we examined the Cu-PTSM distribution *in vitro* with the radioactive and nonradioactive copper. In the short reaction time (5~20 min), Cu-PTSM was rapidly accumulated to the mitochondria from cytosol and retained in the mitochondria. In the previous study we reported that the chelate structure of Cu-PTSM has been ruptured after reduction (8). From our proposed Cu-PTSM retention mechanism in the brain, Cu-PTSM may serve as a cerebral blood flow agent, as long as the mitochondrial electron-transport chain remains normal. But if this system was injured by some causes such as ischemia-reperfusion, encephalic Cu-PTSM accumulations would be altered. At that time, Cu-PTSM will provide an additional information for the evaluation of mitochondrial functions. In addition, differences of reactivities between the normal and the tumor cell would indicate the possibility of Cu-DTS complexes as a qualitative diagnostic agent for the diseased tissue.

REFERENCES

(1) Y. Fujibayashi, et al. - J Nucl Med 30 , 1989 : 1838 - 1842
(2) Y. Fujibayashi, et al. - J Nucl Med 29 , 1988 : 930
(3) A. Yokoyama, et al. - Radioisotopes 35, 1986 : 249 -255
(4) MA. Green, et al. - Nucl Med Biol 14, 1987 : 59 - 61
(5) MA. Green, et al. - J Nucl Med 29, 1988 : 1549 - 1557
(6) CH. Chan-stier et al. - Bioinorg Chem 6, 1976 : 203 - 217
(7) DT. Minkel et al. - Can Res 38, 1978 : 117 - 123
(8) Y. Fujibayashi, et al. - Bio Pharm Bull 16(2), 1993 : 146 - 149
(9) DH. Petering - "Metal Ions in Biological Systems," ed. by H. Sigel, Marcel Dekker Inc., New York, 1980, pp. 197 - 229

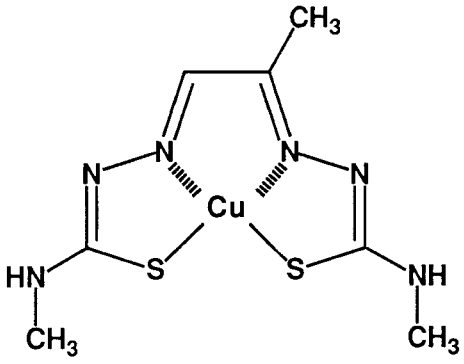

Fig.1 Structure of Cu-PTSM

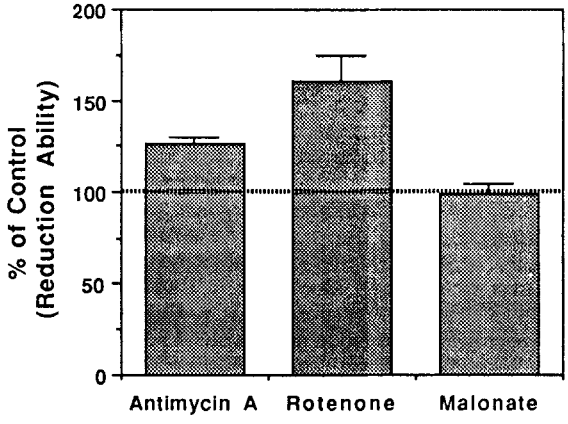

Fig.2 The Effect of Electron Transport System Inhibitors on Cu-PTSM Reduction

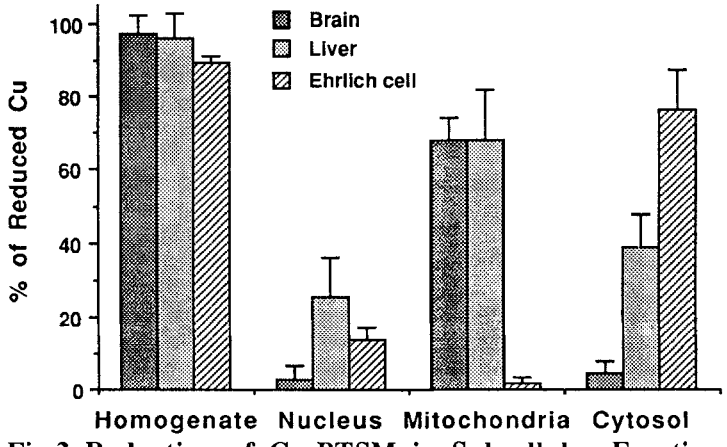

Fig.3 Reduction of Cu-PTSM in Subcellular Fractions (Brain,Liver,Ehrlich cell)

Structure-Distribution Relationships for Gallium *Tris*(salicylaldimine) and Related *Tris*(aminophenol) Complexes.

GREEN, M.A.; MATHIAS, C.J.; TSANG, B.W.; Neumann*, W.L.; and Woulfe*, S.R.
*Mallinckrodt Medical, Inc., St. Louis, MO 63134 and Department of Medicinal Chemistry, Purdue University, West Lafayette, IN 47907.

Radiopharmaceuticals labeled with generator-produced gallium-68 could facilitate the clinical use of positron emission tomography in hospitals lacking the cyclotron facilities needed for production of more commonly used PET radionuclides (^{15}O, ^{13}N, ^{11}C, and ^{18}F). Tripodal hexadentate *tris*(salicylaldimine) ligands with the general structure shown below have been of interest in this

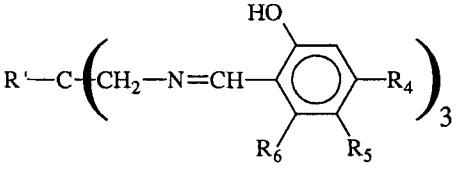

regard because they provide a nearly octahedral $N_3O_3^{3-}$ coordination sphere for the Ga^{3+} ion (1,2). The resulting uncharged lipophilic complexes of ^{68}Ga have been investigated as potential radiopharmaceuticals for evaluation of myocardial perfusion (2-4). In our initial work with the lead compound Ga[(5-MeOsal)$_3$tame] (R' = CH_3; R_5 = OCH_3; R_4 = R_6 = H) (3) we were able to obtain ^{68}Ga images of the dog heart that qualitatively mapped the pattern of tissue perfusion determined independently with [^{15}O]water; however, the relatively low heart/blood ratios obtained with this compound necessitated a blood pool subtraction protocol for satisfactory myocardial image quality. Subsequent studies showed that heart/blood ratios could be improved by altering the pattern of -OCH_3 substitution on the aromatic rings (4). More recently, we have shown that derivatization at the central carbon atom with an alkyl ether function (*e.g.* R' = -$CH_2OCH_2CH(CH_3)_2$) results in ^{68}Ga tracers that exhibit high myocardial uptake and high heart/blood ratios at short times post-injection (2). However, these highly lipophilic tracers also clear rather rapidly from the heart, imposing imaging times that may be undesirably short for use with a ^{68}Ga tracer (2).

We report here a more extensive investigation of gallium *tris*(salicylaldimine) complexes containing a variety of substituents on the aromatic rings and at the central carbon of the tripodal ligand framework (5,6) (Figure 1). In addition, we have examined four related ligands in which the imine -CH=N- linkage is replaced with an amine -CH_2-NH- linkage (Figure 2). The ^{67}Ga complexes of each of these ligands was prepared by ligand exchange from [^{67}Ga]*tris*(2,4-pentanedionato)-gallium(III) in ethanol solution. The measured octanol/water partition coefficients, *P*, for these tracers range from *log P* = 0.98 to *log P* = 4.0. Following dilution to 5% ethanol:30% propylene glycol:65% saline and filtration through a 0.2 μm PTFE membrane, the biodistribution of each of these tracers was determined by intravenous administration to ether-anesthetized rats (Table 1).

The most promising results were obtained with the ^{67}Ga complex of ligand **11**. This tracer exhibited slightly higher myocardial uptake than the previous best tracer of this type, Ga[(sal)$_3$tame-O-*iso*-Bu], and excellent heart/blood ratios (18.7 ± 1.7, 8.8 ± 0.9, and 6.6 ± 0.3 at 1, 5, and 60 minutes post-injection, respectively). Progressive liver accumulation of ^{67}Ga continued to be consistently observed whenever a salicylaldimine complex lacks substituents at the R_4, R_5, or R_6 positions of the aromatic rings, but is not observed with the ring-substituted complexes. Liver accumulation of tracer can also be avoided by saturation of the imine C=N double bond (ligands **5-8**); however, these *tris*(aminophenol) complexes exhibited rather poor myocardial uptake relative to the *tris*(salicylaldimine) and *tris*(alkoxysalicylaldimine) complexes. Poor myocardial uptake was also observed for the *tris*(salicylaldimine) complexes with ester substituents on the aromatic rings. With all of the complexes investigated, the ^{67}Ga radiolabel was cleared relatively quickly from the myocardium (Table 1). In no case was there evidence that the ^{67}Ga tracer could penetrate the blood-brain barrier.

Figure 1. Structural formula of tripodal hexadentate salicylaldimine ligands and octanol/water partition coefficients (*P*) for their ^{67}Ga-complexes.

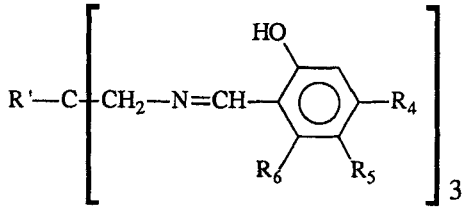

Ligand #	R'	R_4	R_5	R_6	*log P*
1	$-CH_3$	$-OCH_2C(O)O$-*t*-Bu	H	H	3.88 ± 0.17
2	$-CH_2OCH_2CH_2OCH_3$	H	H	H	1.53 ± 0.01
3	$-CH_3$	H	$-CH_2C(O)OEt$	H	2.34 ± 0.01
4	$-CH_3$	$-OCH_2C(O)OEt$	H	H	0.98 ± 0.01
9	$-C(O)O$-*t*-Bu	H	H	H	2.5 ± 0.1
10	$-CH_3$	$-OCH_3$	$-CH_3$	H	3.4 ± 0.1
11	$-CH_2OCH_2CH_2CH_3$	$-OCH_3$	H	H	3.2 ± 0.1
12	$-CH_2OCH_2CH_2CH_3$	$-OCH_3$	$-CH_3$	H	3.7 ± 0.1
13	$-CH_2OCH_2CH(CH_3)_2$	$-OCH_3$	H	$-OCH_3$	4.0 ± 0.1

Figure 2. Structural formula of tripodal hexadentate aminophenol ligands and octanol/water partition coefficients (*P*) for their ^{67}Ga-complexes.

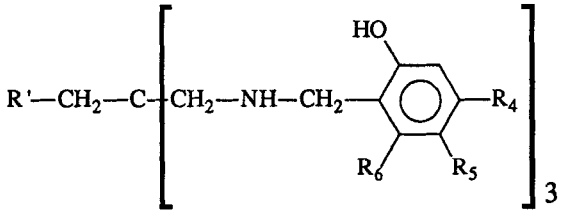

Ligand #	R'	R_4	R_5	R_6	*log P*
5	H	H	$-CH_3$	H	2.19 ± 0.02
6	$-NH_2$	H	H	H	1.60 ± 0.13
7	H	H	H	H	0.71 ± 0.03
8	$-OCH_2CH(CH_3)_2$	H	H	H	2.41 ± 0.01

Table 1. Myocardial Uptake of ^{67}Ga-Complexes in the Rat Following Intravenous Injection.

LIGAND	Percentage of Injected Dose in the Heart*		
	1 minute	5 minutes	60 minutes
1	0.96 ± 0.07	0.28 ± 0.04	0.008 ± 0.001
2	1.20 ± 0.03	0.45 ± 0.03	0.026 ± 0.005
3	0.59 ± 0.04	0.24 ± 0.01	0.009 ± 0.001
4	0.24 ± 0.03	0.088 ± 0.011	0.005 ± 0.001
5	0.36 ± 0.03	0.23 ± 0.02	0.054 ± 0.012
6	0.21 ± 0.02	0.065 ± 0.010	0.010 ± 0.002
7	0.28 ± 0.06†	0.18 ± 0.04†	0.04 ± 0.01†
8	0.56 ± 0.07	0.41 ± 0.08	0.10 ± 0.01
9	2.56 ± 0.19	1.08 ± 0.06	0.12 ± 0.02
10	2.08 ± 0.25	0.41 ± 0.05	0.19 ± 0.02
11	2.90 ± 0.35	0.86 ± 0.06	0.38 ± 0.03
12	3.04 ± 0.77	1.12 ± 0.05	0.36 ± 0.02
13	2.21 ± 0.18	1.59 ± 0.02	0.56 ± 0.04

*Values shown represent the mean ± standard deviation of data obtained from four (†three) rats.

1. Green M.A., Welch M.J., and Huffman J.C. - J. Am. Chem. Soc. 106:3689 (1984).
2. Green M.A., Mathias C.J., Neumann W.L., *et al.* - J. Nucl. Med. 34: 228 (1993).
3. Green M.A., Welch M.J., Mathias C.J., *et al.* - J. Nucl. Med. 26: 170 (1985).
4. Green M.A. - J. Labelled Comp. Radiopharm. 23: 1227 (1986).
5. Dunn T.J., Neumann W.L., Rogic M.M., and Woulfe S.R. - J. Org. Chem. 55: 6368 (1990).
6. Neumann W.L., Woulfe S.R., Rogic M.M., and Dunn T.J. - J. Nucl. Med. 31: 897 (1990).

Kinetics of Hybridization of MRNA of c-myc Oncogene with In-111 Labeled Antisense Deoxyoligonucleotide (INASDON) Probes by High Pressure Chromatography Technique. M.K. DEWANJEE, A.K. GHAFOURIPOUR, M. KAPADVANJWALA, A.N. SERAFINI, G.N. SFAKIANAKIS. Division of Nuclear Medicine, Department of Radiology, University of Miami, Miami, FL USA.

The selection of appropriate nucleotide sequence is of vital importance in inducing translational arrest, polymerase chain reaction and fluorescent in situ hybridization (ISH). ISH of probe with mRNA was carried out by Northern blotting technique. We recently prepared and used several radiolabeled antisense probes (In-111, Tc-99m, Ga-67, Sm-153) for noninvasive diagnosis of oncogenes (c-myc, e-erbB2, c-myb) in leukemia and solid tumors (1-8). Previously, separation of mRNA and Northern blotting of radiolabeled probe, autoradiography and densitometry were extensively used in this evaluation (7,8). We have developed the molecular sieving technique (high pressure liquid chromatography: gel-filtration with TSK-300 SW column) for the qantitation of hybridization of mRNA with In-111 labeled deoxyoligonucleotide; different length (12-25 mer) and sequence (sense, antisense and scrambled) of c-myc oncogene were evaluated by HPLC-hybridization technique.

The mRNA was purified from the P388 cells; P388 cells washed with phosphate-buffered saline and sucrose, were lysed with NP-40 and total RNAs, protein and DNA were separated by CsCl density gradient centrifugation (Beckman Inc., LT-55). The ribosomal RNA was separated from mRNA with polyadenylate tail, by oligo-deoxythymidylate conjugated cellulose column (Boehringer-Mannheim Inc., Germany). The murine leukemic cells (P388: log phase) and purified mRNA are incubated directly with In-111 antisense probe for 60 min at 37°C and the degree of hybridization was quantified by gel-filtration. The retention times of probe, mRNA and probe-mRNA complex were calibrated by injecting 10 μl of In-111 labeled probe, c-myc mRNA of interest and probe-mRNA-complex (Waters Inc., Model 600E, Detector 486). The radioactivity and absorbance were traced and peak areas were integrated for the amount of free and bound probe.

The kinetics of hybridization was studied by incubation of cytoplasmic extracts of c-myc mRNA with sense and antisense probes. The mRNA-probe complex, unbound radiolabeled oligonucleotide and degradation products, were analyzed by the HPLC analysis (size exclusion) technique; the retention time of the probe-mRNA complexes, probe and probe-fragments was 8.0-9.5, 16.1 and 17.0-18.0 minutes respectively. The integrated areas under the curve permitted the study of the kinetics of hybridization of antisense probe with c-myc mRNA and the hybridization reaches a saturation value at 45-50 minutes of incubation of cells, cell-lysate and purified mRNA. More than 70-80% of the antisense probe was bound to mRNA at 60 min. of incubation. On the other hand, there is very little binding of the sense probe with the c-myc mRNA. In addition to the pure probe and probe-mRNA complex, a small fraction of degraded probe and their bound fraction with mRNA, could also be detected with slightly lower values of the corresponding retention times. The absorbance values of mRNA, oligonucleotide and complexes at 254 nm, also corroborate the presence of these species in the incubated media. The column retention was also evaluated by measuring the injected and eluted radioactivity; about 95-98% of the radiolabeled probe and fragments and complexes is eluted from the HPLC column.

The hybridization of probe with mRNA and probe-uptake in intact cells followed parallel curves; the cellular binding is lagging behind the direct hybridization of probe with mRNA extracted from cell-lysate. Similar parallel curves were generated with several radionuclides and same probe sequence, suggesting that majority of cellular incorporation is due to hybridization of permeable probe with intracellular mRNA. In stead of purified mRNA, cell-lysate could also be used for following the kinetics of hybridization. Radiolabeled probe along with HPLC technique provided a simple, sensitive and quantitative technique for the evaluation of hybridization kinetics of probe with mRNA. Efficient and fast kinetics of hybridization suggested that antisense oligonucleotides may be suitable vehicle for DNA damage and tumor cell-killing by ß-emitting radionuclides.

References

1. Dewanjee M.K., Ghafouripour A.K., Werner R.K., Serafini A.N., Sfakianakis G.N. - Development of sensitive radioiodinated anti-sense oligonucleotide probes by conjugation technique. Bioconj Chem 2: 195-200(1992)
2. M.K. Dewanjee, G.K. Panoutsopoulos, A.K. Ghafouripour, M. Kapadvanjwala, T. Ionescu, A. Ganju-Krishan, S. Glenn, T. Boothe, R. Werner, R. Vargas-Cuba, A.N. Serafini, G.N. Sfakianakis. - Metabolic fate of indium-111 labeled anti-sense deoxyoligonu-cleotide (ASDON) in a pig model. Proc. Miami Bio/Technology Winter Symposium, January 17-22, 1993, p 112.
3. M. K. Dewanjee, A. K. Ghafouripour, M. Kapadvanjwala, R. Vargas-Cuba, G. Panoutsopolous, T. D. Ionescu, S. Glenn, A. N. Serafini, G. N. Sfakianakis - A new direct method of cell-labeling in whole blood by administration of In-111 labeled anti-sense oligonucleotide. NHLBI/AAMI Conferenece on Cardiovascular Science and Technology, Bethesda MD, Dec. 8-10 (1992) p 56.
4. Dewanjee M.K. Preiss I.L. - Decay of samarium isotopes: ^{140}Sm, ^{141m}Sm, ^{142}Sm and $^{143(m+g)}$Sm. J Inorg Nucl Chem 34: 1105-1117(1972)
5. Dewanjee M.K. and Kahn P.C. - Myocardial mapping techniques and the evaluation of In-113m labeled polymethylenephosphonate for myocardial imaging. Radiology 117: 723-726(1975)
6. Dewanjee M.K. - Radiolabeled antisense oligonucleotides: diagnosis and therapy. Diagnostic Oncology (1993)
7. Warren W.J. and Vella G. - Analysis of synthetic oligodeoxynucleotides by capillary gel electrophoresis and anion-exchange HPLC. BioTechniques 14: 598-606 (1993)
8. Crooke S.T. - Progress toward oligonucleotide therapeutics. pharmacodynamic properties. FASEB J 7:533-539 (1993)

Supports by NHLBI (HL47201, Shannon Award), NIH-NS22603-08, Baxter Healthcare Corporation, Department of Energy grant DE-FG05-88ER60728 and Florida High Technology and Industry Council are gratefully acknowledged.

Figure 1. Kinetics of intracellular hybridization of mRNA of c-myc oncogene with indium-111 labeled antisense deoxyoligonucleotide probes in leukemic cells (P388). The kinetics of AS probe-mRNA complex formation was studied from samples taken at 10, 20, 60, 90 and 120 minutes of incubation by HPLC with a TSK-300 column eluted by phosphate-buffered saline (0.1 M, pH: 7.4).

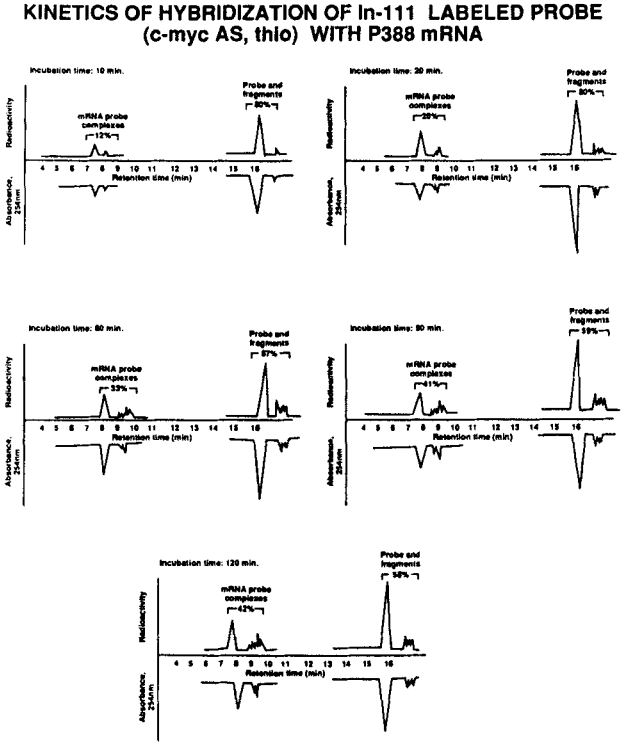

Gallium-67 Labelling of Antisense Deoxyoligonucleotide (GAASDON) Probes and Uptake in Leukemic Cells (P388). M.K. DEWANJEE, A.K. GHAFOURIPOUR, T. BOOTHE, W. MALLIN, L. WILLEM, A. GANJU-KRISHAN, M. SUBRAMANIAN, M. HANNA, M. KAPADVANJWALA, A.N. SERAFINI, G.N. SFAKIANAKIS. University of Miami and Mount Sinai Medical Center, Miami FL and Biotechnology Research Institute, Rockville MD.

The antisense nucleotide sequence complements the coding strand of DNA, selectively binds the strand of specific mRNA by base-pairing and interferes with its translation into protein. The antisense oligonucleotides are finding potential applications in biotechnology, pharmaceuticals and agricultural biotechnology. The c-myc oncogene is amplified in several types of cancer (leukemia, colon/rectum, breast, prostate and lung) making the c-myc mRNA a suitable cytoplasmic receptor-like target for noninvasive imaging of oncogene activation (1-6). Antisense probes have been labeled with radionuclides of In-111, Ga-67 and Tc-99m (1-5); these probes may be more specific than other conventional pharmaceuticals (6). The kinetics of uptake of Ga-67 labeled antisense (AS), sense (SN, control) and oxo and thio derivatives by P388 cells was evaluated. The 15-mer oligonucleotide sequence for the initiation-codon domain was synthesized, aminolinked [sense (SN) and antisense (AS) phosphodiester (O) and monothioester (S)] and coupled to isothiocyanates of DTPA and THOA (tetraethylene-hexaamineoctaacetate); aliquots (10μg) were lyophilized. Ga-67 citrate (5-10 mCi, Medi-Physics, Inc.) was oxidized with conc. nitric acid and the solution was evaporated to dryness and redissolved in sterile saline. Ga-67 (100-500 μCi) was chelated to probe (10 μg) and solution sterilized by membrane filtration (Figure 1); aliquots of 1-2 μCi (0.1 μg) was added to P388s cells ($10X^6$ cells/ml in log[L] and plateau[P] phase) and incubated at 37°C for 10, 20, 40 and 60 minutes, washed and cell-uptake CU(%) was shown in the following table:

	10 min,L	**60 min,L**	**10 min,P**	**60 min,P**
AS(S)	11.5±2.7	35.2±9.3	2.7±0.5	7.0±1.5
SN(S)	2.8±0.3	15.7±4.3	1.7±0.4	3.6±1.7
AS(O)	10.5±1.9	33.1±7.8	2.2±0.5	4.5±1.3
SN(O)	2.5±1.1	4.1±2.2	1.5±0.6	3.9±0.8

Labeled cells were lysed and radioactivity bound to membrane, total RNAs, mRNA, protein and DNA were separated by CsCl density gradient centrifugation, followed by oligo-dT column. The ribosomal RNA was separated from mRNA with polyadenylate tail, by oligo-deoxythymidylate conjugated cellulose column (Boehringer-Mannheim Inc., Germany); 20%, 2%, 78% and 40%, 9%, 51% of AS and S-probe were found associated with protein, DNA and RNA fraction respectively. More than 70-80% of the antisense probe was bound to c-myc specific mRNA. The cells in log phase with more mRNA copies hybridized more INASON probes than plateau phase cells; CU(%) of sense (O) and (S) probes was significantly lower ($p < 0.001$). The thio and oxo probes showed similar high CU(%) suggesting probe transport, hybridization for noninvasive imaging of proliferation.

The P388 log phase cells were grown in roller bottles in media (RPMI 1640) supplemented with 10% fetal bovine serum, 24 hours prior to experiments and used at a concentration of $(1.1\text{-}1.9)10^6$/ml. For plateau phase cultures, these cells are diluted 6-fold and cultured for 48 hours in serum supplemented media followed by 24 hour incubation in serum free media (RPMI and

antibiotics) and used at a density of (1.5-2.0)X10^6 cells/ml.

The kinetics of hybridization was studied by incubation of cytoplasmic extracts of c-myc mRNA with sense and antisense probes. The mRNA-probe complex, unbound radiolabeled oligonucleotide and degradation products, were analyzed by the HPLC analysis (size exclusion) technique; the retention time of the probe-mRNA complexes, probe and probe-fragments was 8.0-9.5, 16.1 and 17.0-18.0 minutes respectiovely. The integrated area under the curve permitted the study of the kinetics of hybridization of antisense probe with c-myc mRNA and the binding reaches a saturation value at 45 minutes. On the other hand there is very little binding of the sense probe with the c-myc mRNA. The low rate constant values for the sense probe also indicated lower level of binding. This new HPLC technique of hybridization study may permit evaluation of other oncogenes amplified in cancer cells and tumor tissues.

References

1. Dewanjee M.K. and Kahn P.C. - Myocardial mapping techniques and the evaluation of In-113m labeled polymethylenephosphonate for myocardial imaging. Radiology 117:723-726(1975)
2. Dewanjee M.K. Ghafouripour A.K. Werner R.K. Serafini A.N. Sfakianakis G.N. - Development of sensitive radioiodinated anti-sense oligonucleotide probes by conjugation technique. Bioconj Chem 2: 195-200(1992)
3. M.K. Dewanjee, G.K. Panoutsopoulos, A.K. Ghafouripour, M. Kapadvanjwala, T. Ionescu, A. Ganju-Krishan, S. Glenn, T. Boothe, R. Werner, R. Vargas-Cuba, A.N. Serafini, G.N. Sfakianakis. Metabolic fate of indium-111 labeled anti-sense deoxyoligonu-cleotide (ASDON) in a pig model. Proc. Miami Bio/Technology Winter Symposium, January 17-22, (1993) p 112.
4. Dewanjee M.K. - Radiolabeled antisense oligonucleotides: diagnosis and therapy. Diagnostic Oncology (1993) (Miami Symposium Supplement).
5. Dewanjee M.K. Beh B. Hnatowitch D.J. - Ga-68 labeled polymethylene phosphonate for positron scintigraphy. J Nucl Med 17: 1003-1007(1976)
6. Holman B.L., Kaplan W.D., Dewanjee M.K., Fliegel C.P., Davis M.A., Skarin A.T., Rosenthal D.S. and Chaffey J. - Tumor detection and localization with Tc-99m tetracycline. Radiology 117: 723-726(1975)

Supports by NHLBI (HL47201, Shannon Award), NIH-NS22603-08, Baxter Healthcare Corporation, Department of Energy grant DE-FG05-88ER60728 and Florida High Technology and Industry Council are gratefully acknowledged.

Figure 1. General scheme of radiolabeling of antisense deoxyoligonucleotide probes with DTPA-derivatives for labeling with Ga-67 radionuclide.

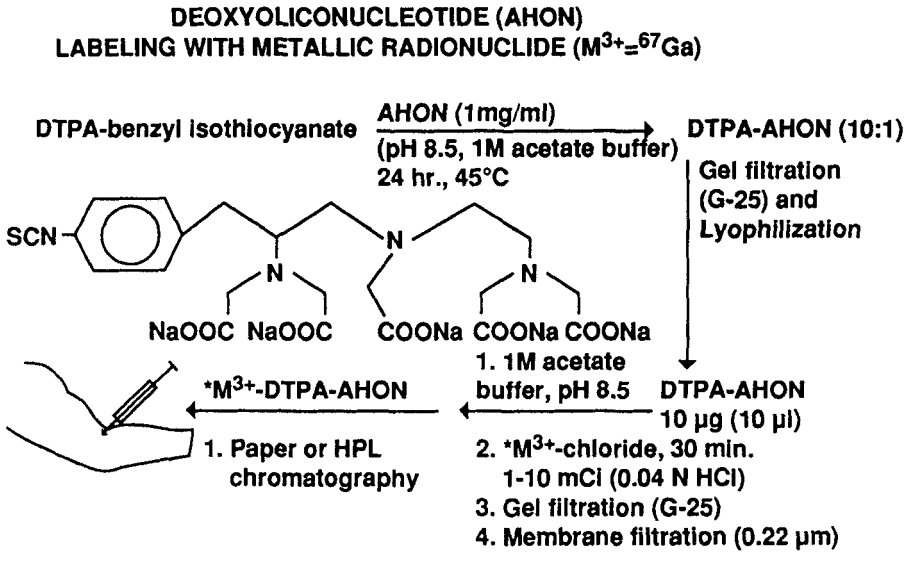

The Synthesis of DTPA-D-Phe^1-Octreotide by Solid-Phase Synthesis

W.B. Edwards, C.J. Anderson, M.J. Welch, C.G. Fields* and G.B. Fields*. Mallinckrodt Institute of Radiology, Washington University School of Medicine, St. Louis, MO 63110 and *Department of Laboratory Medicine and Pathology, University of Minnesota, Minneapolis, MN 55455.

The somatostatin analogue, octreotide (Sandostatin®), when conjugated to DTPA and labeled with ^{111}In, is a useful SPECT imaging agent of tumors containing somatostatin receptors (1). In the development of a somatostatin receptor imaging agent for PET, a relatively simple and inexpensive method for synthesizing octreotide-bifunctional chelate conjugates is desirable. Although octreotide is commercially available, the cost often prohibits the purchase of the amounts needed for the research and development of new conjugates. We have developed a solid-phase synthesis of DTPA-D-Phe^1-octreotide using Fmoc methodology.

The most challenging aspect in the development of a synthesis of an octreotide conjugate is the formation of the C-terminal alcohol. One method requires treatment of the resin with boron hydrides, cleaving the peptide from the resin and simultaneously forming the C-terminal alcohol (2). However, this method may be incompatible with carboxylate-containing bifunctional chelates conjugated prior to cleavage. Furthermore, reductive cleavage precludes the formation of the disulfide bond while the peptide is still on the resin. Another method requires the synthesis of a complex linking molecule where the C-terminal alcohol is attached to the linker via an acetal bond (3). This method involves a time-consuming, multi-step synthesis of the linker. The method we have developed is based on a previously published aminolysis by an amino-alcohol (4). In the synthesis of DTPA-D-Phe^1-octreotide, the target peptide is conveniently cleaved from the solid support by aminolysis with threoninol (Figure 1). The advantages of this technique are that aminolysis is compatible with bifunctional chelates and the disulfide bond can be formed while the peptide is on the resin.

FIGURE 1

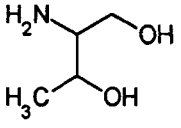

THREONINOL

The fully side-chain protected peptide (Figure 2) was assembled on a p-benzyloxybenzyl alcohol (Wang) resin by modified FastMoc® chemistry (5). Cyclization of the peptide was performed on-resin by oxidation with $Tl(TFA)_3$ in DMF. Cyclic anhydride of DTPA (cDTPAA) was added in portions until a Kaiser test was negative. The peptide was cleaved

from the resin by aminolysis using threoninol in DMF over 18 hours. After filtration from the resin, the reaction mixture was concentrated *in vacuo* and deprotected with 95% TFA in water. The product was purified by reversed-phase HPLC. The product was identified by comparing the retention time on reversed-phase HPLC to that of a DTPA-D-Phe^1-octreotide standard and by electrospray mass spectroscopy. The product was labeled with ^{111}In and eluted at the same time as a ^{111}In-DTPA-D-Phe^1-octreotide standard.

FIGURE 2

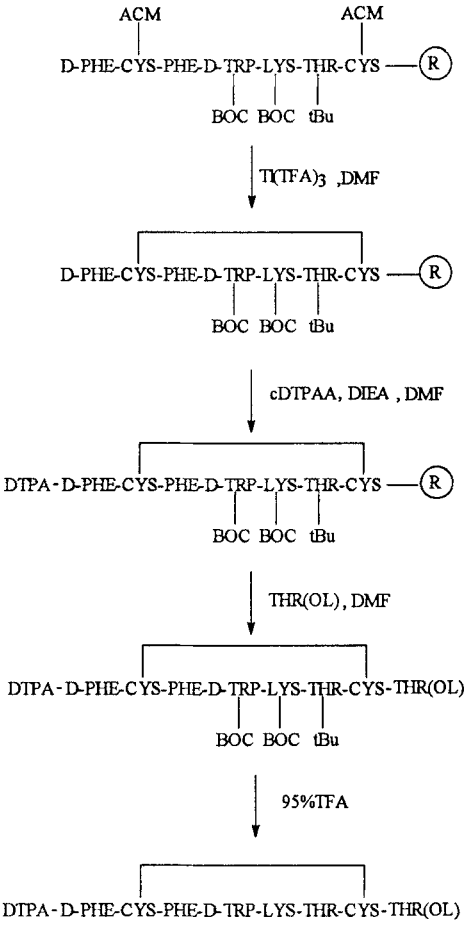

ACKNOWLEDGEMENTS

This work was supported by DOE grant DE-FG02-84ER60218 (MJW), NIH grant HL 13851 (MJW), NIH grant KD 44494 (GBF) and McKnight-Land-Grant Professorship (GBF). The authors wish to thank Gregory A. Grant, PhD., Dept. of Molecular Biology and Pharmacology, Washington Univ. School of Medicine, for the mass spectral data. We also thank Mallinckrodt Inc. for DTPA-D-Phe^{1}-octreotide (Octreoscan®).

REFERENCES

1. Bakker WH, Krenning EP, Reubi JC, et. al. Life Sci 49: 1593 (1991)
2. Stewart JM and Morris DH, Pennwalt Corporation, U.S. Patent 4254023 (1981)
3. Mergler M, Hellstern H, Wirth W, et. al., Poster, 12th American Peptide Symposium, Boston 292 (1991)
4. Fields CG, Fields GB, Nobel RL and Cross TA Int. J. Protein Peptide Res. 33:298 (1989)
5. Fields CG, Lovdahl CM, Miles AJ et. al. Biopolymers 33 : in press (1993)

In vitro and *in vivo* Evaluation of [^{64}Cu-CPTA-D-Phe^1]-Octreotide: An Agent for Quantitating Somatostatin Receptors with PET.

C.J. Anderson, W.B. Edwards, T.S. Pajeau, B.E. Rogers, K.R. Zinn*, H.V. Lee and M.J. Welch. Mallinckrodt Institute of Radiology, Washington University School of Medicine, St. Louis, MO 63110 and *University of Missouri Research Reactor, Columbia MO 65211.

The somatostatin analogue octreotide (Sandostatin®) has been labeled with ^{123}I ($T_{½}$ = 13 h)[1] and ^{111}In ($T_{½}$ = 67 h)[2] for SPECT imaging, as well as ^{68}Ga ($T_{½}$ = 1.1 h)[3] and ^{18}F ($T_{½}$ = 1.8 h) [4] for potential PET imaging of tumors. The best SPECT images of tumors in patients obtained after administration of ^{111}In-DPTA-D-Phe^1-octreotide were taken 24 hours post-injection because of the lower background activity in the body. The shorter half-lives of ^{68}Ga and ^{18}F may not allow for optimal imaging times when labeled to octreotide. The positron-emitting radionuclide ^{64}Cu ($T_{½}$ = 12.8 h) has been used to label the anti-colorectal carcinoma monoclonal antibody 1A3 and PET images of primary colon cancer tumors and metastases have been obtained in patients 24 hours post-injection.[5] The longer half-life of ^{64}Cu may be more suitable for PET imaging of somatostatin receptors in tumors. In this study ^{64}Cu has been labeled to octreotide that has been conjugated to the macrocyclic bifunctional chelate 4-[(1,4,8,11-tetraazacyclotetradec-1-yl)-methyl]benzoic acid (CPTA) (Figure 1). The synthesis of CPTA-D-Phe^1-octreotide and its labeling with ^{64}Cu along with an *in vitro* and *in vivo* analysis are described. The *in vitro* and *in vivo* results are compared to results obtained with ^{111}In-DPTA-D-Phe^1-octreotide.

FIGURE 1

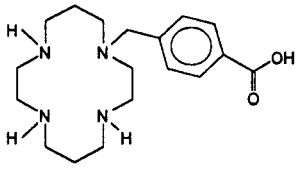

CPTA

The bifunctional chelate CPTA was synthesized by the one-step procedure of Studer and Kaden.[6] CPTA-octreotide was synthesized from commercially available octreotide as shown in Figure 2. The N-terminal amine of the Boc-protected octreotide was conjugated to the carboxylic acid on CPTA with diisopropylcarbodiimide (DIC) in DMF using hydroxybenzotriazol (HOBT) as a catalyst. The product, CPTA-D-Phe^1-octreotide, was identified by electrospray mass spectrometry. CPTA-octreotide was labeled with ^{64}Cu-acetate in 0.1 M ammonium acetate buffer, pH 5.5. ^{64}Cu-CPTA-octreotide was prepared in > 98% yield with a specific activity of > 400 μCi/μg.

FIGURE 2

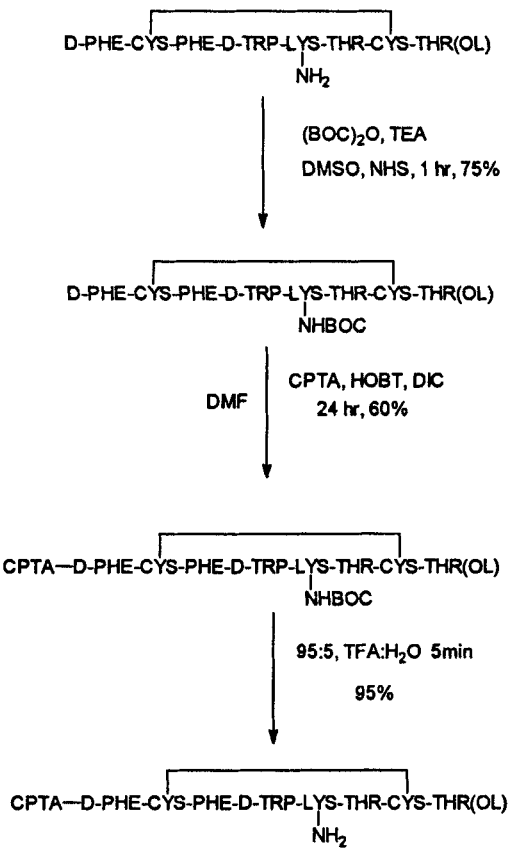

The somatostatin receptor binding characteristics of both ^{64}Cu-CPTA-D-Phe^1-octreotide and ^{111}In-DTPA-D-Phe^1-octreotide were investigated in AtT20 rat pituitary tumor cell membranes. A preliminary Scatchard analysis showed comparable binding between the two radiolabeled octreotide compounds, with a K_d of 4.7 nM for ^{111}In-DTPA-D-Phe^1-octreotide and a K_d of 4.3 nM for ^{64}Cu-CPTA-D-Phe^1-octreotide.

Biodistribution was carried out in normal Sprague-Dawley rats. The rats were co-injected with ^{64}Cu-CPTA-D-Phe^1-octreotide and ^{111}In-DTPA-D-Phe^1-octreotide. The blood clearance of the two agents was similar out to three hours post-injection. After three hours, the ^{111}In-DTPA-D-Phe^1-octreotide continued to clear from the blood, whereas the amount of ^{64}Cu-

CPTA-D-Phe^1-octreotide in the blood remained constant at approximately 0.1 % ID/g. The uptake of ^{64}Cu-CPTA-D-Phe^1-octreotide in the adrenal glands, an organ known to contain somatostatin receptors, was 2.5 times that of ^{111}In-DTPA-octreotide at times 1 and 24 hours. As previously shown[7] there is minimal observed ^{111}In-DTPA-D-Phe^1-octreotide activity in the liver; however, there is some retention in the kidneys (1.53 $\pm$ 0.36 %ID/g at 24 hours post-injection). ^{64}Cu-CPTA-D-Phe^1-octreotide is retained both in the liver (3.50 $\pm$ 0.15 %ID/g at 24 hours) and kidneys (2.72 $\pm$ 0.45 %ID/g at 24 hours).

The synthesis of CPTA-D-Phe^1-octreotide and labeling with ^{64}Cu at high specific activity for potential PET imaging of somatostatin receptors has been described. Although ^{64}Cu-CPTA-D-Phe^1-octreotide has an affinity for the somatostatin receptor similar to ^{111}In-DTPA-D-Phe^1-octreotide both *in vitro* and *in vivo*, the high liver and kidney uptake *in vivo* make this agent less than desirable for PET imaging in humans. Further investigation of different macrocyclic bifunctional chelate-octreotide conjugates for complexing ^{64}Cu are being performed.

Acknowledgements: This work was supported by DOE grant DE-FG02-84ER60218 and a grant from Mallinckrodt Medical, Inc. The authors would like to thank Edward Deutsch, Ph.D. and Mallinckrodt Medical, Inc. for the gifts of Sandostatin® and DTPA-D-Phe^1-octreotide (Octreoscan®).

REFERENCES

1. Kwekkeboom D.J., Krenning E.P., Breeman W.A.P., et al. - J. Nucl. Med. 32:1845 (1991).
2. Krenning E.P., Bakker W.H., Kooij P.P.M., et al. - J. Nucl. Med. 33:652 (1992).
3. Smith-Jones P., Stolz B., Albert R., Reist H., Bruns C. and Mäcke H. - J. Lab. Comp. Radiopharm. 32:422(1993).
4. Wester H.J., Bruns C. and Stöcklin G. - J. Nucl. Med. 34:80P(1993) (abstract).
5. Philpott G.W., Schwarz S.W., Anderson, C.J., et al. - J. Nucl. Med. 34:81P(1993) (abstract).
6. Studer M. and Kaden T.A. - Helv. Chim. Acta 69:2081(1986).
7. Bakker W.H., Krenning E.P., Reubi J.-C., et al. - Life Sciences 49:1593 (1991).

Fluorine-18 Labeled Chemotactic Peptide: A Potential Agent for the PET Imaging of Focal Infection.

VAIDYANATHAN, G.; AFFLECK, D.A.; WELSH, P. and ZALUTSKY, M.R.
Department of Radiology, Duke University Medical Center, Durham, N.C. 27710.

A promising approach for labeling leukocytes to image infection or inflammation is to use chemotactic peptides. Fischman et al. (1) have labeled a number of chemotactic peptides with In-111 and demonstrated the feasibility of imaging focal *E. coli* infections in the rat. Recently, these investigators also have reported successful labeling of a chemotactic peptide with Tc-99m and its suitability for imaging focal inflammation in non-human primates (2). Because of the imaging advantages inherent in PET, we were interested in developing an approach for labeling chemotactic peptides with a positron-emitting nuclide. Previously, we have developed a method for the fluorine-18 labeling of monoclonal antibodies using *N*-succinimidyl 4-[^{18}F]fluorobenzoate, SFB (3). In the present study, we report on the use of a modification of this method to label a chemotactic peptide, *N*-formyl-norleucyl-leucyl-phenylalanyl-norleucyl-tyrosyl-lysine (FNleLFNleYK) with F-18 and describe its preliminary *in vitro* and *in vivo* evaluation.

The unlabeled fluorinated peptide was prepared by reacting FNleLFNleYK with an excess of SFB in dimethylformamide (scheme 1). Using human polymorphonuclear leukocytes (PMN), it was shown that increasing concentrations of this modified peptide displaced binding of [^{3}H]FMLF chemotactic peptide with an IC_{50} value of 49.8 nM. In comparison, the IC_{50} value for FNleLFNleYK was 10.7 nM, suggesting a reduction in binding affinity due to SFB conjugation. However, in another assay, the IC_{50} value for superoxide production for the fluorinated peptide was 4.2 nM. For FNleLFNleYK the corresponding value was 6.1 nM, suggesting less of a perturbation due to peptide modification.

For F-18 labeling, an improved method of SFB preparation was utilized. Originally, a reaction time of 25 min was used for the fluorodequaternization step (3). With a reaction time of only 5-8 min, identical yields were obtained. Di-*N*-succinimidylcarbonate/pyridine reagent converted 4-[^{18}F]fluorobenzoic acid to its *N*-succinimidyl active ester in 80-100% yield in 1-3 min at 150°C. Using a 25-30 mM solution of the peptide in DMF (10μL), more than 80% radiochemical yield was obtained in 5 min for its reaction with [^{18}F]SFB. The total time for the preparation of the F-18 labeled peptide is 100 min and the maximum specific activity attained so far is 200-300 Ci/mmole.

Binding of the F-18 labeled peptide to human PMN was 25% *in vitro*. This binding was displaceable; binding could be reduced to half-maximal levels with 840 nM of the unlabeled peptide. A potential problem with using chemotactic peptides is their ability to induce severe neutropenia. To investigate this possibility, mice were given 20 μCi of F-18 labeled chemotactic peptide and white blood cell counts were determined prior to and serially after injection. As shown in Figure 1, the F-18 labeled chemotactic peptide preparation did not cause neutropenia. The biodistribution of the labeled peptide was measured in normal mice (Table 1). As expected (1), rapid clearance of activity was seen except in kidneys and small intestine. The activity cleared from the blood with a half-life of 20 min. These results suggest that F-18 labeled chemotactic peptides warrant further investigation as agents for imaging focal infections using PET.

REFERENCES

1. Fischman, A.J., Pike, M.C., Kroon, D., Fucello, A.J., Rexinger, D., tenKate, C., Wilkinson, R., Rubin, R.H. and Strauss, H.W. *J. Nucl. Med.* 1991; 32:483-491.

2. Fischman, A.J., Rauh, D., Solomon, H.F., Abrams, M.J., Babich, J.W., Kroon, D., Strauss, H.W. and Rubin, R.H. *J. Nucl. Med.* 1993; 34:104P.

3. Vaidyanathan, G. and Zalutsky, M.R. *Nucl. Med. Biol.* 1992; 19:275-281.

Table 1. Tissue Distribution of [^{18}F]FNleLFNleYK-SFB in Normal Mice
% Injected Dose/Organ*

Tissue	5 min	30 min	60 min	120 min
Liver	16.34±2.86	1.89±0.62	0.51±0.35	0.46±0.34
Spleen	0.26±0.07	0.07±0.03	0.02±0.01	0.40±0.07
Lungs	0.91±0.31	0.23±0.09	0.08±0.02	0.10±0.04
Heart	0.29±0.05	0.04±0.02	0.02±0.01	0.01±0.02
Kidneys	16.28±1.31	3.91±0.95	1.57±0.66	0.30±0.04
Stomach	0.90±0.18	0.33±0.21	0.08±0.06	0.05±0.01
Small Intestine	4.68±0.98	8.16±1.00	5.73±1.38	0.84±0.53
Large Intestine	1.06±0.50	0.20±0.08	0.68±0.86	2.15±1.50
Muscle	10.87±2.65	2.82±1.00	1.23±0.45	0.96±0.56
Bone†	6.88±0.23	2.73±1.30	0.50±0.21	0.84±0.39
Blood	6.06±0.95	1.09±0.38	0.24±0.16	0.09±0.05
Testicles	0.23±0.29	0.09±0.02	0.04±0.01	0.04±0.27

*Mean ± S.D. (n = 6)
†n = 3

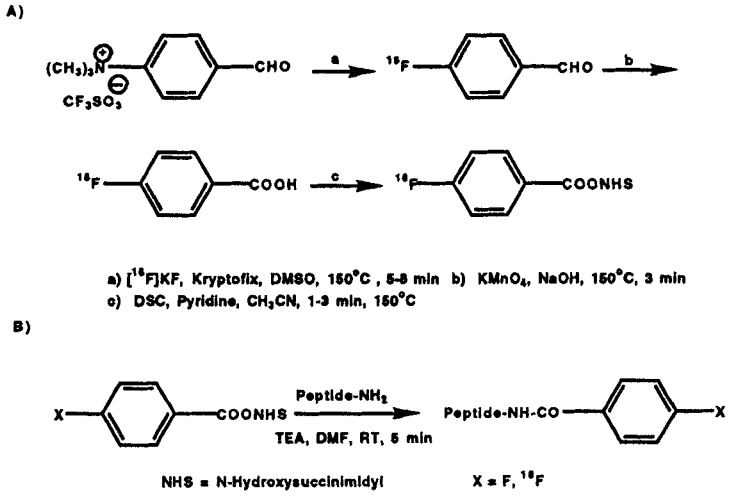

Scheme 1. Synthesis of [^{18}F]ForNleLFNleYK-SFB

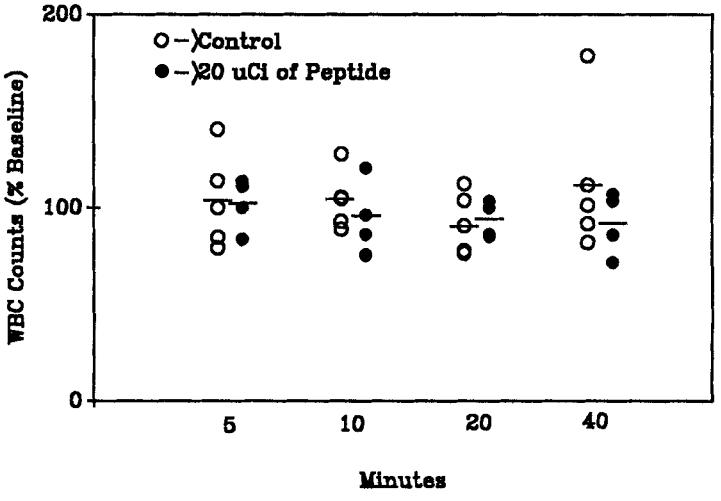

Figure 1. Effect of [^{18}F]ForNleLFNleYK on WBC Counts

A Novel Radioiodination Reagent for Antibodies with an Ester Bond to Release an Iodohippuric Acid. Y. Arano[1], K. Wakisaka[1], Y. Ohmomo[2], T. Mukai[1], T. Uezono[1], H. Motonari[1], H. Sakahara[3], J. Konishi[3], C. Tanaka[2], and A. Yokoyama[1]. Faculty of Pharmaceutical Sciences[1] and Medicine[3], Kyoto University, Sakyo-ku, Kyoto 606, and Osaka University of Pharmaceutical Sciences[2], Matsubara, 580, Japan.

Development of radiolabeled antibodies to induce target selective radioactivity localization has been a subject of great importance for radioimmunoimaging and radioimmunotherapy. Recently, we have shown that conjugation of a hippurate-like radiometal chelate proximal to the antibody via an ester bond enhanced the target/non-target radioactivity ratio without reducing target radioactivity delivery (1). These results stimulated us to expand this design to other radionuclides of potential clinical applications. We selected a radioiodine as the radionuclide, and designed a novel radioiodinating reagent with an ester bond to release *meta*-iodohippuric acid. This reagent, N-[3-(tri-n-butylstannyl)hippuriruoxyethyl]maleimide (HIM) (Fig. 1), consists of a maleimide group for site-specific and proximal attachment to proteins, organotin moiety for selective and high yield radioiodination and an ester bond to release *meta*-iodohippuric acid, a compound of high urinary excretion with stable C-I bond against *in vivo* deiodination (2).

The synthetic procedure for HIM is shown in Fig. 1. The hydroxy group of N-hydroxyethylmaleimide, prepared by a two-step reaction from maleimide, was activated with trifluoromethanesulfonic anhydride to form an ester bond with Boc-glycine. After deprotecting the Boc group, the amine residue was reacted with N-succinimidyl 3-(tri-n-butylstannyl)benzoate (ATE) (2), and subjected to silica gel column chromatography to produce HIM as a colorless oil.

Radioiodination of HIM was carried out with ^{131}I in the presence of N-chlorosuccinimide at room temperature for 45 min. After the addition of $NaHSO_3$ to neutralize the oxidant, the reaction mixture was evaporated to dryness under a stream of nitrogen. For the biological evaluation of HIM, galactosyl-neoglycoalbumin (NGA) (3) and monoclonal antibody against osteogenic sarcoma (IgG_1, OST7) were labeled with ^{131}I-HIM. Prior to conjugation with ^{131}I-HIM, NGA or OST7 was treated with dithiothreitol or mercaptoethanol, respectively to generate thiol groups. Conjugation was carried out at pH 6.0, followed by purification with Sephadex G-25 column chromatography. For comparison, NGA and OST7 were also conjugated with ^{131}I-ATE.

In biodistribution studies, ^{131}I-HIM-NGA demonstrated a faster clearance rate from the parenchymal cells of the liver than that of ^{131}I-ATE-NGA (Fig. 2). At 6 h post-injection of ^{131}I-HIM-NGA and ^{131}I-ATE-NGA, 78.4 % and 63.2 % of injected radioactivity were excreted in the urine, respectively. Analyses of urine samples after injection of ^{131}I-HIM-NGA indicated that all the radioactivity was excreted as the *meta*-

iodohippuric acid. No significant differences were observed in radioactivity localization in the neck (thyroid) and stomach between the two ^{131}I-labeled NGA. In biodistribution of radiolabeled OST7 (Fig. 3), ^{131}I-HIM-OST7 indicated a comparable blood clearance of radioactivity to ^{131}I-ATE-OST7 up to 6 h post-injection. After this post-injection time, a faster radioactivity clearance rate from blood was observed with ^{131}I-HIM-OST7.

The gathered results indicate that while the ester bond of HIM has a practical stability in plasma, it was cleaved rapidly after accumulation in non-target tissues, followed by the excretion of *meta*-iodohippuric acid in urine as an intact form. Such chemical and biological characteristics of HIM would be promising as an iodination reagent of antibodies for radioimmunoimaging and radioimmunotherapy.

References

(1) Arano Y., Inoue T., Mukai T., et al. J. Nucl. Med. **34**, 59P (1993).
(2) Zalutsky MR. and Narula AS. Appl. Radiat. Isot. **38**, 1051-1055 (1987).
(3) Ashwell G. and Haford J. Ann. Rev. Biochem. **51**, 531-554 (1982).

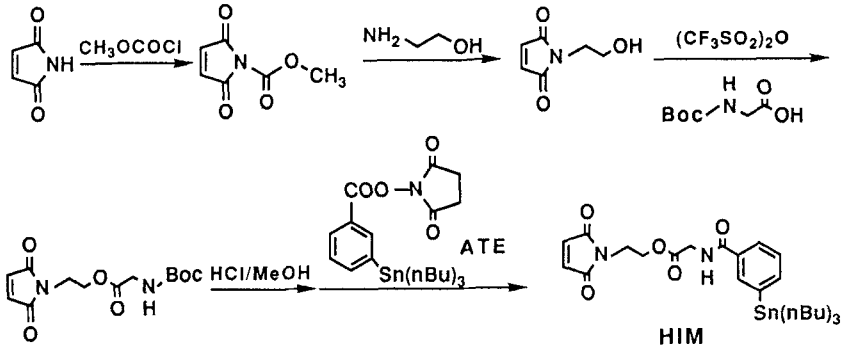

Fig. 1 Synthesis of N-[3-(tri-n-butylstannyl)hippuriruoxyethyl]maleimide (HIM)

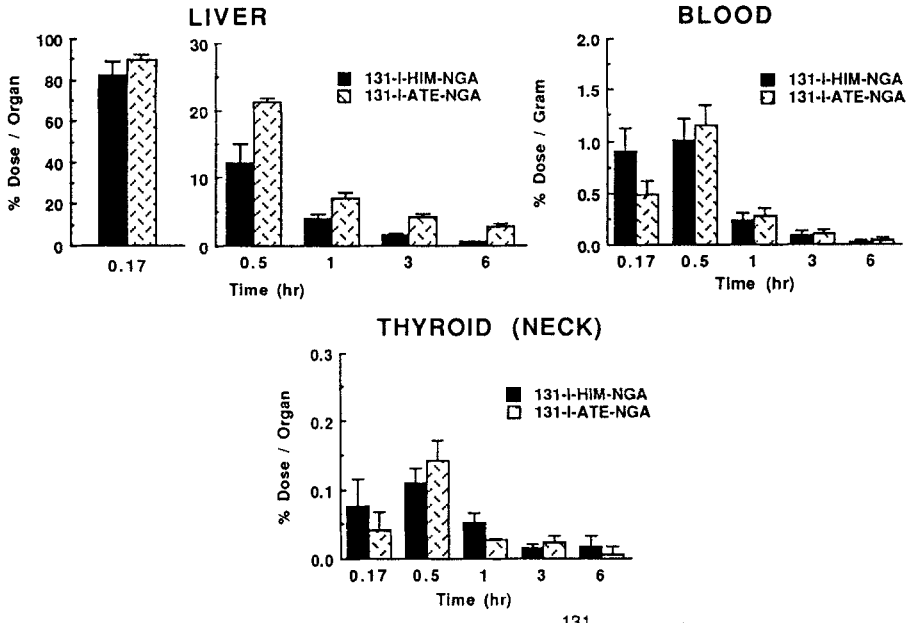

Fig. 2 Biodistribution of radioactivity after injection of ^{131}I-HIM-NGA and ^{131}I-ATE-NGA in mice

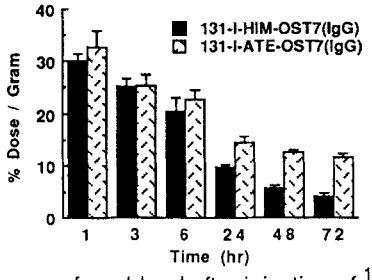

Fig. 3 Radioactivity clearance from blood after injection of ^{131}I-HIM-OST7 and ^{131}I-ATE-OST7 in mice

A Novel Bifunctional Chelator for Labelling Proteins with ^{64}Cu and ^{67}Cu

SCHMIDT, P.; SMITH, S. V.; DI BARTOLO, N., LAMBRECHT, R. M. ;
Biomedicine and Health Program, Australian Nuclear Science Technology Organisation, Menai, 2234, N.S.W., Australia.

In recent years considerable effort has been directed towards the synthesis of bifunctional chelating agents for the coupling of radiometals to proteins for tumour targetting. Of particular interest is the design of chelators for radiolabelling with copper for use in diagnostic and therapeutic applications.[1,2,3] Copper-64 ($t_{1/2}$ = 12.4 h, β^+) for use in PET imaging, while copper-67 ($t_{1/2}$ = 61.9 h, γ = 184.6 KeV, β^- = 391 KeV, 57%) is effective in therapy and SPECT imaging. The present study involves a high yielding synthesis of a novel di-amino-hydroxyaryl containing derivative of EDTA (DAHA-EDTA) and its radiolabelling chemistry.

The first step in the synthesis involves the refluxing of EDTA anhydride in the presence of 4-nitro-2-amino-phenol in acetonitrile to produce the dinitro derivative (DNHA-EDTA) in > 95% yield. This precursor is then reduced in the presence of activated palladium charcoal with sodium borohydride under an inert atmosphere at room temperature. The reaction mixture is acidified and the catalyst removed. The final product (2) is obtained with a yield >90 % (refer Scheme 1).

The ^{67}Cu complexes of DAHA-EDTA, DNHA-EDTA and the parent ligand (DNP-EDTA) were prepared. Copper-67 in sodium acetate (0.2M, pH 4.5) was added to a solution of the ligand at metal:ligand ratio of 4:1 and allowed to react at RT for 15 min. For each ligand in excess of 95% of the ^{67}Cu was incorporated and verified by instant thin layer chromatography-silica gel (ITLC-SG) using a ethanol:water mobile phase (9:1).

Serum stability was determined over a 24 hr period for the copper complex of DHA-EDTA. Separation of radioactive species by size exclusion chromatography demonstrated that the ^{67}Cu complex was stable during that period (Fig. 1). The biodistribution of the ^{67}Cu complex of DAHA-EDTA was determined in balb/c mice. Rapid renal clearance of the complex was observed.

The ^{67}Cu labelling of proteins (eg. HSA and IgG, $F(ab')_2$ fragment) with the new chelator DAHA-EDTA was accomplished. The procedure involved the addition of ^{67}Cu DAHA-EDTA complex in sodium acetate to protein (4 mg/ml) in phosphate buffered saline, in the presence of an excess of 1-ethyl-3-(3-dimethylaminopropyl) carbodiimide. The reaction mixture was left at 37°C for 1 hr. The ^{67}Cu- labelled protein was then purified by gel filtration chromatography.

As the ligand DAHA-EDTA has two anilino nitrogens which may be involved in linking to the protein, it was important to establish if any cross-linking of protein molecules had occurred. The purified ^{67}Cu- labelled protein was characterized by HPLC using a size exclusion column Biorad Bio-sil Sec-250. No evidence of cross-linking of the proteins was observed.

The study shows that DAHA-EDTA may be prepared in high yield, forms complexes with ^{67}Cu rapidly in high radiochemical purity and is stable in serum. Efficient radiolabelling of protein has been demonstrated and hence illustrates the potential this ligand has for use in tumour targetting. Further work will involve the use of DAHA-EDTA for the radiolabelling of monoclonal antibodies and other site specfic proteins.

References:

1. Anderson, C.J. et al, *J. Nucl. Med.*, 1992, **33**, 1685.
2. Smith-Jones, P.M. et al, *Bioconjugate Chem.*, 1991, **2**, 415.
3. Morphy, R.J. et al, *J. Chem. Soc., Perkin Trans.*, 1990, **2**, 573.

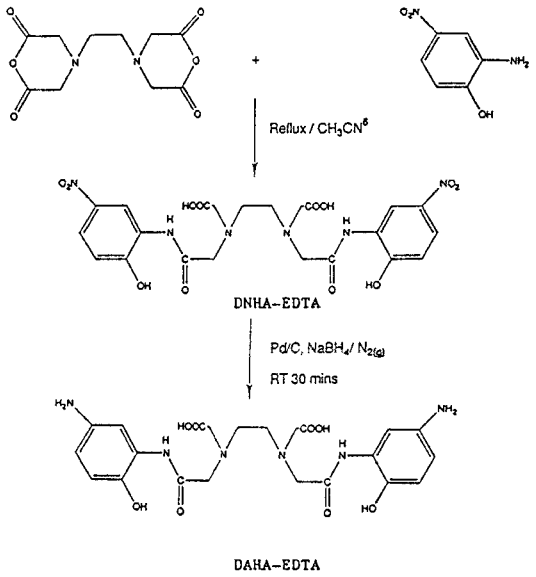

SCHEME 1.

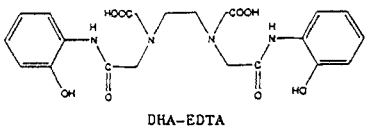

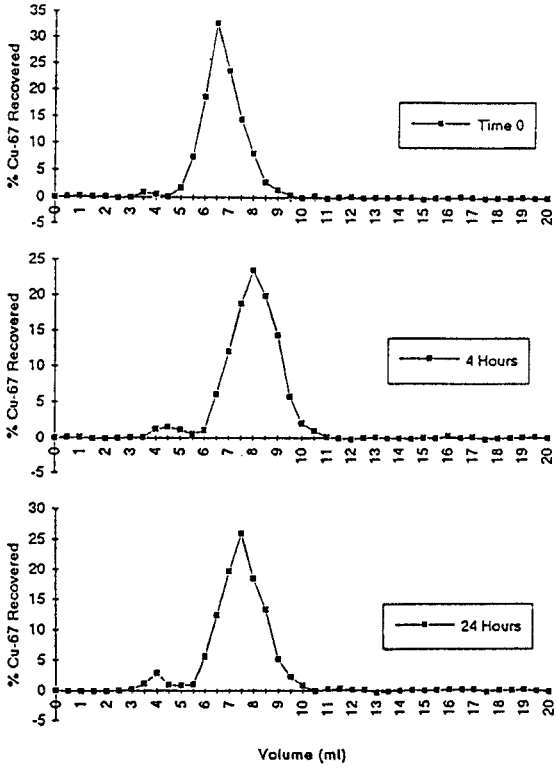

Figure 1. Selected serum stability data.

Development and Evaluation of Copper-67 Labeled DOTA and TETA Immunoconjugates for Radioimmunotherapy

MAUSNER, L.F.; SRIVASTAVA, S.C.; KOLSKY, K.L; MEASE, R.C.; JOSHI, V.; MEINKEN, G.E.; KURCZAK, S.; CHATAL*, J.F. AND STEPLEWSKI**, Z. Medical Department, Brookhaven National Laboratory, Upton, NY 11973, USA, *INSERM, Unit 211, University of Nantes, Nantes, France; **Wistar Institute, Philadelphia, PA, USA.

The radionuclide ^{67}Cu ($t_{1/2}$ 2.6d, $E\beta$ avg 141 keV, $E\gamma$ 184 keV) is attractive for radioimmunotherapy (1). For therapy, large amounts of radioactivity with high specific activity and low metal impurity levels are required. We report here developments to improve the ^{67}Cu production yield and metal content. We also report ^{67}Cu labeling and in-vivo results with an anti-CEA monoclonal antibody. Two bifunctional chelating agents (BCA), 1,4,7,10-tetraazacyclododecane and 1,4,8,11-tetraazacyclotetradecane-N,N',N'',N'''-tetraacetic acid (DOTA and TETA respectively), synthesized with a simple, large scale method, and functionalized as mono-NHS ester using one of the carboxylate groups (2) were used. To increase production yield, we changed from a single 35g ZnO target to two Zn metal powder targets, 50g each. This straightforward modification caused multiple problems in processing chemistry. The existing method (3) consists of extracting Cu into dithizone in CCl_4, followed by extraction of ^{67}Ga into isopropyl ether, and anion exchange elution to remove remaining Zn, Co, Mn and Fe isotopes. This method has been modified by washing the dithizone/CCL_4 after Cu extraction with 0.5N HCl to remove extra Zn, and fuming the solution after the ether extraction with HNO_3/HCl to destroy traces of ether and dithizone. We also removed all Cu components from the hot cells and used closed vessels whenever possible. The entire separation scheme is shown in Figure 1. The overall Zn separation factor has improved to $2.5x10^{-8}$. The average Cu recovery improved 15%, and the average specific activity improved 20% to ~2.0 mCi/μg. The production yield increased from 115mCi to 530mCi at EOB. Further improvement of a factor of 2.5 in yield and specific activity can be obtained with the proposed upgraded BLIP facility.

Labeling of the anti-CEA F(ab')$_2$ fragment was typically accomplished as follows. To approximately 300μg of the anti-CEA F(ab')$_2$-BCA conjugate (1.5-3 BCA/MAb) in 0.1M $NaHCO_3$ buffer, pH 8.2, were added an acetate buffer pH 5.5, and ~10-25μl of the $^{67}CuCl_2$ (0.5-5.0mCi) solution in 0.1M HCl. The mixture, final pH ~7.5, was incubated for 2h at 25°C. Ten μl of 0.05M EDTA was then added and the mixture allowed to react for 10 min to chelate unbound or nonspecifically bound copper. Purification was carried out using size exclusion HPLC (Zorbax GF-250; 0.1M phosphate, pH 7.0) to give the monomeric labeled conjugate. Labeling yields were 90±5%, the in-vitro serum stability at 4d was ~98%, and the retention of immunoreactivity was 80±10%. In nude mice xenografted with LS-174T human tumor cells, tumor (T) uptake (% injected dose per g) at 24 and 96h, respectively, was as follows: DOTA-1NHS, 32.4 and 14.6; TETA-1NHS, 35.7 and 17.1. The liver uptake of DOTA-NHS conjugate was slightly higher than that of the TETA-NHS conjugate whereas the opposite was true for the kidneys. The data are summarized in Table 1. This study demonstrates that ^{67}Cu can be produced in greater quantities with good radiopurity and specific activity, and that high tumor uptake and favorable tumor to blood, liver, and kidney ratios make the ^{67}Cu-DOTA (or TETA) anti-CEA (Fab')$_2$ system worthy of further investigation for radioimmunotherapy.

1. Mausner, L.F.; and Srivastava S.C. Med. Phys. 20:503 (1993).
2. Mease, R.C.; Chinol, M.; Mausner, L.F.; Steplewski, Z; and Srivastava, S.C.; J. Nucl. Med. 33:942 (1992).
3. DasGupta, A.K.; Mausner, L.F.; Srivastava, S.C. Appl. Radiat. Isot. 42:371 (1991).

Work supported by the US Department of Energy under Contract No. DE-AC02-76CH00016 and by the NCI under Grant No. U01 CA51958-03. The anti-CEA antibody was supplied by J.C. Saccavini, Compagnie ORIS Industrie, Gif Sur Yvette, France.

Figure 1. Separation of NCA ^{67}Cu from Zn Metal and Oxide Targets

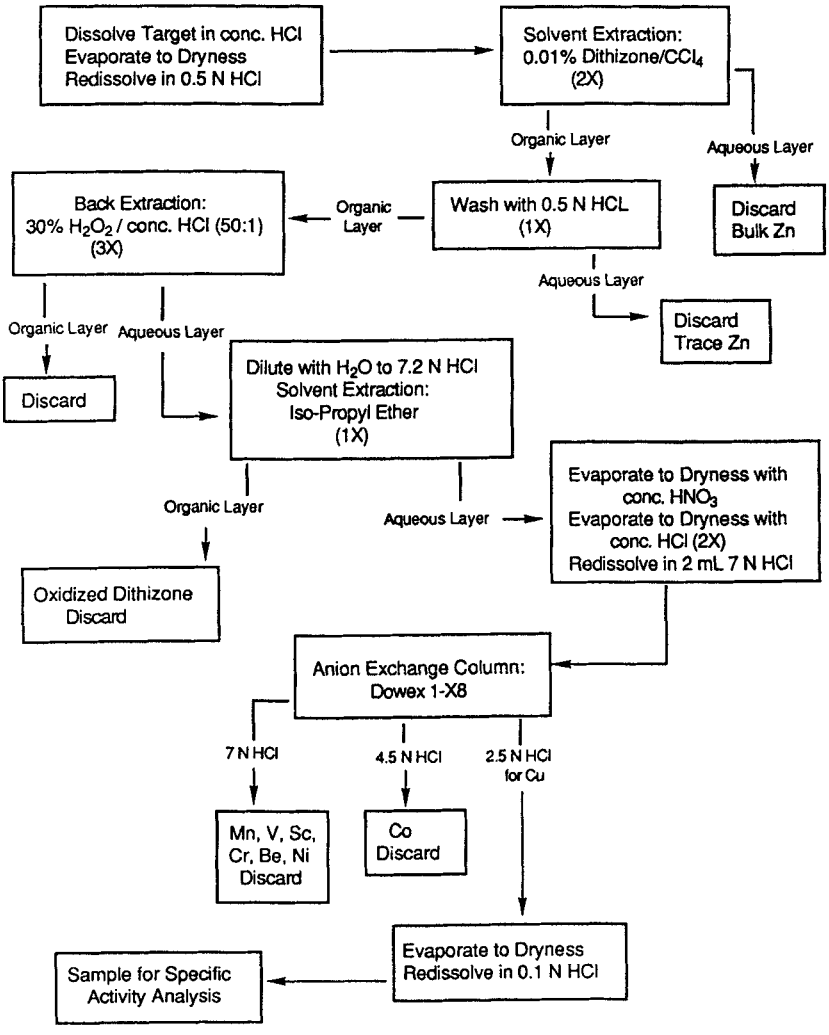

Table 1. Biodistribution (% Dose/g) of ^{67}Cu Labeled Anti-CEA $F(ab')_2$ Immunoconjugates in Nude Tumor Mice*

Ligand	Time (Hr)	Tumor	Blood	Liver	Kidney	Whole Body (% Dose)
DOTA-1NHS	24	32.36 ± 1.94 --	6.16 ± 0.14 (5.2)	14.74 ± 0.48 (2.2)	4.78 ± 0.10 (6.8)	92 ± 3
	96	14.60 ± 0.94 --	0.72 ± 0.05 (20.3)	7.01 ± 0.08 (2.1)	4.11 ± 0.24 (3.6)	50 ± 4
TETA-1NHS	24	35.68 ± 2.11	4.73 ± 0.38 (7.5)	10.44 ± 0.32 (3.4)	12.84 ± 1.41 (2.8)	90 ± 3
	96	17.06 ± 1.84	0.46 ± 0.02 (37.2)	5.34 ± 0.62 (3.2)	8.59 ± 0.45 (2.0)	44 ± 4

*LS-174T tumor xenografts; n = 5. Tumor to organ ratios in parentheses

A Simple and Efficient Method of Antibody Labelling with Zirconium

MEIJS[1] W.E., HERSCHEID[1] J.D.M., HAISMA[2] H.J., WIJBRANDTS[1] R. and PINEDO[2] H.M. [1]RadioNuclideCentre(RNC), Free University, [2]Department of Oncology, Free University Hospital, Amsterdam, The Netherlands.

With the increasing interest in PET-studies, there is need for a method to label proteins, for instance antibodies, with positron emitters. The labelled antibodies might be useful for non-invasive quantitative measurements of the biodistribution of these conjugates in patients, necessary for dosimetric calculations in radioimmunotherapy. With respect to the biological half-life of antibodies, especially positron emitters with a physical half-life in the order of days would be suitable for this purpose. ^{89}Zr with a half-life of 78.4 hours has the necessary characteristics to be a good candidate for labelling antibodies: it decays for 23% by positron emission to stable ^{89}Y with a positron energy of 900 keV.
Proteins can be labelled with metal ions making use of bifunctional chelating agents. Desferal (Df) is a promising chelating agent for labelling proteins with ^{89}Zr, because it forms very stable complexes with Zr. These complexes are formed efficiently and fast [1].
In this report we describe a method to label the antibody 323A3 with Zr by using the Df-approach. For these experiments ^{88}Zr was used as a tracer in stead of ^{89}Zr because of its more convenient half-life for *in vitro* experiments ($t_{1/2}$ = 83.4 days).

For the coupling of Df to the antibody 323A3, both Df and the antibody were modified (scheme 1). Maleimide groups have been incorporated into the protein with the aid of succinimidyl 4-(N-maleimidomethyl)cyclohexane-1-carboxylate (SMCC). The amino group of Df was converted into a thioester with N-succinimidyl S-acetylthioacetate (SATA). This thioester of Df was converted into the free thiol with hydroxylamin to react with the maleimide groups of the antibody. The excess of Df was removed by gelfiltration and the antibody solution was freeze dried. These modification steps were also performed with ^{125}I-labelled 323A3. Compared with the unmodified I-labelled antibody, no detectable loss of immunoreactivity was observed .

^{88}Zr was produced by a (p,2n)reaction on ^{89}Y, separated from Y and other metal ions with a hydroxamate column and dried under vacuum. The previously modified antibody was dissolved in 0.1 M ammonium acetate pH=5 at a final protein concentration of 0.5 mg/ml and added to the ^{88}Zr. Non-specificly bound Zr could be removed by addition of citrate, while the citrate did not remove the Df-bounded ^{88}Zr. The percentage of ^{88}Zr bound to the protein was determined by ITLC and gelfiltration and found to be more than 95% after 1 hour of labelling.

For an impression of the *in vivo* behaviour of the ^{88}Zr-labelled 323A3, $^{88}ZrDf$ and ^{88}Zr-citrate, animal experiments with non-tumor-bearing mice were performed. The blood pool activity of these compounds during 24 hours is depicted in fig 1. $^{88}ZrDf$ was found to be cleared very fast by the kidneys: after 15 minutes nearly half of the injected dose was present in the urine. ^{88}Zr-citrate has a longer biological half-life and is mainly accumulated in the bone, which accentuates the necessity of a stable bond between the Zr and the antibody.
Comparison of the biodistribution of the ^{88}Zr labelled 323A3 in non-tumor-bearing mice with that of ^{123}I labeled antibody revealed a higher liver accumulation with the ^{88}Zr labelled antibody. Although during the timespan of our experiments the percentage radioactivity in blood in case of I-labelled antibody was higher than for the Zr-labelled 323A3, the blood clearance pattern of the two radioimmunoconjugates is approximately the same (fig. 1). Since hardly any ^{88}Zr accumulation in bone was observed, it seems justified to assume that the ^{88}Zr labelled 323A3 is stable *in vivo* for at least 24 hours.

Desferal was shown to be a very promising chelating agent for the labelling of antibodies with Zr-isotopes. The method of labelling is simple and efficient and might even be applicable in kit-form. The obtained radioimmunoconjugate seems to be stable *in vitro* as well as *in vivo*.

[1] Meijs,W.E., Herscheid,J.D.M., Haisma,H.J. and Pinedo,H.M. -Appl. Radiat. Isot. 43:1443(1992)

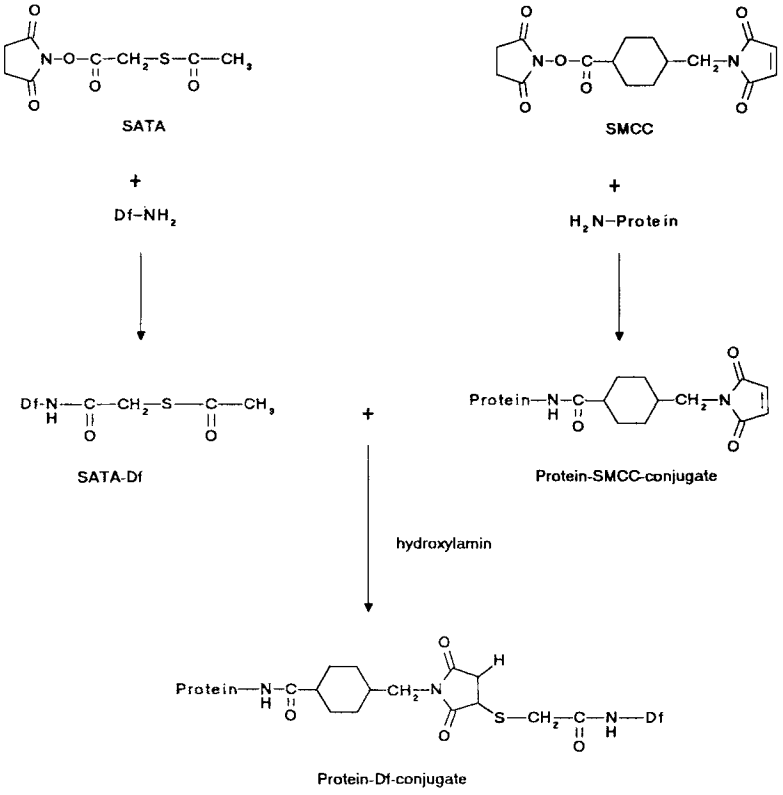

Scheme 1

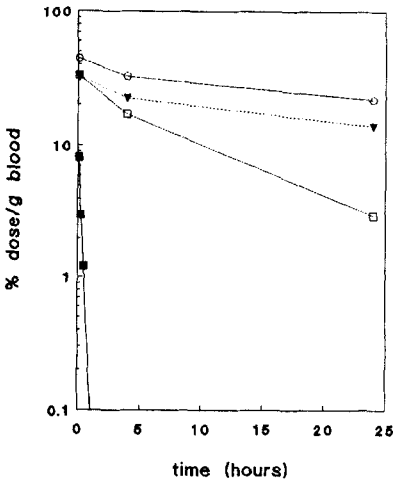

FIGURE 1 Bloodclearance of ^{88}ZrDf (■), ^{88}Zr-citrate (□), ^{88}Zr-323A3 (▾) and ^{123}I-323A3 (o) in non-tumor-bearing mice.

Biodistributions of 169Yb-, 153Sm-, and 111In-labelled monoclonal antibodies against TAG-72 - Preliminary results

SCHOMÄCKER, K.; SCHEIDHAUER, K.; SCHARL*, A.; SCHICHA, H.; HAUSCH, A.; SCHULZ, M.; SCHULTE, S.; SHUKLA**, S.K. Clinic of Nuclear Medicine and *Clinic of Obstetrics and Gynaecology, Cologne Medical School, **Nuclear Research Council of Italy, Hospital St. Eugenio (Department of Nuclear Medicine)

The monoclonal antibody MAb B72.3-GYK-DTPA against the tumour associated glycoprotein TAG-72, which is in 111In-labelled form commercially available as "Oncoscint" (Eurocetus) was labelled with 111 In, 169Yb or 153Sm. The radionuclides were applied for labelling 153Sm is a therapeutically relevant radionuclide and 169Yb is used as "standard" because its biokinetics in various chemical forms is well investigated by our group. The quality control of the labelling products was carried out with HPLC, performed on a gel (2000 SW) column and with TLC. The efficiency of the 169Yb- and 153Sm-labelling was >95 % and of the 111In-labelling > 97%. The labelled products were injected via the tail vein into mice bearing mamma carcinoma. The biodistributions after injection of the different labelled antibodies were compared at 24 h p.i..

We found in the tumour after injection of the 169Yb- or 153Sm-labelled products radioactivity concentrations which were lower by ca. 50 % in comparison with the 111In-labelled antibody. On the other hand, also the bone, blood- and muscle radioactivities were lower as in the case of the 111In-compound. Consequently, the tumour/background-ratios could be increased by the factor 2-5 by replacing In by Yb or Sm. The disturbing radioactivity accumulation in the liver after the application of 169Yb- and 153Sm-antibodies could be reduced by the factor 10 by coapplication of EDTMP.